AD-A113 253 E-SYSTEMS INC ST PETERSBURG FL ECI DIV F/G 9/5
ELECTRONICALLY TUNABLE PHASE LOCKED LOOP OSCILLATOR.(U)
FEB 82 M BALASIS, M R DAVIS, C R JACKSON F30602-80-C-0133
UNCLASSIFIED 60-62244 RADC-TR-81-400 NL

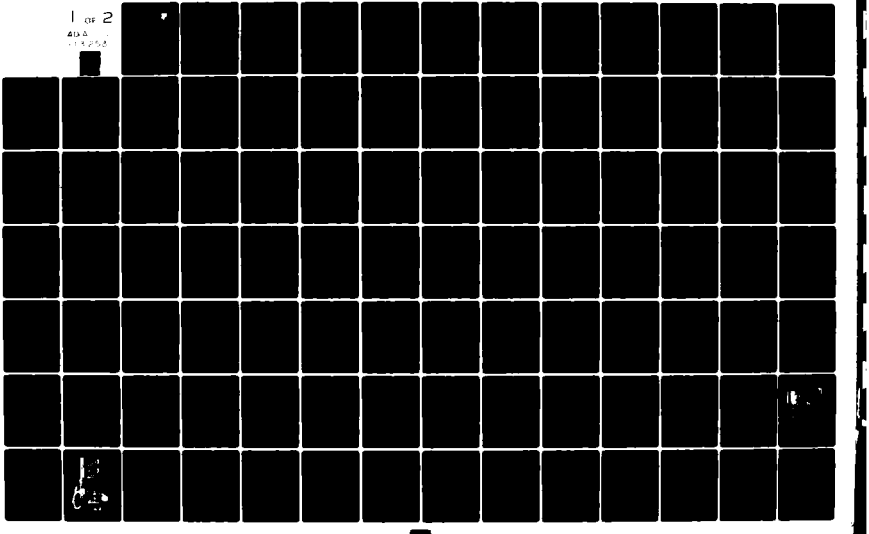

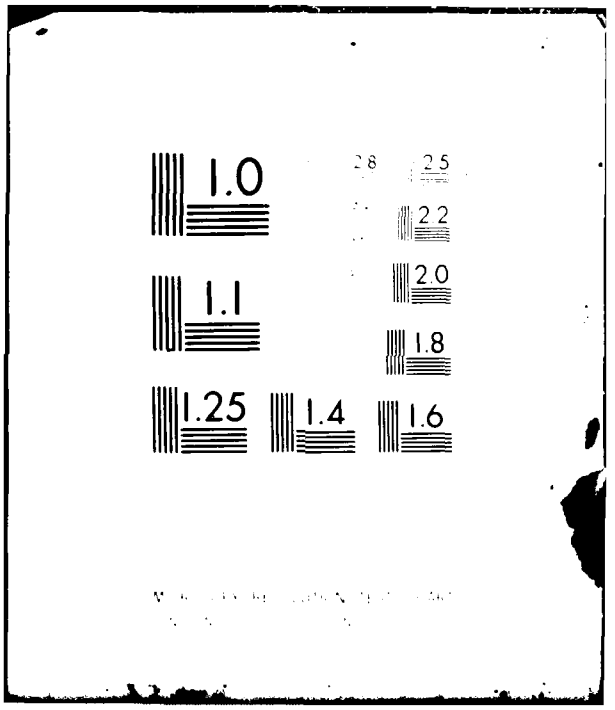
1.0
2.8
2.5
2.2
2.0
1.1
1.8
1.25
1.4
1.6

(12)

RADC-TR-81-400
Final Technical Report
February 1982

ELECTRONICALLY TUNABLE PHASE LOCKED LOOP OSCILLATOR

E-Systems, Inc.

Mathew Balasis
Michael R. Davis
Charles R. Jackson

APPROVED FOR PUBLIC RELEASE; DISTRIBUTION UNLIMITED

DTIC
ELECTE
MAR 9 1982
S D
A

AD A113253

DTIC FILE COPY

ROME AIR DEVELOPMENT CENTER
Air Force Systems Command
Griffiss Air Force Base, New York 13441

82 04 12 004

This report has been reviewed by the RADC Public Affairs Office (PA) and is releasable to the National Technical Information Service (NTIS). At NTIS it will be releasable to the general public, including foreign nations.

RADC-TR-81-400 has been reviewed and is approved for publication.

APPROVED: Thomas E. Baustert

THOMAS E. BAUSTERT
Project Engineer

APPROVED: David C. Luke

DAVID C. LUKE, Colonel, USAF
Chief, Reliability & Compatibility Division

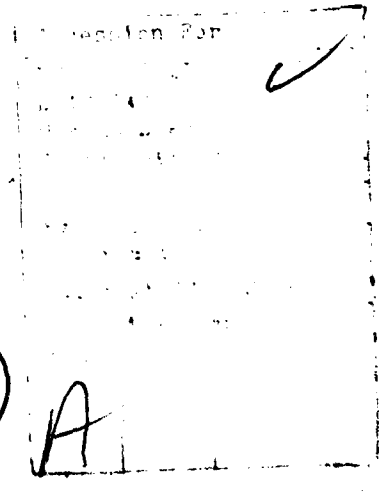

DTIC
COPY
INSPECTED
2

FOR THE COMMANDER: John P. Huss

JOHN P. HUSS
Acting Chief, Plans Office

If your address has changed or if you wish to be removed from the RADC mailing list, or if the addressee is no longer employed by your organization, please notify RADC (RBCT) Griffiss AFB NY 13441. This will assist us in maintaining a current mailing list.

Do not return copies of this report unless contractual obligations or notices on a specific document requires that it be returned.

UNCLASSIFIED

SECURITY CLASSIFICATION OF THIS PAGE (When Data Entered)

REPORT DOCUMENTATION PAGE		READ INSTRUCTIONS BEFORE COMPLETING FORM
1. REPORT NUMBER RADC-TR-81-400	2. GOVT ACCESSION NO. AD-A113 253	3. RECIPIENT'S CATALOG NUMBER
4. TITLE (and Subtitle) ELECTRONICALLY TUNABLE PHASE LOCKED LOOP OSCILLATOR		5. TYPE OF REPORT & PERIOD COVERED Final Technical Report 10 Mar 80 - 12 Jun 81 6. PERFORMING ORG. REPORT NUMBER GO-62244
7. AUTHOR(s) Mathew Balasis Michael R. Davis Charles R. Jackson		8. CONTRACT OR GRANT NUMBER(s) F30602-80-C-0133
9. PERFORMING ORGANIZATION NAME AND ADDRESS E-Systems, Inc., ECI Division 1501 72nd St. No. St. Petersburg FL 33733		10. PROGRAM ELEMENT, PROJECT, TASK AREA & WORK UNIT NUMBERS 62702F 23380412
11. CONTROLLING OFFICE NAME AND ADDRESS Rome Air Development Center (RBCT) Griffiss AFB NY 13441		12. REPORT DATE February 1982 13. NUMBER OF PAGES 154
14. MONITORING AGENCY NAME & ADDRESS(if different from Controlling Office) Same		15. SECURITY CLASS. (of this report) UNCLASSIFIED 15a. DECLASSIFICATION/DOWNGRADING SCHEDULE

16. DISTRIBUTION STATEMENT (of this Report)

Approved for public release, distribution unlimited.

17. DISTRIBUTION STATEMENT (of the abstract entered in Block 20, if different from Report)

Same

18. SUPPLEMENTARY NOTES

RADC Project Engineer: Thomas E. Buastert (RBCT)

19. KEY WORDS (Continue on reverse side if necessary and identify by block number)

Electronically Tuned Oscillator
Electronically Tuned Resonators
High Power Oscillators
Voltage Controlled Oscillators
Electromagnetic Compatibility
Phase Noise

20. ABSTRACT (Continue on reverse side if necessary and identify by block number)

This technical report describes the design and development of a low noise, high power, variable oscillator incorporating a high "Q" electronically tunable resonator as the frequency determining element. The VCO provides improved EMC performance in phase locked synthesizers which are a part of communications equipments. The oscillator combines a low noise VMOS transistor with the selectivity and out-of-band attenuation of a coaxial resonator to provide superior EMC performance.

DD FORM 1 JAN 73 1473 EDITION OF 1 NOV 65 IS OBSOLETE

UNCLASSIFIED

SECURITY CLASSIFICATION OF THIS PAGE (When Data Entered)

Several oscillator designs were examined and the basis for the final configuration is presented.

Oscillator noise is discussed and models for analysis are explained.

A brass board model was constructed and tested. The technical results are presented and recommendations for further research and development are made.

TABLE OF CONTENTS

TABLE OF CONTENTS (Cont'd)

TABLE OF CONTENTS (Contd)

TABLE OF CONTENTS (Contd)

LIST OF FIGURES

LIST OF FIGURES (Cont'd)

LIST OF FIGURES

LIST OF TABLES

1.0 INTRODUCTION

Many new communications equipment sites require the use of multiple high level transmitters colocated with highly sensitive receivers. In these applications the communications performance is severely affected by the EMC characteristics of each receiver and transmitter on site. Specifically, broadband noise and spurious signals associated with a particular transmitter may fall within the band of a colocated receiver and seriously degrade receiver desensitization and cross-modulation distortion.

These applications stimulate a need for significant improvements in transmitter signal-to-noise and spurious performance and also in receiver dynamic range. A short term solution has been the addition of mechanically tuned band-pass filters to the antenna circuits of receivers and transmitters. Though effective, this approach adds significant cost and complexity to the communication sites. In addition, frequency hopping capabilities for AJ protection is lost due to the relatively slow tune time of mechanical devices.

The subject of this contract is to address the EMC problems of fast tuning frequency agile communications systems. The objective is to provide the design methodology that will lead to the development of synthesized signal sources with significantly improved signal-to-noise (S/N) performance. Specifically a voltage-controlled oscillator (VCO) covering 225 to 400 MHz shall be designed that provides high power output and enhanced S/N.

A brassboard UHF oscillator was designed that meets all technical requirements of the program. This final design was based on the results of a study and test phase where

- o The theory and literature pertaining to low noise oscillators were studied and models refined to predict the noise performance of high power, low noise oscillators.
- o Several oscillator configurations were designed and thoroughly tested.
- o A final oscillator configuration was chosen and a deliverable unit built and tested.
- o Several areas have been identified in which further research would be fruitful.

The program accomplishments are best illustrated by the graph of Figure 1-1 where resultant phase noise of the High Power VCO is compared to a modified ARC-164 UHF transmitter resulting from an earlier RADC program to improve EMC performance. Nearly 40 dB of improvement has been achieved.

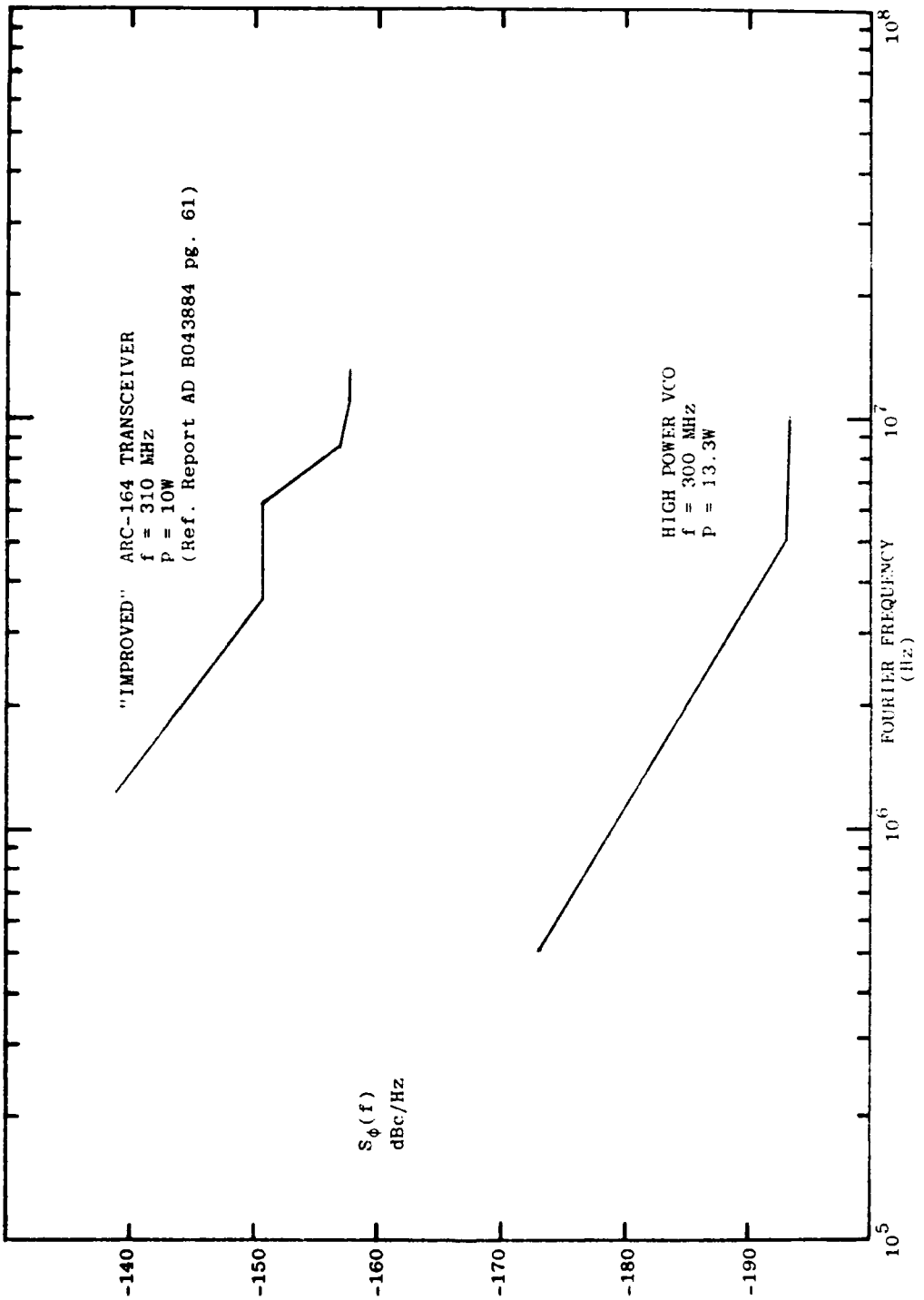

FIGURE 1.1
NOISE COMPARISON OF HIGH POWER
VCO TO ARC-164 TRANSMITTER

2.0 TECHNICAL PROBLEM

2.1 Background of the Problem

During the last decade, modernization programs have led to the development of smaller, lighter, more reliable communications equipments. As a part of these efforts, many receiver and transmitter functions formerly performed by vacuum tubes were designed with modern solid state devices. The vacuum tube transmitter and its mechanically tuned interstage networks were replaced by reliable solid state devices in broadband designs. A typical solid state unit may cover an octave with no tuning required. This freedom from mechanical tuning opened new applications of fast frequency hopping to provide AJ protection. Packaging was simplified, cost and size reduced, reliability increased. A new equipment era was established.

Literally tens of thousands of equipments were manufactured with broadband solid state techniques. As more users appeared, spectrum crowding became common place. Communications sites became more complex, multiple Receiver-Transmitter equipments shared a common locale, perhaps even the same antenna. In these crowded spectrum and colocation conditions, severe deterioration in operation was noted. It became quickly obvious that the broadband transmitter was the offender. For example, broadband transmitters may have 40 dB of gain and a 20 dB noise figure. The resultant broadband noise, 60 dB above thermal, radiates from the transmit antenna. Equipments in the same general locale with less than 50 dB of antenna isolation suffer significant receiver desensitization. Spurious signal interference also became significant. Although equipments were meeting MIL-STD-461 spurious requirements, it was not adequate for the colocation environments. Ironically, older transmitters did not cause this

PRECEDING PAGE BLANK-NOT FILMED

problem because they included narrowband circuits that attenuated the out-of-band noise and synthesizer spurious signals.

Interim solutions have been implemented in critical colocation environments. Narrowband mechanically tuned bandpass filters and multicouplers are placed following the PA to attenuate noise and spurious. These additions cause significant cost, size, and weight increases to the installations. In addition, the frequency hop capabilities required for future systems is lost.

2.2 Conceptual Study

A new concept was developed to solve this very complicated problem by taking a systems approach to the total transmitter design. Consideration was given not only to the power stages but also the exciter and frequency synthesizer. Careful analysis of gain, power level, and noise figure of each stage led to the conclusion that the actual signal generation accomplished within the synthesizer must be substantially improved. This includes increasing the VCO signal level to reduce the broadband gain in the Power Amplifier, and simultaneously decreasing the noise output. These two improvements dramatically enhance signal-to-noise performance at the antenna.

In the late 1970's, E-Systems, Inc., ECI Division performed a preliminary investigation into potential solutions to this problem by merging two state-of-the-art technolgies: (1) High Q Switch-Tuned Resonators and (2) Low Noise High Power VMOS Transistors. The study resulted in a high power low noise oscillator brassboard model that showed significant improvement in signal-to-noise performance. Based on these preliminary results, this contract was awarded.

2.3 Program Tasks

The objective of this effort is to develop the technology and prove the feasibility of combining a low noise, high power, VMOS FET oscillator and a high "Q" electronically tunable resonator to provide a new generation of phase locked frequency synthesizers. To accomplish this objective, the program calls for delivery of a brassboard voltage controlled oscillator covering the UHF military band which provides high power output and significant improvement in signal-to-noise performance over present day military equipment.

2.4 Technical Requirements

In order to demonstrate contract compliance, the experimental model shall meet the following requirements as outlined by the statement of work PR No. N-0-5013.

4.1.1.1 Frequency Range: 225 to 400 MHz

4.1.1.2 Power Output: 2 watts minimum

4.1.1.4 Tuning Capability: Continuous coverage across entire frequency range by combination of digital course tuning and analog fine tuning.

4.1.1.4 Tuning Speed: Tune to a new frequency in 100 uSec or less.

4.1.1.4 Tuning Elements: PIN diode switched capacitor networks for digital course tune and lightly coupled varactor diodes for analog fine tuning.

4.1.1.5 Load Stability: The VCO shall incorporate buffer stages to isolate it from varying load impedances.

4.1.1.6 DC Power: The VCO shall be powered by lab supplies and not incorporate a deliverable supply.

4.1.3 Safety: The VCO shall comply with MIL-STD-454F, Requirement 1.

The experimental model shall be designed for lowest noise against the following technical goal:

4.1.1.3 Output Noise: Not to exceed -150 dBm/Hz, ±500 kHz removed from carrier nor exceed -165 dBm/Hz, ±5 MHz removed.

The experimental model shall be designed to demonstrate the technical soundness of the concept and to provide a device for future testing and experimentation by an engineering organization. It is to be built to best commercial practices.

3.0 DESIGN ANALYSIS AND TRADE STUDY

The following paragraphs provide the results of both a literature search and our analysis concerning the design and trade-offs related to low-noise VCO's. Basic oscillator configurations are analyzed against our Statement of Work to determine the best design approach. We present detailed noise analysis of both simple models and the more complex combinations of oscillator, practical lossy resonators, and buffer amplifiers. Finally we present equations that predict phase noise performance given practical design data like Q, Noise Figure, Gain, etc.

3.1 Oscillator Analysis

Basically, an oscillator is just an amplifier with positive feedback as shown in Figure 3.1-1.

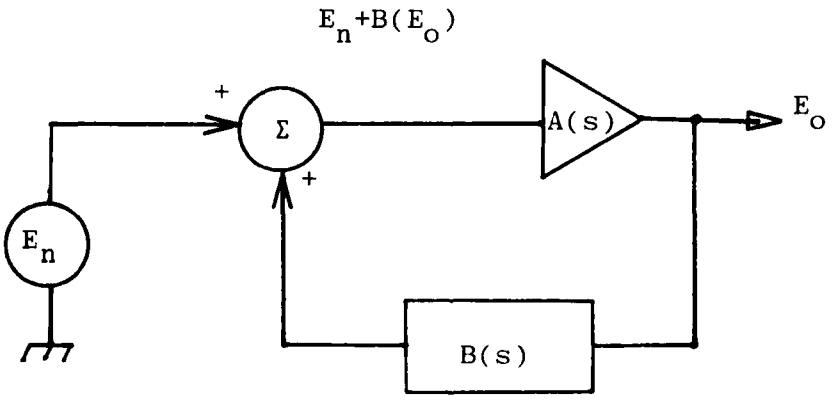

FIGURE 3.1.1
OSCILLATOR FUNCTIONAL BLOCK DIAGRAM

Where:

$A(s)$ = Transfer function of amplifier

$B(s)$ = Transfer function of feedback network

E_n = Noise Voltage

E_o = Output Voltage

The closed-loop expression can easily be shown to be

$$E_o/E_n = \frac{A(s)}{1-A(s)B(s)}$$

Therefore, if the feedback network, $B(s)$, is adjusted such that

$$A(s)B(s) = 1$$

oscillation occurs, since E_o/E_n approaches infinity. The circuit starts with the broadband excitation by thermal noise (E_n) in the circuit. Generally the amplifier and/or the feedback element $A(s)$ and $B(s)$ contains a frequency selective network that determines the frequency of oscillation. More explicitly

$$A(s)B(s) = 1\angle 0^{o} \quad \text{at } f_o$$

3.2 Oscillator Circuit Configurations

Many basic circuit configurations are available for an RF oscillator design. Several of these circuit configurations will be reviewed with respect to potential use in a low noise, high power VCO. Merits of various oscillator configurations were discussed by Clapp[1] in a survey of frequency stable oscillators. Although this work was done for vacuum tubes, some of the conclusions are applicable to VMOS devices.

3.2.1 Basic Clapp Oscillator

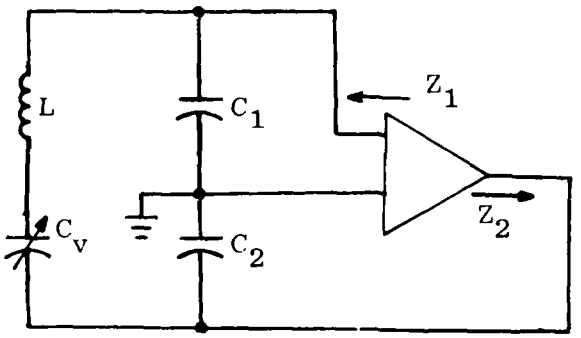

FIGURE 3.2.1
BASIC CLAPP

A basic Clapp oscillator is shown in Figure 3.2-1 in which the inductor is series tuned by the tuning capacitor C_v where:

$$C_v << C_2 \ , \ C_v << C_1$$

C_v provides the variable tuning element. C_1 and C_2 are matching network components which provide the impedance transformations required between the resonant circuit and the active stage.

The Clapp oscillator most often is built around a transcondance amplifier and provides significant improvements in oscillator stability compared to other L-C configurations. However, the Clapp is not well suited for wideband coverage that is, coverage by adjustment of C_v only. Indeed, not only C_v but C_1 and C_2 must be changed to optimize matching over significant band coverage.

The following illustrates this:

The active stage transfer function, g_m, combines with the resonant circuit Z_1, Z_2 to satisfy oscillation as

$$\sqrt{Z_1 Z_2} = 1/g_m$$

since C_v is much less than C_1 and C_2, an approximation follows:

$$Z_1 \simeq R_o (C_v/C_1)^2$$

$$Z_2 \simeq R_o (C_v/C_2)^2$$

Where R_o is the parallel resonant impedance of the tuned circuit.

Solving the above, recalling that

$$Q = \omega C_v R_o$$

we find that

$$g_m = \frac{\omega C_1 C_2}{Q C_v}$$

Knowing the active stage parameter, frequency, and operating Q allows the designer to select optimum tuning and matching elements.

Now - suppose frequency is varied (to ω_2) with C_1, C_2, Q held constant. What characteristic must the amplifier take on?

$$g_{m1} = \frac{\omega_1 C_1 C_2}{Q C_{v1}} \quad (\text{at } f_1)$$

$$g_{m2} = \frac{\omega_2 C_1 C_2}{Q C_{v2}} \quad (\text{at } f_2)$$

and recall that $\omega_1 \simeq 1/\sqrt{LC_{v1}}$

$$\omega_2 \simeq 1/\sqrt{LC_{v2}}$$

$$\text{so } Cv_2/Cv_1 = (\omega_1/\omega_2)^2$$

Thus

$$\frac{g_{m1}}{g_{m2}} = \frac{\frac{\omega_1 C_1 C_2}{Q C_{v1}}}{\frac{\omega_2 C_1 C_2}{Q C_{v2}}} = (\omega_1/\omega_2)^3$$

This shows that g_m must move as the cube of frequency range to optimize performance. The literature suggests a maximum range of about 20% variation (tuning C_v) and therefore the Clapp would not be a good candidate for an oscillator covering nearly an octave.

3.2.2 Basic Seiler Oscillator

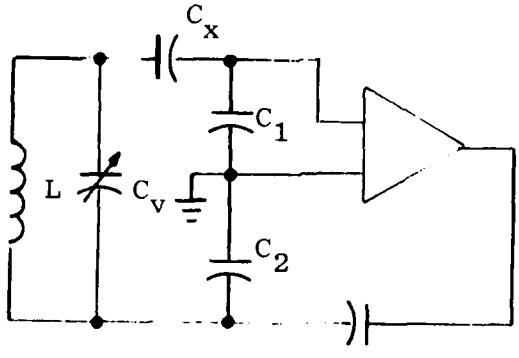

FIGURE 3.2.2
BASIC SEILER

A basic Seiler oscillator configuration is shown in Figure 3.2-2, in which the inductor is parallel tuned with the capacitor C_v. It was shown by Clapp[1] that:

$$g_m \propto \frac{K}{\omega Q}$$

The g_m required for oscillation is proportional to $\frac{1}{\omega}$ and if Q increases with frequency then the amplitude of this oscillator may be relatively constant with tuning over frequency ranges of about 1.8:1.

3.2.3 Basic Colpitts Oscillator

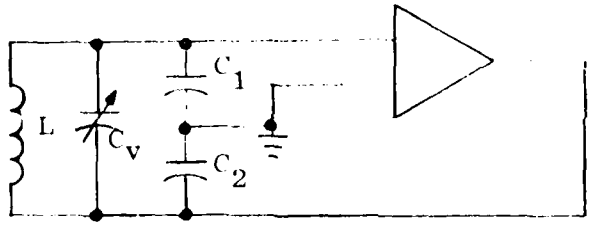

FIGURE 3.2.3
BASIC COLPITTS

The Colpitts oscillator is shown in Figure 3.2-3 is similar to the Clapp oscillator when the series tuned capacitor is eliminated in the Clapp oscillator. The Colpitts oscillator is more stable than the Clapp oscillator.

3.2.4 Basic Hartley Oscillator

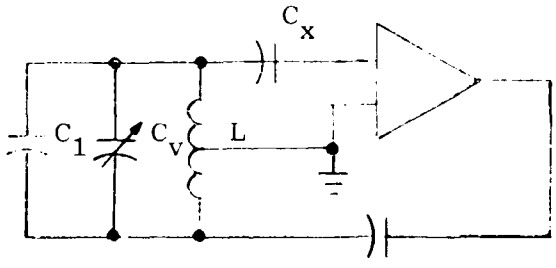

FIGURE 3.2.4
BASIC HARTLEY

The basic Hartley oscillator as shown in Figure 3.2-4 uses a tapped inductor to provide the proper feedback. This circuit may have a tendency to break into spurious oscillation if used over the 225 to 400 MHz band since the tapped inductor may have self-resonance modes at higher frequencies where gain of the active device is greater than unity.

3.2.5 Basic Vackar Oscillator

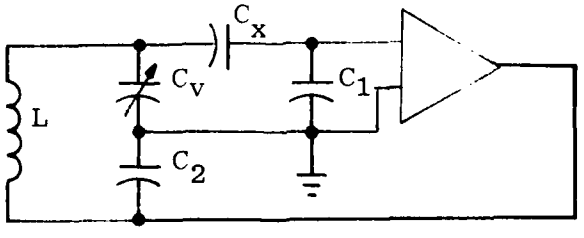

FIGURE 3.2.5
BASIC VACKAR

Vackar[2] describes a circuit combining the features of the series and parallel tuning arrangements as shown in Figure 3.2-5. Clapp[1] shows that the G_m required for oscillation is:

$$G_m = \left(\frac{\omega}{Q}\right)\left(\frac{C_1 C_2}{C_x}\right), \text{ when } C_1 >> C_x \text{ and } C_v >> Cx$$

If Q rises with frequency, then the amplitude remains fairly constant over a tuning range as great as 2.5:1.

Jordon[3] states that this design has the greatest inherent stability of any known configuration except for a design with independent external load feedback. He states three criteria for good stability in this circuit:

a. The peak to peak voltage at the junction of C_v and the tank inductance should be less than twice the B+, but probably greater than one times B+.

b. Since instability will inherently increase with active device closed loop gain, the closed loop gain should be less than about 1.2:1.

c. C_2 and C_1 should be as large as possible.

3.2.6 Transmission Line Oscillators

The five oscillator configurations which have been presented are based on discrete LC components and work well up to about 100 MHz. The discrete inductor is limited in Q at higher frequencies. The unloaded Q of the inductor is important in providing good efficiency and high power output. The Q is even more important in this application of a low-noise VCO because it determines the bandwidth of the phase noise.

High Q inductors are necessary and can be built by using low loss transmission line. The transmission line can be end tuned by a high Q capacitor as shown in Figure 3.2-6.

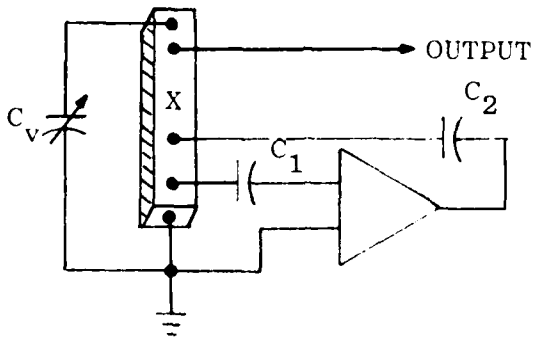

FIGURE 3.2.6
TRANSMISSION LINE OSCILLATOR

This approach simplifies tuning when a wide tuning range is needed since both C_1 and C_2 can be low loss fixed value capacitors. Normally, if C_1 and C_2 are used for tuning in a Colpitts configuration, their values must be changed simultaneously to maintain a constant feedback ratio. This circuit configuraiton has an advantage that the output impedance matching can be adjusted by moving the output tap point. Likewise, the device source and load impedances along with the feedback ratio are all independently adjustable.

3.2.7 Selection of Circuit Configuration

Although discrete LC oscillators are not appropriate for this low noise, high power VCO application, they are presented so that a better understanding of the basic oscillator configurations might lead to an improved design. The inductor in

each of the LC designs may be replaced by a high-Q transmission line. The Clapp oscillator, using a transmission line inductor, will still have a problem with changing amplitude with tuning frequency and is therefore eliminated as a VCO candidate.

The Seiler and Colpitts oscillators are identical except for the location of C_x which allows matching the resonant tank impedance either up or down to the device input impedance. The transmission line oscillator shown in Figure 3.2-6 also allows matching the resonant circuit impedance up or down to the device impedance.

The transmission line oscillator has advantages over the basic Hartley in that it provides more degrees of freedom in selection of impedance matching and the feedback ratio. The basic Vackar oscillator requires a non-grounded inductor which is hard to implement mechanically with a high-Q transmission line as will become apparent later.

In conclusion, the transmission line oscillator, as shown in Figure 3.2-6, appears to be the best basic configuration for a high power, low-noise VCO required to cover the UHF octave.

3.3 Noise Analysis

The noise performance of a VCO is somewhat complex to determine since there are many independent noise sources to deal with such as

a. Noise generated within the active device.
b. Distortion due to non-linearities in the active and tuning devices.
c. Short-term frequency instability of the circuit.
d. Power supply noise and ripple coupled into the circuit.
e. Noise picked up on the tuning line of an electronically tuned circuit (varactor for example).

The objective of this project is to determine design alternatives that enhance signal-to-noise ratios at the VCO output. A careful study must be made therefore, of the noise characteristics.

3.3.1 Noise Modulation of an Oscillator

A good intuitive explanation of oscillator noise is given by Malling[4]. Thermal noise agitation of the oscillator frequency may be considered on a sampling basis as low-level random impulse modulation where the random frequency shifts are represented as unsymmetrical sidebands of the carrier. However, any one of these single random sideband components may be resolved into two pairs of symmetrical and antisymmetrical sidebands representing amplitude and frequency modulation of the carrier, with each pair having half the amplitude of the random component.

The important point is that noise in the oscillator circuit creates both amplitude and frequency jitter. Edson[5] states that the amplitude perturbations produce a continuous spectrum which in typical situations is quite weak and broader than the bandwidth of the resonator in the oscillator feedback path. The phase perturbations disperse the nominal frequency into a continuous distribution which is much stronger and narrower than for the amplitude perturbations. The statistical noise distributions may be quite different during initial oscillator start-up as compared to the steady state condition. Reference 5 contains a good analysis of oscillator noise jitter distribution during start-up and steady state.

Another intuitive approach to incidental frequency modulation performance is illustrated by Figure 3.3.1-1.

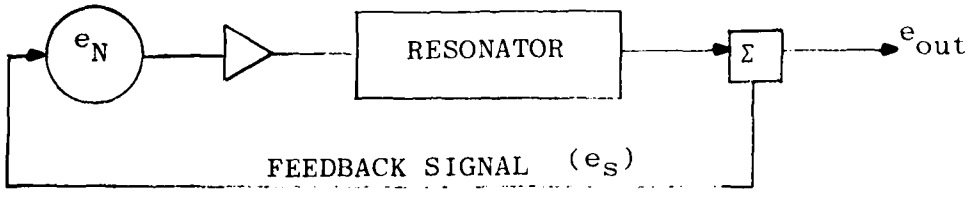

OSCILLATOR

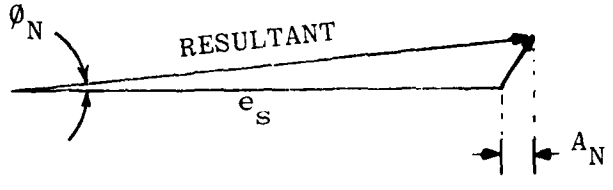

VECTOR DIAGRAM

FIGURE 3.3.1.1
NOISE MODULATION OF OSCILLATOR

All noise contribution is contained in the noise generator e_N and placed in series with the signal path e_s. For oscillation to occur the feedback signal must be at unity gain (or into gain compression) and zero degrees phase.

The vector diagram illustrates the summation of signal and noise voltages at some instant of time. The noise signal, e_N,

actually modulates the carrier and provides both FM and AM energies (ϕ_N and A_N shown). Because most oscillators are designed with gain margin the effects of amplitude modulation by the noise are somewhat surpressed. However, the ϕ_N component forces the oscillator to a new frequency momentarily, determined by the phase slope of the resonator thereby generating a frequency modulation condition. From this picture one clearly determines a path to enhance signal-to-noise.

1. Increase signal power.
2. Decrease noise contributions.
3. Increase the phase slope of the resonator section.

Reference 6 deals with the effects of locking the VCO to an external stable oscillator both in frequency and amplitude resultants.

3.3.2 Characterization of Oscillator Noise

The noise figure (NF) is a convenient quantity for specifying noise characteristics of linear systems since it is related to the signal-to-noise ratio (SNR). But, NF is not a good parameter for specifying SNR of a high power oscillator. The device nonlinearities cause the signal and noise to be treated differently. As a result, the SNR can be sensitive to the operating parameters of the nonlinear oscillator in addition to the strengths of the noise sources.

An oscillator noise model based on physical reasoning[7] consists of a feedback oscillator modeled as a phase locked loop having positive feedback. A mathematical analysis of an oscillator, modeled as an amplifier with a selective feedback filter[8], showed the validity of the physical model. These models did not include the effect of amplifier nonlinearities.

Attempts have been made to predict the noise characteristics for a nonlinear oscillator[9]. Reference 9 treats only noise bandwidth due to broadband thermal noise while ignoring the effects of low frequency noise. A complete generalized nonlinear VCO noise model has not been found which is capable of predicting the output noise spectrum accurately. Recent improvements in measurement capability allow fine resolution spectral density measurements to be made very close to the carrier frequency and show that the shape of the spectral density is more complex than what previous models would predict. A complete generalized nonlinear VCO noise model is not available, and probably would not be too useful for circuit design tradeoff anyhow; the existing models are suitable to aid in circuit synthesis to minimize noise levels. In order to fully utilize these models it is necessary to become familiar with some theoretical definitions.

3.3.3 Definitions

The signal having phase noise may be described by its instantaneous voltage v(t) by:

$$v(t) = A(t)\left[\cos \omega_o t + \phi(t)\right]$$

where:

$A(t)$ = variable amplitude of the signal and does not contribute directly to frequency fluctuations (but in nonlinear devices conversion of AM to PM can occur).

ω_o = constant center frequency in radians/sec

$\omega_o t = 2\pi f_o t$ = linearily growing phase component of v(t) in radians

$\phi(t)$ = a random phase fluctuation with time in radians

$\omega_o t + \phi(t) = \beta$ = instantaneous total phase of v(t) in radians

The instantaneous frequency, f, is equal to the rate of change of the instantaneous phase with time or $\dot{\phi}$.

$$f = \frac{1}{2\pi} \frac{d\beta}{dt} = f_o + \frac{1}{2\pi} \frac{d\phi(t)}{dt} \text{ in Hz}$$

Therefore, phase fluctuations may be related to frequency fluctuations. It is helpful to use FM modulation theory and first consider a signal with sinusoidal frequency modulation and then convert to phase modulation[10].

Let $\phi(t) = \Delta\phi \sin 2\pi f_m t$

then $v(t) = A(t) \cos \left[2\pi f_o t + \Delta\phi \sin 2\pi f_m t\right]$

$$f = f_o + f_m \Delta\phi \cos 2\pi f_m t$$

where

$\Delta\phi = \Delta f / f_m$ = peak phase deviation

$\Delta f = f_m \Delta\phi$ = peak frequency deviation

f_m = rate of frequency deviation

In FM theory $\frac{\Delta f}{f} = m$, the modulation index. Note that since $\Delta\phi = \Delta f / f_m = m$, then v(t) can be either described by phase or frequency deviation because they are related by the rate of modulation (for the case of a single sinusoidal modulation with $m<1$).

By using a Bessel function series expansion, the equation for v(t) can be written to emphasize the frequency components of a sinusoidal frequency or phase modulated signal. Since we are dealing with noise modulation of the carrier we can confine ourselves to the simplification [11].

$$V(t) = J_o(m) \sin \omega_o t + J_1(m) \left[\text{Sin}(\omega_o+\omega_m)t - \text{Sin}(\omega_o-\omega_m)t\right] \bullet\bullet\bullet$$

That applies for $m << 1$. For this case

$$J_o(m) \simeq 1,\ J_1(m) \simeq M/2\ \ J_2,\ J_3 \text{-- } \simeq 0$$

Thus, the waveform appears in the frequency domain as a carrier at f_o with sidebands spaced at $f_o + f_m$ and $f_o - f_m$. The ratio of one sideband amplitude to the carrier amplitude is:

$$\left.\frac{V_{sb}}{V_c}\right|_{dB} = 20 \log \left(\frac{\Delta\phi}{2}\right)$$

The actual spectrum contains more than 2 discrete sidebands and, in fact, is a continuous spectrum which is represented by a power spectral density $S_\phi(f)$ of the phase. Considerable confusion often exists when reference is made to spectral density. The complete RF spectrum as seen on a spectrum analyzer is not a plot of spectral density, unless the analyzer has a 1 Hz noise bandwidth, but may be converted to spectral density if the bandwidth of the analyzer is known. At least four definitions of spectral density[12] are of interest:

1. A(t), the amplitude modulation spectral density, found by passing v(t) through an ideal AM detector,, and measuring the spectrum of the detector output. (This AM spectral noise is usually negligible compared to the FM noise due to both AM noise reduction by nonlinearities or limiting and to enhancement of FM noise by positive feedback in oscillators.
2. $S_\phi(f)$, the spectral density of phase $\phi(t)$ found by passing v(t) through an ideal phase detector, and measuring the detector output spectrum.

3. $S_{\dot{\phi}}(f)$, the spectrum of $\phi(t)$, obtained by spectral analysis of the output of an ideal FM detector.

4. $S_y(f)$, the spectral density of normalized frequency fluctuations.[13]

The most useful spectral representation is usually either $S_{\phi}(f)$ or $S_{\dot{\phi}}(f)$. The derivative of $\phi(t)$ is $\dot{\phi}(t)$ and since differentiation in the time domain is equivalent to multiplication by $j\omega$ in the frequency domain or multiplication by ω^2 in terms of spectral densities then[12],

$$S_{\dot{\phi}}(\omega) = \omega^2 S_{\phi}(\omega)$$
$$S_{\dot{\phi}}(f) = (2\Pi f)^2 S_{\phi}(f)$$

The fourth definition of spectral density $S_y(f)$ was suggested[13] as a standard frequency domain definition of frequency stability because of its invariance with multiplication. The National Bureau of Standards (NBS) proposes to standardize the spectral density of fractional frequency fluctuations, y(t), so as to have a dimensionless quantity, where: $y(t) = \Delta f(t)/f_o$

$$S_y(f_m) = \frac{1}{f_o^2} S_{\phi}(f_m) = \left(\frac{f_m}{f_o}\right)^2 S_{\dot{\phi}}(f_m)$$

Use of y(t) and $S_y(f)$ permits a better comparison of relative noise between sources with different carrier frequencies.

There are other methods of measurement and specification of oscillator noise including residual FM noise and time domain stability. The residual FM noise is the total RMS frequency deviation within a specified bandwidth, commonly related to a voice channel of about 300 Hz to 3 kHz. Residual FM noise specifications have three components: power level, bandwidth, and frequency region relative to f_o.

Time domain stability can be specified by fractional frequency deviation. A quantitative measure of fractional frequency deviation is given by the Allan variance[14], $\sigma_y^2(\tau)$, which is the proposed standard measure of frequency stability.[10]

$$\sigma_y^2(\tau) \approx \frac{1}{2(m-1)} \sum_{k=1}^{m-1} (\bar{Y}_{k+1} - \bar{Y}_k)^2$$

where $\bar{Y}_k$ is the average fractional frequency difference of the kth sample, measured over the sample time, τ. The differences between consecutive sample pairs are averaged over a large number (e.g. m>100) of samples. The measurement is dependent on averaging time, τ, and therefore it is meaningless to specify fractional frequency deviation without a statement of averaging time.

Conversions from the frequency domain to the time domain and vice versa, are very complex and beyond the scope of this report. Mathematical treatments of these conversions are given in references 15, 16, and 17. A Table of practical conversion formula is given in reference 10.

3.3.4 Characterizing Oscillator Noise

The spectral density of the noise $S_\phi(f)$ is not flat with frequency but has several different slopes[10]. Figure 3.3.4-1 illustrates the five dominant examples often encountered in various oscillators even though any one design will be dominated by at most three of these.

The following general remarks relate to these oscillator characteristics:

a. Random Walk FM (f^{-4})

- Usually relates to oscillator's physical environment; shock, vibration, temperature.

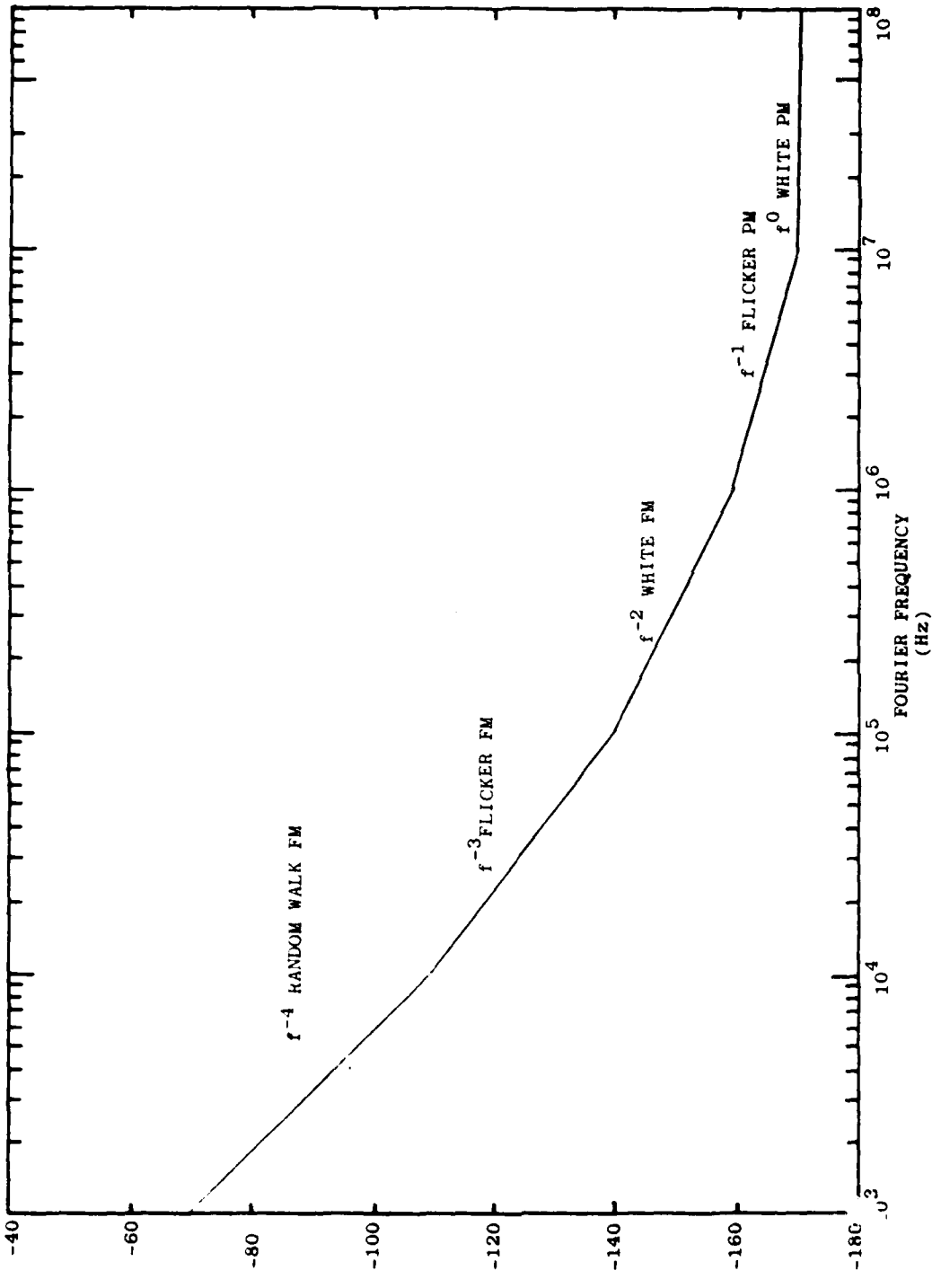

FIGURE 3.3.4.1
SINGLE SIDED PHASE NOISE SPECTRA

- Normally not a dominant factor.
- Often very close to the carrier and thereby very difficult to measure accurately.

b. Flicker FM (F^{-3})

- Related to physical resonances within the oscillator.
- Distinguished in very high quality oscillators like quartz resonator designs.
- Affected by electronic parts choices.

c. White FM (F^{-2})

- Generally the dominant noise characteristic.
- Found in oscillators with a high Q resonant element determining center frequency.

d. Flicker PM (F^{-1})

- May relate to physical resonance in the oscillator.
- Often caused by noisy components.
- May be contributed by amplifier or multiplier stages following oscillator.

e. White PM (F^{0})

- Broadband phase noise that has little or nothing to do with the resonance mechanism.
- Stages of amplification following resonator are generally responsible.

White noise, F^{0}, is lowered by good amplifier design practices. Increasing oscillator output and minimizing buffer gains provide the most significant improvements. F^{-1} noise

often is caused by device nonlinearities through which the carrier is phase modulated by low frequency noise. This device dependent characteristic may occur in the range of from 1 kHz to 1 MHz removed from carrier. A typical cause is carrier density fluctuations in the base resistance of a bipolar transistor. Flicker noise may be improved by rf feedback techniques, by bias stabilization, and by maintaining low input matching impedances at low frequencies.

Noise close in to the carrier (F^{-2}, F^{-3}, F^{-4}) increases due to the positive feedback at frequencies within the bandwidth of the resonator. A common expression for this noise is[18]

$$\Delta f_{RMS} = \frac{f_o}{Q} \sqrt{\frac{KTBF}{P_S}}$$

where:

KTBF = the thermal noise

P_S = signal power at input of active input

Q = loaded Q of feedback resonator

This simple expression shows that the oscillator noise density can be minimized by selecting a device with the lowest NF at the desired signal level and by designing a resonator with maximum loaded Q. The improvement of stability with increased Q will only occur if the source of instability is caused by circuit elements other than the resonator. If the instability is caused by temperature sensitivity or nonlinearities within the resonator, then increasing the Q_L will not improve oscillator stability as much as would be expected.

What really determines the high-Q resonator noise performance is not its narrow amplitude response but the rapid change in phase with frequency that accompanies it[19]. Any network with a phase-frequency response of sufficient slope could replace a high-Q resonator if its amplitude response is properly adjusted. Thus there are alternatives to the use of high-Q resonators in the design of low-noise oscillators.

Phase slope is the traditional parameter that determines an oscillator's stability[20]. Phase slope, if constant, can be defined as the ratio of the change in loop phase to the resulting change in oscillator frequency $\Delta\phi/\Delta f$, and is related to the Q_L of a single cavity or LC resonator by:

$$\frac{\Delta\phi}{\Delta f} = \frac{2Q_L}{f_o}$$

or stability is:

$$\frac{\Delta f}{f_o} = \frac{\Delta\phi}{2Q_L}$$

where: Δf is the change in oscillator frequency

$\Delta\phi$ is the phase shift in radians which causes the frequency change.

When the feedback path consists of a device other than a single cavity or LC resonator, such as a SAW delay line[21], an equivalent "Q" is used to represent the same phase slope as the circuit in question. The equivalent "Q" is the Q that a single LC circuit would have if it had the same phase slope as the circuit in question and it is useful in comparing methods of feedback. In a real oscillator there are several sources of

instability and Q is not a suitable parameter for analysis of the combined effects. It is more desirable to use group delay when analyzing the effects of all the components on overall frequency stability. A single LC resonator is related to the group delay by: $Q = \pi f_o \tau_R$

where τ_R= delay time or group delay of resonator, then

$$\frac{\Delta f}{f_o} = \frac{\Delta \phi}{2\pi f_o \tau_R}$$

The effects of all the major components of an oscillator, such as a resonator having delay τ_R, an amplifier having delay τ_A, and a matching network having delay τ_M with corresponding independent phase shifts of $\Delta\phi_R$, $\Delta\phi_A$, and $\Delta\phi_M$ is[22]:

$$\frac{\Delta f}{f_o} = \frac{\Delta \phi_R + \Delta \phi_A + \Delta \phi_M}{2\pi f_o(\tau_R + \tau_A + \tau_M)}$$

It is possible to show that the closed loop group delay is equal to the open loop group delay so that open loop measurements can be used for predicting overall closed loop stability. These equations do not apply during initial turn on, for frequency dependent parameters, and for nonlinearities such as AM to PM conversion.

3.3.5 Leeson's Oscillator Noise Model

The previous section presented insights from a somewhat physical point of view regarding the causes and effects of noise in oscillators. We now analyze performance from a more detailed viewpoint.

Leeson's oscillator model describes the phase noise in free-running oscillators[13,7]. The summary of considerable analysis and algebra is an expression for the single sided power spectral density.

$$S_{\phi}(f) = \frac{FKT}{2P_S}\left[f_{\alpha}\left(\frac{f_o}{2Q}\right)^2 f^{-3} + \left(\frac{f_o}{2Q}\right)^2 f^{-2} + f_{\alpha}f^{-1} + 1\right]$$

where:

F = device noise figure measured at operating level

P_S = device input signal power at center frequency

f_{α} = the frequency where flicker noise equals white noise

f_o = the oscillator center frequency

f = the noise modulation frequency

Q = loaded Q of feedback network

K = Boltzman's constant

T = Temperature = $290^{o}K$

The plot of this equation is shown in Figure 3.3.5-1 for the following UHF oscillator.

F = 10 dB

f_o = 300 MHz

Q = 50 and 100

P_S = 10 mW

f = 40 kHz

3.3.6 General Oscillator Noise Model

Leeson's simple model assumes the output is taken from the amplifier as follows:

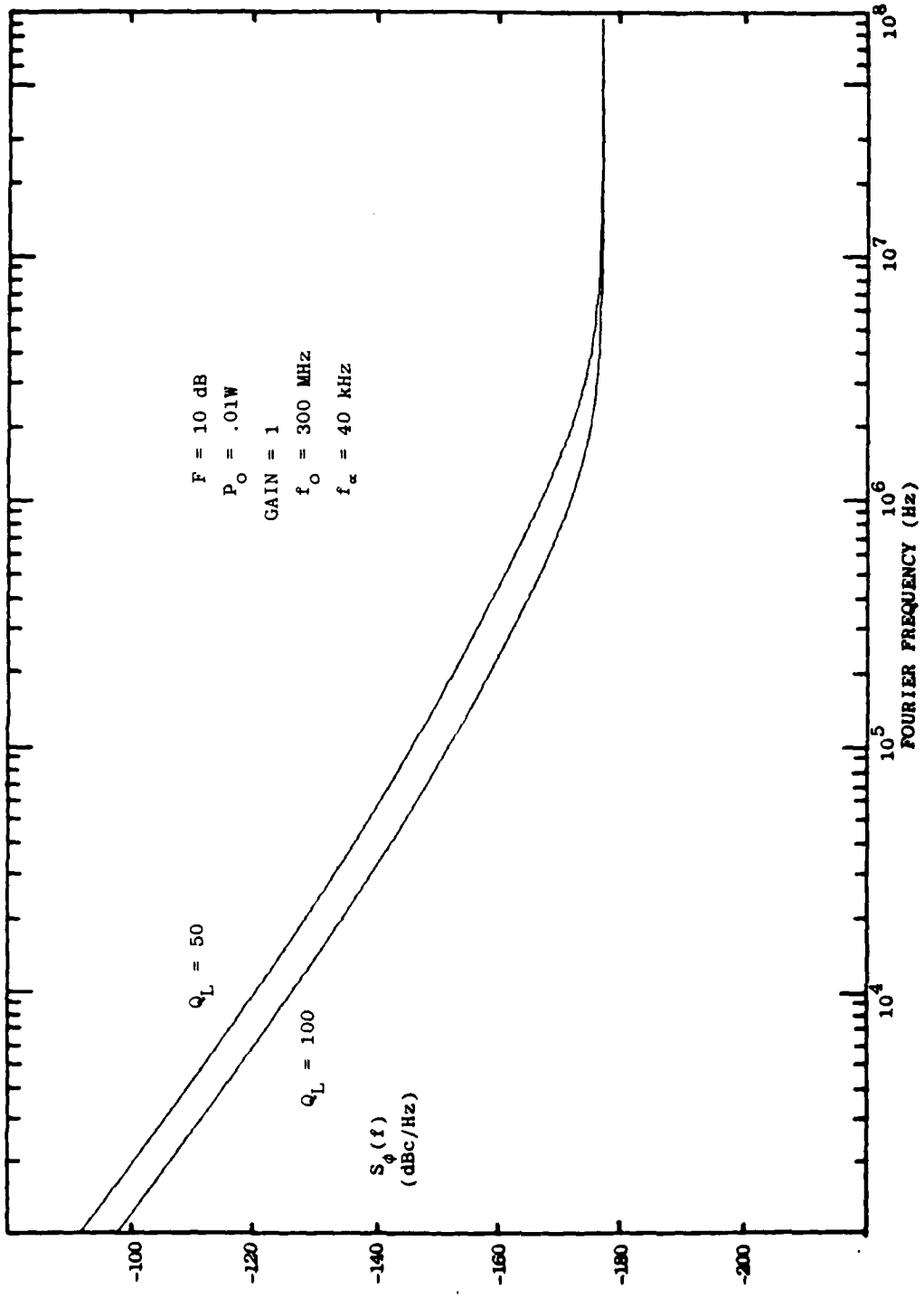

FIGURE 3.3.5.1
OSCILLATOR PHASE NOISE
LEESON'S SIMPLE MODEL

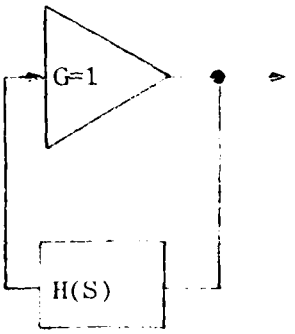

FIGURE 3.3.5.2
UNITY GAIN
OSCILLATOR MODEL

The model assumes a unity gain active device with a loss-less frequency selective network in the feedback path.

A more realistic model includes:

- An active stage that has gain greater than one,
- A frequency selective network that has finite loss,
- An adjustable feedback path that sets desired loop gain, and
- A tap for the output taken directly from the frequency selective network.

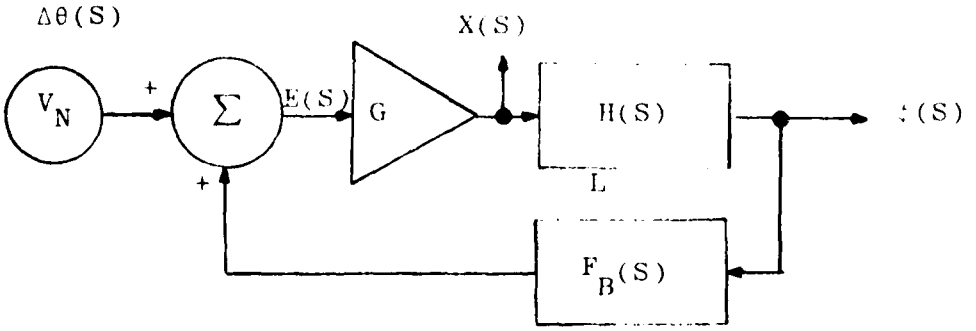

FIGURE 3.3.5.3
REALIZED OSCILLATOR MODEL

Where:

$H(S)$ = resonator transfer function
$F_B(S)$ = feedback transfer function
$E(S)$ = amplifier input
$\Delta\theta(S)$ = input phase noise
$\phi(S)$ = output phase noise
$X(S)$ = output phase noise for Leeson's model
G = power transfer of active stage (≥ 1)
L = power transfer of frequency selective network (≤ 1)

The analysis of this model leads to the following equation. The reader is referred to Appendix A for full mathematical development.

The single sided phase noise spectra is defined by

$$S_{\phi(f)} = \frac{FKT\ GL}{2P_o F_B} \left(\frac{f_o}{2Q_L}\right)^2 \left[\frac{f_\alpha}{f^3} + \frac{1}{f^2}\right]$$

Note the absence of both 1/f noise and flat noise when the output is referenced to the output of the filter. Assumption was made that the filter does not have floors in the region of interest.

A plot of this last equation is compared to measured test data in Figure 3.3.6-1. The oscillator measured was an experimental fixed tuned cavity oscillator.

3.3.7 Oscillator Model with Finite Filter Floor

The previous results are based on a single pole resonator with attenuation increasing at a slope of 6 dB per octave forever. But practical filters have finite attenuation floors, especially those designed for UHF. A low pass equivalent transfer function with a finite attenuation floor has the form:

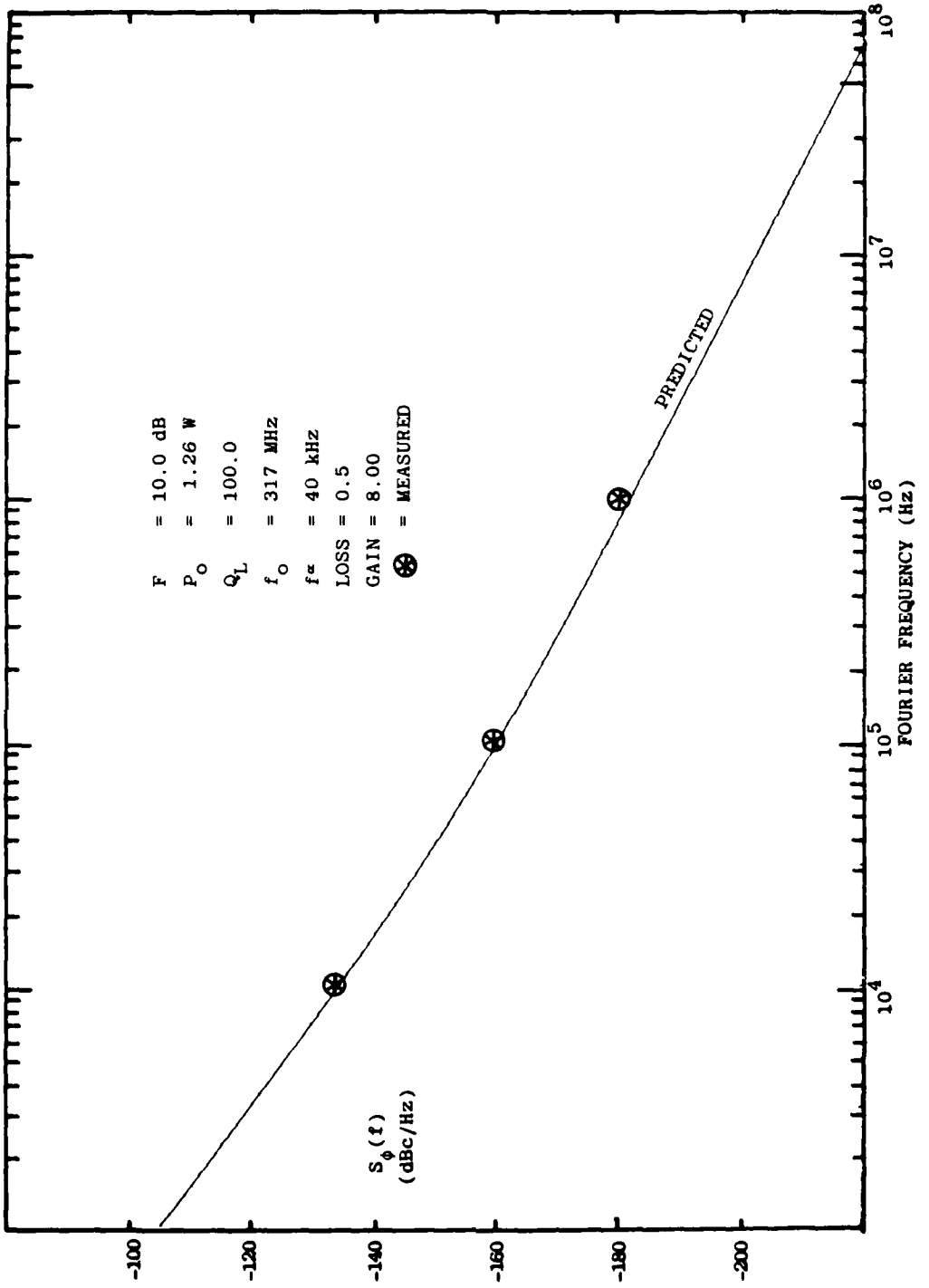

FIGURE 3.3.6.1 OSCILLATOR PHASE NOISE
LEESON's MODEL WITH GAIN AT FILTER OUTPUT
PREDICTED vs MEASURED

$$H(j\omega) = \sqrt{L}\left(\frac{\omega_1(j\omega+\omega_2)}{\omega_2(j\omega+\omega_1)}\right)$$

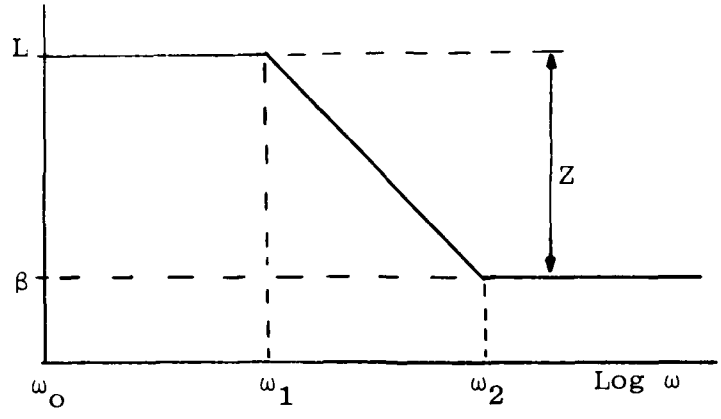

Where:

L = midband power loss of BPF

β = filter floor loss

Z = relative filter floor loss

$\omega_1 = \omega_o/2Q_L$

ω_2 = cutoff frequency where filter slope changes to unity

$Z^2 = \beta - L = 20 \log (\omega_2/\omega_1)$

$\frac{\omega_2}{\omega_1} = 10^{Z/20}$

The resultant single sided phase noise spectra is represented by the expression

$$S_{\phi(f)} = \frac{FKT\ G^2L^2}{2P_o(1 - 10^{-Z/20})^2}\left[f_\alpha\left(\frac{f_o}{2Q_L}\right)^2 f^{-3} + \left(\frac{f_o}{2Q_L}\right)^2 f^{-2} + f_\alpha 10^{-Z/10} f^{-1} + 10^{-Z/10}\right]$$

A plot of this equation is shown in Figure 3.3.7-1 for filter floors of 20, 30, and 40 dB.

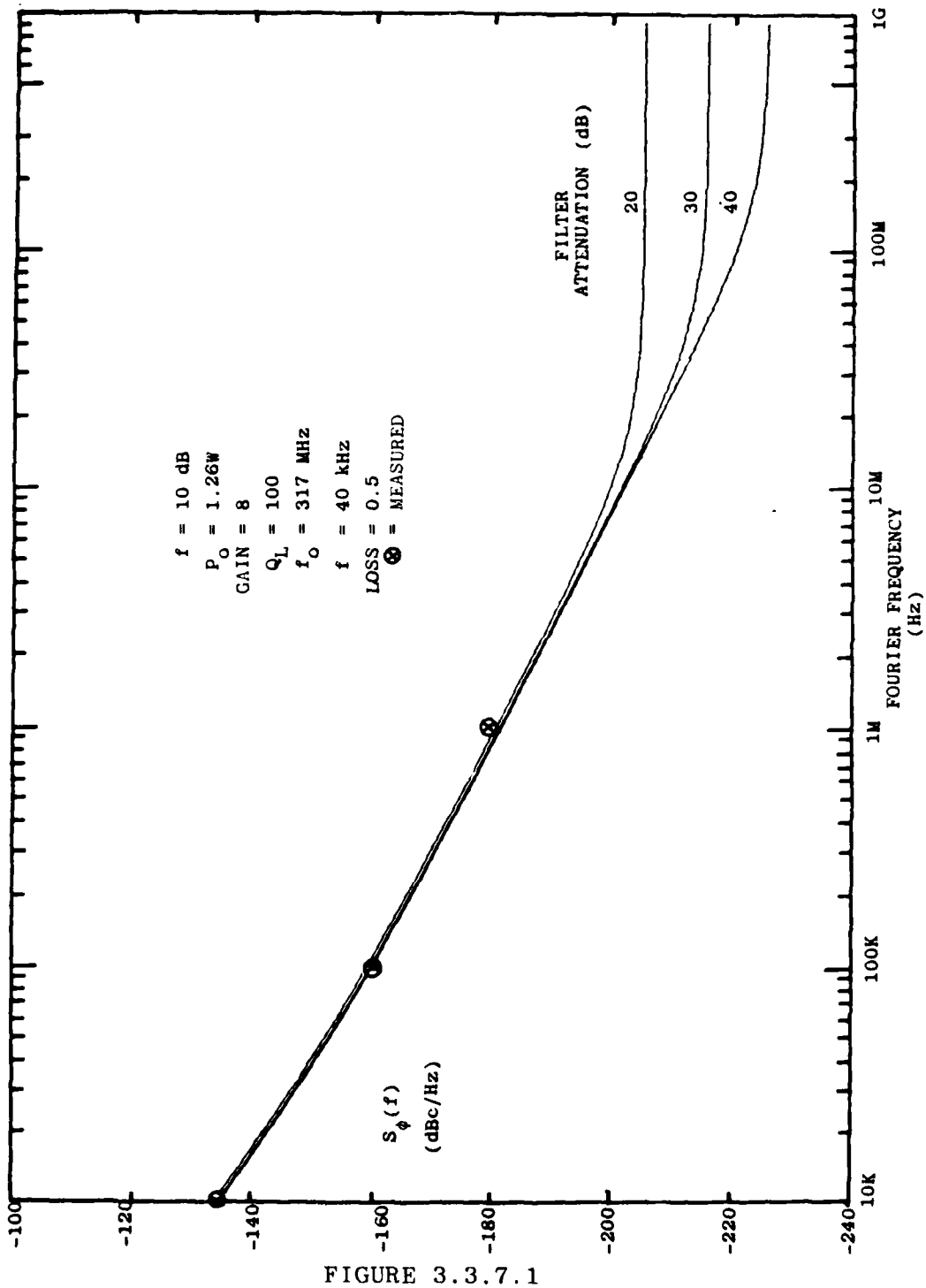

FIGURE 3.3.7.1
OSCILLATOR PHASE NOISE AT FILTER OUTPUT
WITH FINITE FILTER ATTENUATION

3.3.8 Oscillator Model with Buffer Stages

Generally a buffer amplifier is necessary to isolate the oscillator from non-ideal loads. Often the rf generator system must provide fully compliant signal purity into high VSWR loads. Most oscillator designs suffer significant frequency pulling effects if subjected to the infinite varieties of magnitude and phase angle provided by practical systems. A second need, in addition to VSWR isolation, is the increase of signal power such as in UHF transmitter applications. We now model our oscillator with a following amplifier with gain G_A noise figure F_A, flicker noise cutoff frequency $F_{\alpha A}$ and output power P_A.

The composite single sided phase noise spectral density is expressed by

$$S_{\phi(f)} = \frac{FKTG^2L^2}{2P_o(1-10^{-z/20})^2}\left[f_\alpha\left(\frac{f_o}{2Q_L}\right)^2 f^{-3}+\left(\frac{f_o}{2Q_L}\right)^2 f^{-2}+f_\alpha 10^{-z/10}+\right.$$

$$\left.10^{-z/10}\right] + \frac{F_A KT}{2P_o}\left[f_{\alpha A}\, f^{-1}+ 1\right]$$

This equation is plotted in Figure 3.3.8-1 for the case of a buffer amplifier with various values of noise figure.

This oscillator may be used with a high power amplifier in a transmitter, and, if the modulation does not add any noise, the relative phase noise spectral density is not degraded with higher output power.

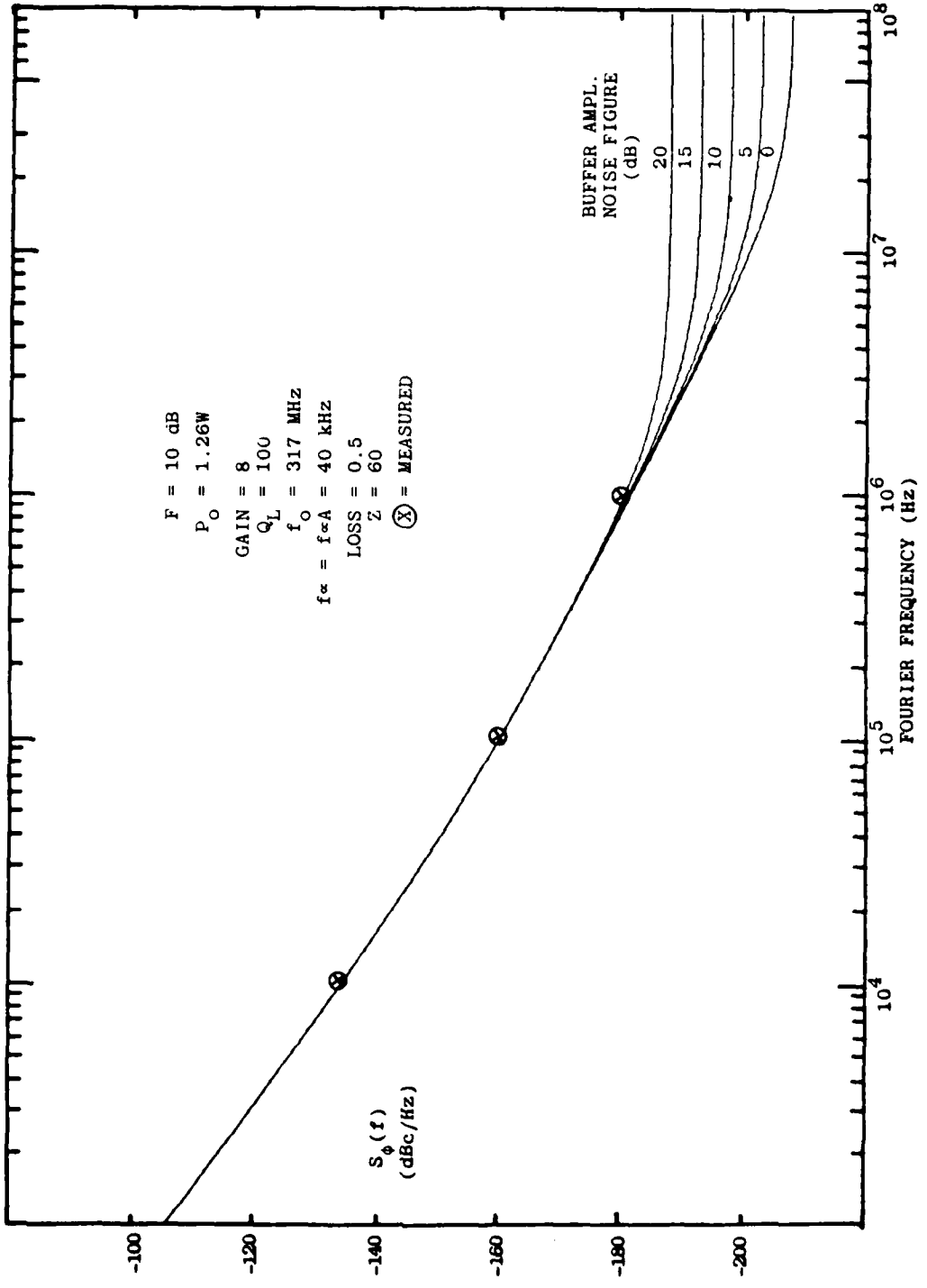

FIGURE 3.3.8.1
OSCILLATOR PHASE NOISE AT FILTER OUTPUT
WITH BUFFER AMPLIFIER AND FINITE FILTER ATTENUATOR

3.3.9 Effects of Nonlinearity

The oscillator noise models presented are based on linear operation. A practical nonlinear oscillator noise model has not been found during the literature search for this study. A derivation of noise in nonlinear oscillators is given in Reference 9., but does not even consider low frequency noise which modulates (or is translated to) the carrier frequency by nonlinear operation. The complexity of the problem may be emphasized when one considers the possible modes of limiting in a FET oscillator.[23] The amplitude of the oscillations can be limited by the supply voltage, by the I_{DSS} of the FET, or by the FET gain in UHF oscillators operating near the maximum frequency limits of the FET. Noise is increased when nonlinear junction capacities are periodically varied.

Previous authors [24] have increased the noise figure value to account for nonlinear mixing of noise. The excellent fit of the data implies that this degradation of the effective noise figure may well be an adequate description of the effect of nonlinearity.

3.4 Bias Considerations

The bias circuit and device circuit configuration are very important considerations for low noise oscillator design. The bias circuit should not add noise to the active device noise. The active device noise can be minimized by selecting a configuration that allows DC shorting at the device noise generator.

The active device will have nonlinearities which translate its 1/f noise to the carrier frequency in the oscillator. The level of 1/f noise is dependent on the external device termination at the device port associated with the equivalent noise generator. The noise figure of a transistor power amplifier

with 20 watts output can be improved from 30 dB to 20 dB, at 1 MHz from fc of 35 MHz, when the base has a low impedance at low frequency[25]. It may be assumed that an improvement might also be obtained with a FET when the gate is terminated in a low impedance at low frequency.

Components in the bias circuit should be selected so that noise is not added to the circuit. Usually, capacitors and inductors do not add any significant noise. But, resistors can have noise that is 30 dB above KTBR noise due to current noise. Current noise has a 1/f spectrum and depends primarily on the resistor material and construction. Also, it increases with current and resistance values[26]. The following table shows the relative noise levels of various resistor types:[27]

TABLE 3.4
RESISTOR NOISE LEVEL CONTRIBUTIONS

	Noise in dB/Decade
Bulk metal film	-50
Wirewound	-35
Evaporated metal film	-20
Cermet	+20
Carbon film	+20
Carbon composition	+30

The conclusion is that carbon or cermet type resistors should never be used in bias circuits for low noise amplifiers or oscillators.

3.5 Device Selection

A detailed trade study between various types of semiconductor devices is desirable. This trade study may be approached in at least three different ways:

1. Prediction of device performance based on device physics
2. Prediction of device performance based on manufacturer's data sheets
3. Test actual devices in an amplifier configuration at the desired operating point.

First, an approximate prediction of device noise performance is possible by knowing pertinent parameters of the internal device construction such as doping levels and critical dimensions. Such information is normally considered to be proprietary to the device manufacturers and would not be available. Therefore, performance predictions based on device physics will not be done in this trade study.

Secondly, the device performance could be compared by comparing information on manufacturers data sheets. The problem in making this device comparison is that the parameters required to predict high power performance are not in general included on manufacturers data sheets. Therefore, the only approach left is to obtain representative device samples and measure the required performance parameters.

3.6 Amplifier Design

A good starting point in the design of an oscillator is to follow established guide-lines for stable amplifier operation.

A description of a computer-aided design approach using both small signal and large signal device parameters was presented by Gonda[28] in which a circuit is built up step-by-step to meet performance objectives of: spurious free oscillation, output power, efficiency, electronic tuning range, and low FM noise. Unfortunately, this reference does not contain either the computer programs or sufficient detail to create the computer programs.

An example of a power transistor amplifier design using large-signal S-parameters at UHF is given in Reference 29. Measurement of large-signal S-parameters must be made with bias conditions similar to those in the intended circuit. The nonlinearity of the device at high drive levels generates harmonics which must be properly accounted for in the measurement.[30]

An example of a common gate FET oscillator, with a FET buffer amplifier, using a step-by-step design procedure based on S-parameters is given in Reference 31.

3.7 Cavity Interface

A high Q tuned circuit is required for this oscillator in order to obtain high power and low phase noise. Greater power output can be obtained for the same loaded Q by using a higher unloaded Q resonator. Phase noise may be lowered by using a higher loaded Q resonator.

In conventional discrete LC UHF oscillators, the Q of the inductor usually determines the resonator unloaded Q. However, high Q inductors can be synthesized by using a low loss transmission line, end tuned by a high Q capacitor.

Figure 3.7-1 shows the theory for the transmission line tuning approach. The basic transmission line equation for a lossless line gives the input impedance as:

$$Z_{in} = \frac{Z_o Z_1 + jZ_o^2 \tan\phi}{Z_o + jZ_1 \tan\phi}$$

where

ϕ = electrical length
Z_o = line impedance
Z_1 = load impedance

1. Prediction of device performance based on device physics
2. Prediction of device performance based on manufacturer's data sheets
3. Test actual devices in an amplifier configuration at the desired operating point.

First, an approximate prediction of device noise performance is possible by knowing pertinent parameters of the internal device construction such as doping levels and critical dimensions. Such information is normally considered to be proprietary to the device manufacturers and would not be available. Therefore, performance predictions based on device physics will not be done in this trade study.

Secondly, the device performance could be compared by comparing information on manufacturers data sheets. The problem in making this device comparison is that the parameters required to predict high power performance are not in general included on manufacturers data sheets. Therefore, the only approach left is to obtain representative device samples and measure the required performance parameters.

3.6 Amplifier Design

A good starting point in the design of an oscillator is to follow established guide-lines for stable amplifier operation.

A description of a computer-aided design approach using both small signal and large signal device parameters was presented by Gonda[28] in which a circuit is built up step-by-step to meet performance objectives of: spurious free oscillation, output power, efficiency, electronic tuning range, and low FM noise. Unfortunately, this reference does not contain either the computer programs or sufficient detail to create the computer programs.

with the proper choice of Φ and Z_1, Z_{in} will appear inductive even when Z_1 is capacitive. Since one side of capacitor C is referenced to ground, the effective inductance value may be changed by switching different capacitors onto the line with PIN diodes. This permits the oscillator frequency to be coarse tuned. Eight capacitors theoretically allow tuning to within 1 MHz over the 225 to 400 MHz band.

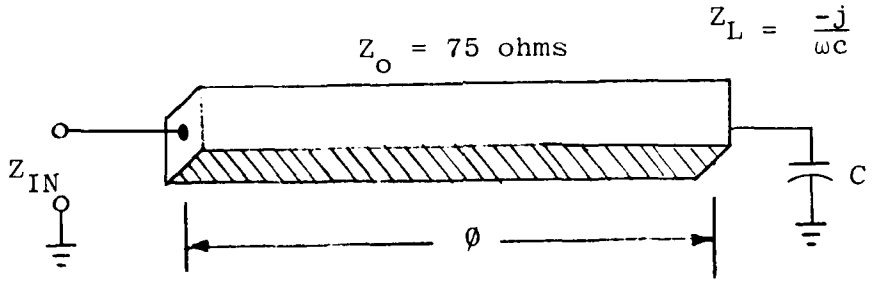

Figure 3.7-1 Synthesis of High Q Inductor

3.7.1 Resonator Implementation

Integration of the structures described with input and output coupling networks forms a usable high Q resonator. Because the resonant transmission lines are foreshortened by the capacitive loading of the tuning network, the resonators are directly analogous to those in a classical combline or similar structure.

Tuning is accomplished by switching the bias on the PIN diodes. The diodes are biased ON with a high forward current to achieve low series resistance. A high reverse bias voltage is used to permit large RF voltage excursions without forward biasing the part and increasing harmonic output levels. TTL logic levels are converted to the bias voltages required with a solid state driver. A look-up ROM is used to convert the frequency or tuning code to the filter bias code. Thus, the interface to any system is easily handled with standard logic circuits. Fine tuning can be accomplished with a conventional phase lock loop with the addition of a lightly coupled varactor diode to the tuning network.

Tuning speed is a function of driver switching speed, delay in the bias decoupling network, diode reverse carrier recovery time, and the settling time of the phase lock loop. Resonator switching times of less than 25 microseconds have been achieved to date with a simple decoupling network. Additional speed can be achieved at the expense of a power handling capability or insertion loss; however, the tuning time will ultimately be determined by the response time of the phase locked loop.

3.8 Load Isolation

Loads with changing VSWR, such as modulators, must be isolated from the VCO in order to prevent frequency pulling. Frequency pulling may be defined as the total frequency excursion observed as the VCO load of a specified VSWR varies over 180 electrical degrees.

VCO load isolation may be provided by either an attenuator or a buffer amplifier. An attenuator is not desirable since noise level is dependent on the NF of the stage following the VCO. A VCO and buffer amplifier would interface with a typical transceiver as shown in Figure 3.8-1.

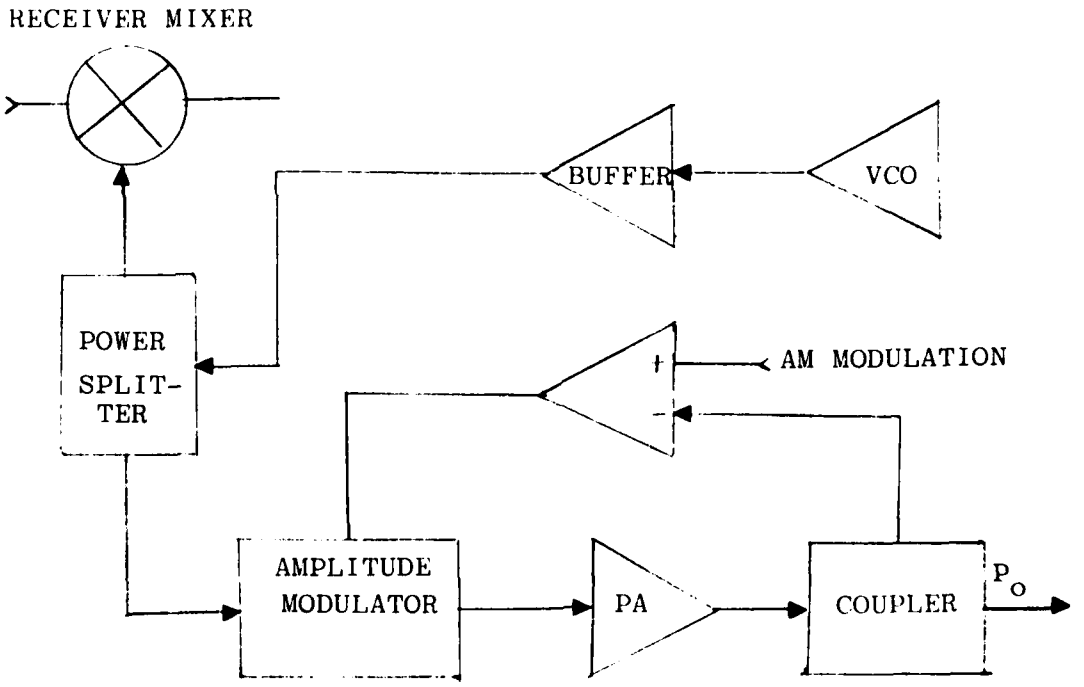

Figure 3.8.1 Functional Block Diagram
VCO Interface

Oscillator frequency pulling can be represented by a Rieke diagram[32] where lines of constant frequency roughly correspond to lines of constant reactance on a Smith chart and lines of constant power to lines of constant resistance. Therefore, load isolation may be designed to provide a specified frequency error and power change while avoiding loads which will cause oscillations to stop.

Given the maximum allowable source frequency deviation and load VSWR, the minimum amount of isolation may be calculated[33] as follows:

$$\text{Isolation} = 10 \log \left[\frac{3K}{\Delta F_{MAX}} \bullet \left(\frac{VSWR_L - 1}{VSWR_L + 1} \right) \right]$$

Where:

K = experimentally determined deviation factor, in H_z, that an oscillator xperiences when subjected to a standard mismatch of 2:1 rotated through all phases

ΔF_{MAX} = maximum allowable oscillator deviation

$VSWR_L$ = Maximum expected load VSWR

This experimental approach is applicable if an oscillator is available, but is not useful for prediction of isolation requirements before the oscillator is built. A better approach for prediction of isolation requirements may be derived from the effect of frequency pulling in an injection locked oscillator where a low level external signal is injected into the oscillator output port. This low level signal represents the reflected power from a mismatched load. The frequency change due to injection locking is:

$$\Delta F = \frac{f_o}{Q_L}\sqrt{\frac{P_i}{P_o}}$$

Where:

Q_L = loaded Q of oscillator resonator

f_o = center frequency

P_i = injection power or reflected power from load

P_o = oscillator forward power

since

$$\frac{P_i}{P_o} = \left(\frac{VSWR_L - 1}{VSWR_1 + 1}\right)^2$$

$$\Delta F = \frac{f_o}{Q_L}\left(\frac{VSWR_L - 1}{\sqrt{VSWR_L} + 1}\right)$$

and the maximum tolerable load VSWR for a given ΔF_{MAX} is:

$$VSWR_L\Big|_{MAX} = \frac{1 + \Delta F_{MAX} Q_L / f_o}{1 - \Delta F_{MAX} Q_L / f_o}$$

If the actual load VSWR is greater than $VSWR_{L\ MAX}$ then additional isolation is required. The additional isolation may be derived as follows:

$$\text{let } \rho = \frac{VSWR - 1}{\sqrt{VSWR} + 1}$$

$$\Delta F = \frac{f_o}{Q_L}\ \rho\ ,\ \rho = \frac{\Delta F Q_L}{f_o}$$

The return loss, RL, with isolation is:

$$RL = RL_{load} + 2\ (\text{Isolation})$$

$$\text{Isolation} = \frac{RL}{2} - \frac{RL_L}{2} = 10 \log \frac{1}{\rho} - 10 \log \frac{1}{\rho_L}$$

$$\text{Isolation} = 10 \log \left(\frac{f_o}{\Delta F Q_L}\right) - 10 \log \left(\frac{VSWR_L+1}{VSWR_L-1}\right)$$

$$\text{Minimum Isolation} = 10 \log \left[\left(\frac{f_o}{\Delta F_{MAX} Q_L}\right) \left(\frac{VSWR_L-1}{VSWR_L+1}\right)\right]$$

For example:

$VSWR_L = 2:1$

$f_o = 400$ MHz

$Q_L = 100$

$$\text{Isolation} = 10 \log \left[\frac{4X10^8}{\Delta F_{MAX} 100} \left(\frac{1}{3}\right)\right]$$

$$= 61.3 - 10 \log (\Delta F_{MAX})$$

if $\Delta F_{MAX} = 10$ kHz

Isolation = 21.3 dB

4.0 DESIGN TRADE-OFFS

Three different approaches to implementing the high power VCO in hardware have been considered. One method was chosen for further development and test. In this section the three approaches are described, data presented and the reasons for the choice of one method discussed.

4.1 Cavity Oscillator

The original oscillator work on which this contract is based was performed by E-Systems, ECI Division in 1977. The experimental oscillator developed at that time was of the cavity oscillator type. The cavity is utilized as a high-Q tuned circuit with the active device an integral part.

The original experimental oscillator hardware was fixed tuned, but was modified under this contract to variable mechanical tuned and electrical switched tuned. The tuning range of the variable tuned oscillators was limited, with amplitude variations within the operating frequency band as shown in Fig. 4.1.1. The original noise data was repeated in the mechanical tuned versions, but electrical tuning degraded noise performance as shown in Fig. 4.1.2.

A second model of the cavity oscillator was constructed which also revealed tuning and start-up problems. Most of these problems were traced to device dependent parameters and the difficulty of matching the VMOS FET device to the cavity across a wide band.

Because of the unreliable oscillator performance, this approach to a broadband oscillator was rejected.

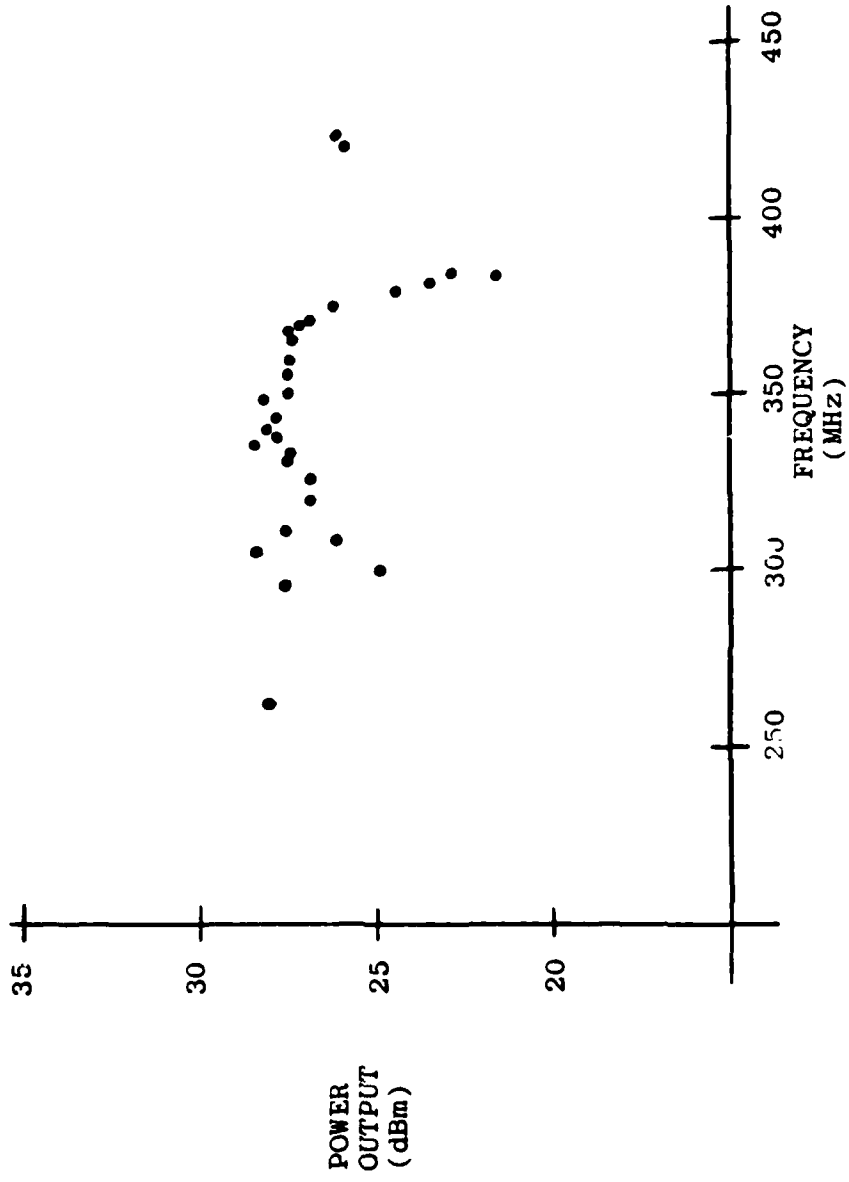

FIGURE 4.1.1.1·
AMPLITUDE VARIATIONS OF
CAVITY TUNED OSCILLATOR

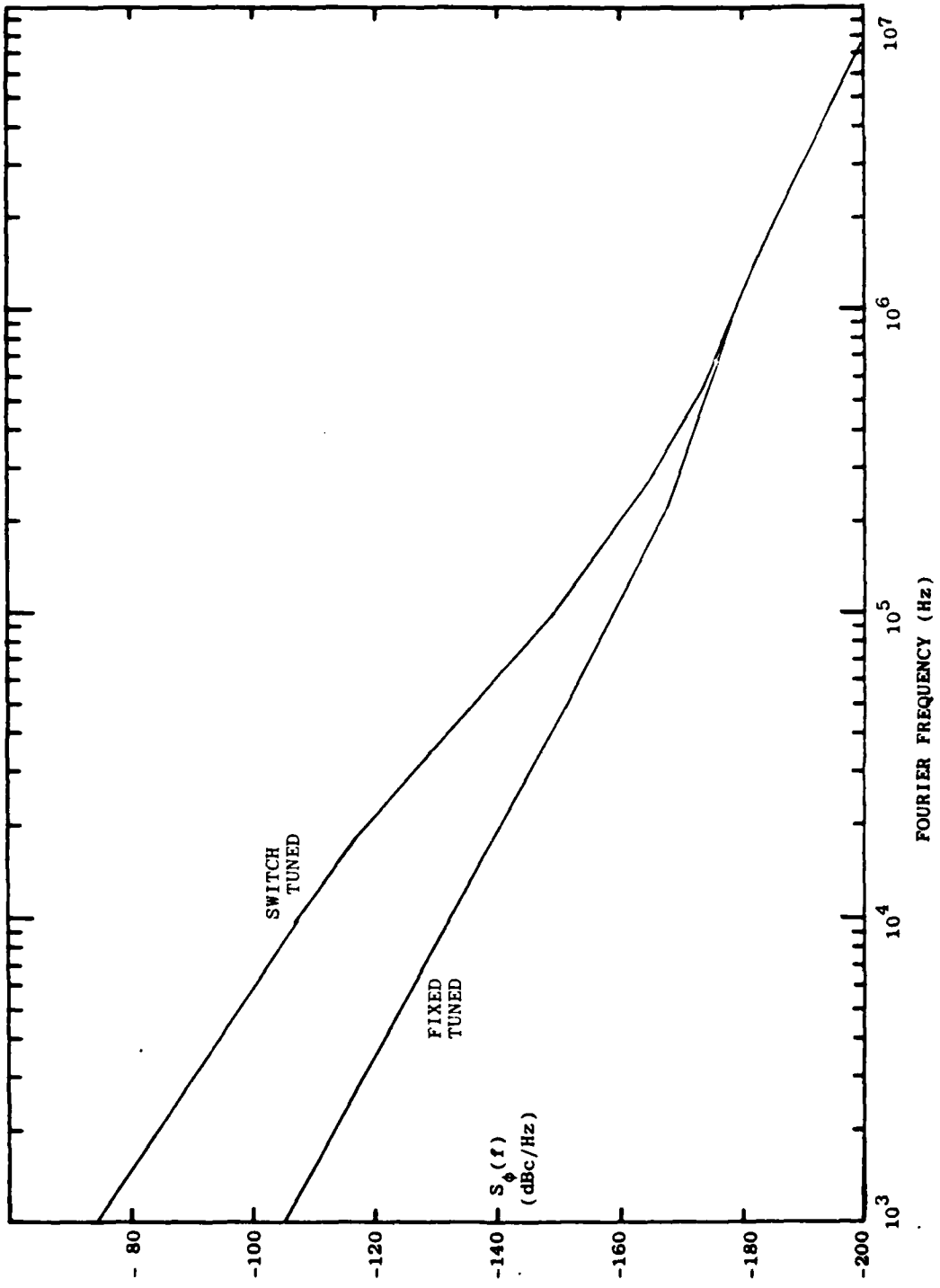

FIGURE 4.1.2
NOISE PERFORMANCE OF FIXED
TUNED vs SWITCHED TUNED OSCILLATOR

4.2 LC (Negative Impedance) Oscillator

An intensive investigation of the S parameters of different FET devices was conducted, including the Motorola EV-1 and EV-3 transistors and the CTC-CF4 transistors. The need for this evaluation was addressed in section 3.5, and some parameters of the devices are presented in Table 4.2.1.

The investigation revealed that all devices exhibit a negative S_{22} (output impedance). These devices, when terminated in reactive loads matched to the device, will oscillate at high power with low noise output. The load can be a lumped LC network or a high-Q cavity which is switched tuned to control oscillator frequency. Noise performance on several circuits is shown in Fig. 4.2.1.

The approach offers some interesting possibilities for size reduction and simplicity in the oscillator, but suffers from several problems. One is in coupling the active device to the high-Q load, and in extracting the power from the device. Transistors with large reverse transfer capacity (S_{12}) seem to work best in this respect. Another problem is that the output frequency is as much device dependent as circuit dependent. Thus, devices must be carefully measured and device parameters identified for selection, and the possibility of degraded temperature performance exists. For these reasons this method of oscillator design was rejected.

TABLE 4.2.1
V_{MOS} DEVICE PARAMETERS

A) COMMON SOURCE S-PARAMETERS
MOTOROLA EV-1 S/N #65

BIAS: 15V @100 ma

	S11		S12		S21		S22	
FREQ (MHz)	dB	DEGREES	dB	DEGREES	dB	DEGREES	dB	DEGREES
225	-1.9	-143°	-23.2	-66°	8.0	7°	-5.2	-130°
265	-1.8	-161°	-23.8	-86°	6.8	-16°	-5.2	-141°
305	-1.6	-167°	-24.8	-99°	4.4	-34°	-4.5	-153°
345	-1.6	-171°	-25.5	-110°	3.5	-48°	-3.6	-153°
385	-1.8	-177°	-26.0	-121°	2.2	-66°	-3.8	-154°

BIAS: 15V @200 ma

225	-2.0	-147°	-23.6	-64°	8.8	8°	-5.5	-136°
265	-1.9	-162°	-24.3	-83°	6.8	-15°	-5.6	-146°
345	-1.6	-171°	-25.9	-107°	3.7	-49°	-4.4	-155°
385	-1.9	-177°	-26.3	-117°	2.8	-65°	-4.1	-155°

BIAS: 15V @300ma

224	-2.1	-150°	-24.3	-62°	8.4	8°	-5.6	-141°
265	-1.9	-164°	-24.7	-81°	6.7	-15°	-5.8	-150°
305	-1 7	-170°	-25.4	-93°	5.1	-34°	-5.0	-158°
345	-1.6	-173°	-25.8	-104°	4.0	-48°	-4.1	-157°
385	-1.9	-179°	-26.2	-115°	3.3	-65°	-4.2	-150°

B) COMMON SOURCE S-PARAMETERS
MOTOROLA EV-1 S/N #67

BIAS: 15V @200 ma

	S11		S12		S21		S22	
FREQ (MHz)	dB	DEGREES	dB	DEGREES	dB	DEGREES	dB	DEGREES
225	-1.8	-143°	-23.7	-69°	8.1	9°	-5.1	-140°
265	-1.7	-159°	-24.3	-86°	6.5	-12°	-5.2	-148°
305	-1.5	-165°	-25.4	-100°	4.8	-32°	-4.5	-159°
345	-1.4	-170°	-26.0	-110°	3.6	-48°	-3.5	-157°
385	-1.7	-177°	-26.3	-121°	2.9	-64°	-3.7	-156°

TABLE 4.2.1
V_{MOS} DEVICE PARAMETERS (Contd)

C) COMMON GATE S-PARAMETERS
MOTOROLA EV-1 S/N #66

BIAS: 15V @150 ma

	S11		S21		S12		S22	
FREQ (MHz)	dB	DEGREES	dB	DEGREES	dB	DEGREES	dB	DEGREES
225	-3.4	-172°	4.9	-106°	-14.8	-34°	1.8	-65°
245	-3.4	-175°	5.1	-121°	-14.8	-48°	2.4	-70°
265	-3.4	-177°	5.1	-136°	-15.2	-61°	2.6	-79°
285	-3.2	-177°	4.7	-150°	-15.9	-70°	2.8	-85°
305	-2.6	-182°	4.2	-166°	-16.7	-76°	3.0	-97°
325	-2.2	-175°	3.9	170°	-17.5	-81°	3.3	-100°
345	-1.8	171°	3.8	164°	-18.2	-83°	3.5	-105°
365	-1.7	169°	3.7	150°	-18.7	-83°	3.5	-108°
385	-1.3	163°	3.8	136°	-19.0	-79°	3.6	-112°

BIAS: 15V @300 ma

225	-3.2	-177°	4.7	-107°	-16.2	-34°	1.4	-68°
245	-3.3	-180°	5.0	-121°	-16.2	-44°	2.0	-76°
265	-3.2	-182°	4.9	-137°	-16.6	-55°	2.4	-80°
285	-2.9	176°	4.6	-152°	-17.3	-63°	2.8	-89°
305	-2.5	173°	4.3	-165°	-18.0	-68°	3.0	-98°
325	-2.2	170°	4.1	-171°	-18.6	-71°	3.1	-102°
345	-1.9	166°	4.1	171°	-19.0	-72°	3.3	-106°
365	-1.5	162°	4.0	158°	-19.2	-70°	3.3	-110°
385	-1.3	158°	4.1	146°	-18.4	-66°	3.4	-113°

D) COMMON SOURCE S-PARAMETERS
CTC CF4-28 S/N #3

BIAS: 15V @100 ma

	S11		S12		S21		S22	
FREQ (MHz)	dB	DEGREES	dB	DEGREES	dB	DEGREES	dB	DEGREES
225	-2.1	-148°	-20.4	-87°	5.8	24°	-2.7	-142°
265	-1.9	-161°	-21.1	-107°	4.1	3°	-2.7	-152°
305	-1.6	-166°	-22.0	-123°	1.8	-15°	-2.4	-163°
345	-1.4	-169°	-23.3	-135°	.4	-28°	-1.9	-162°
385	-1.6	-174°	-23.7	-147°	-.4	-42°	-2.2	-163°

BIAS: 15V @200 ma

225	-2.0	-148°	-22.3	-84°	7.4	0°	-3.2	-152°
265	-1.8	-156°	-23.1	-103°	5.6	-20°	-3.3	-162°
305	-1.5	-158°	-24.5	-117°	3.4	-37°	-2.9	-172°
345	-1.3	-158°	-25.2	-128°	2.7	-50°	-2.5	-171°
385	-1.5	-161°	-25.5	-139°	1.2	-63°	-2.8	-172°

TABLE 4.2.1
V_{MOS} DEVICE PARAMETERS (Contd)

D) COMMON SOURCE S-PARAMETERS
CTC CF4-28 S/N #3 (Contd)

BIAS: 15V @300 ma

	S11		S12		S21		S22	
FREQ (MHz)	dB	DEGREES	dB	DEGREES	dB	DEGREFS	dB	DEGREES
225	-2.4	-158°	-24.1	-82°	8.4	0°	-3.2	-154°
265	-2.1	-169°	-25.0	-98°	6.7	-14°	-3.3	-169°
305	-2.0	-173°	-26.3	-111°	4.5	-36°	-2.9	-178°
345	-1.6	-175°	-26.9	-120°	3.2	-44°	-2.5	-176°
385	-1.8	-180°	-27.2	-130°	2.8	-630°	-2.4	-177°

E) COMMON GATE S-PARAMETERS
CTC CF4-28 S/N #3

BIAS: 20V @100 ma

	S11		S12		S21		S22	
FREQ (MHz)	dB	DEGREES	dB	DEGREES	dB	DEGREES	dB	DEGREES
225	-3.4	174°	-13.9	-63°	4.9	-141°	1.9	-70°
265	-3.4	174°	-13.3	-81°	5.0	-161°	2.9	-78°
305	-3.2	181°	-13.7	-110°	4.5	167°	3.0	-102°
345	-3.1	180°	-14.4	-127°	3.9	146°	3.3	-108°
385	-3.2	174°	-14.4	-143°	4.2	124°	3.7	-115°
BIAS 20V @200 ma								
225	-2.5	172°	-15.4	-62°	5.2	-138°	1.8	-67°
265	-2.5	172°	-15.0	-79°	5.3	-157°	2.9	-75°
305	-2.4	178°	-15.3	-105°	5.0	172°	3.0	-47°
345	-2.4	176°	-16.2	-170°	4.5	151°	3.1	-103°
385	-2.4	170°	-16.2	-134°	4.7	129°	3.5	-109°
BIAS 20V @200 ma								
225	-2.1	172°	-16.1	-67°	5.2	-138°	1.7	-66°
265	-2.2	172°	-15.9	-74°	5.3	-156°	2.5	-74°
305	-2.0	177°	-16.3	-104°	5.0	174°	2.6	-96 °
345	-2.0	175°	-17.2	-118°	4.8	153°	3.0	-102°
385	-2.0	169°	-17.2	-129°	4.9	131°	3.4	-107°

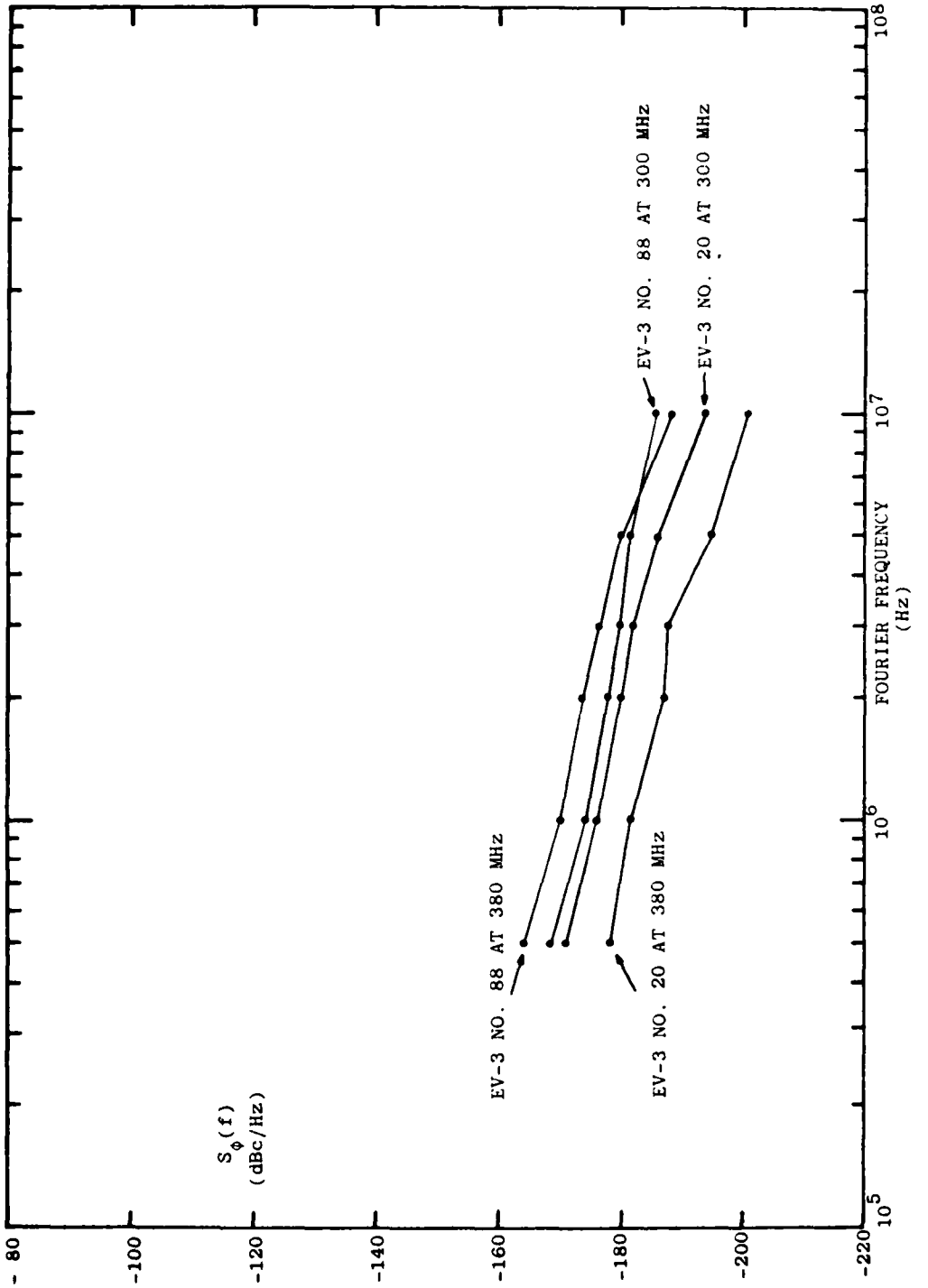

FIGURE 4.2.1
NEGATIVE IMPEDANCE OSCILLATOR
NOISE PERFORMANCE

4.3 Transmission Line Oscillator

Section 3.1 discusses the use of an amplifier with a feedback network as an oscillator. The noise performance of such an oscillator is discussed in Section 3.3, with the concept of phase slope introduced in 3.3.4. The oscillator chosen for detailed testing on this project is of this design. This method of low noise amplifier/high-Q filter/high phase slope produces an oscillator which is low in noise, relatively independent of active device parameters, and tunable over the entire band with nearly constant high output power. The physical implementation of this oscillator is far more straight-forward and predictable than the previous two methods, and thus has been chosen for the final oscillator construction and testing.

See Fig. 5.2.1b for a block diagram of the electrical configuration. A low noise VMOS FET amplifier is followed by a high power dual amplifier. The circuit drives a high "Q" 2 pole filter to provide the output frequency. Part of the output signal is fed back to the input of the FET amplifier through a phase shifter. The phase shifter has over 360^{o} tuning range, and adjusts total loop phase to 0^{o}, a criterion for oscillation.

A schematic diagram of the oscillator gain stages is shown in Fig. 4.3.1. R.F. drive from the phase shifter is connected to the resistive attenuator at the input to the VMOS amplifier. Q3 is a VMOS field effect transistor. T1 and C3 provide gate input matching from 50 ohms. L4, C4, C5 and C6 output match the FET drain to 50 ohms. Q1 and Q2 form a d.c. switch commanded from control line BO that allows the B+ on the Buffer Q3 to be varied.

The Buffer Amplifier output is connected to the input of the dual power amplifier. See Fig. 4.3.1a. The bias on the

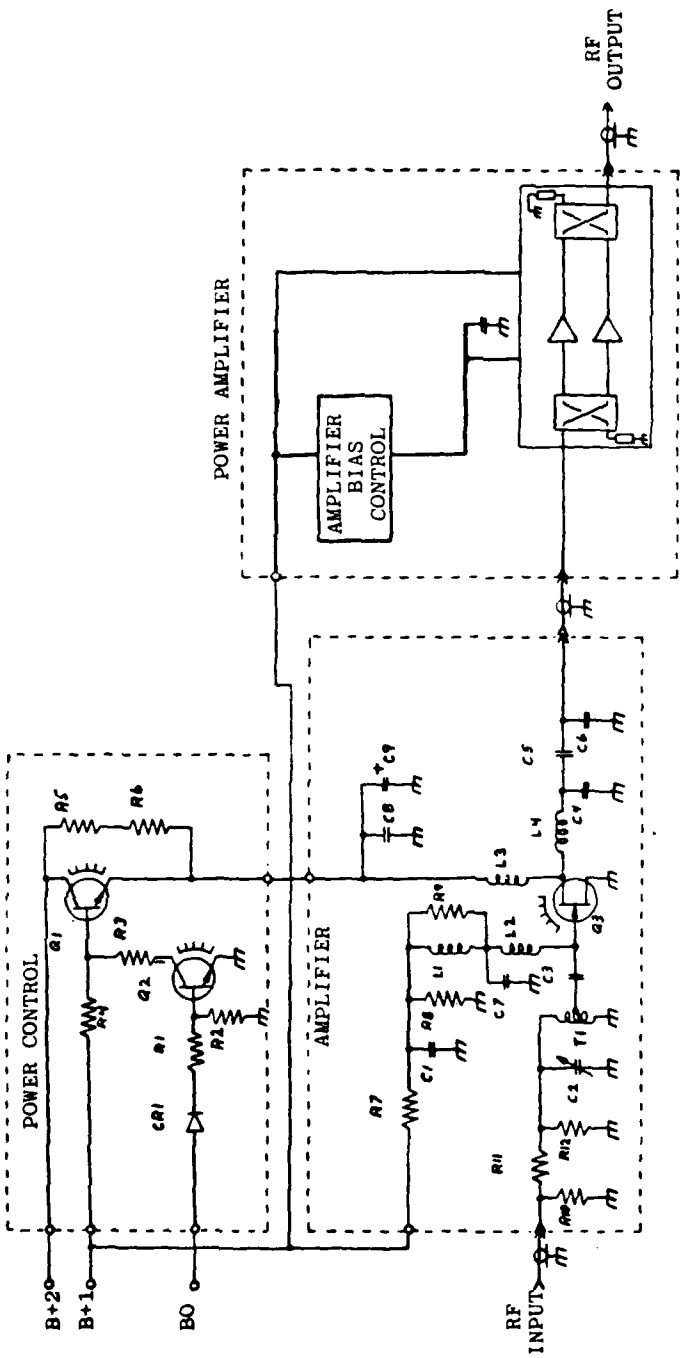

FIGURE 4.3.1
OSCILLATOR GAIN STAGE
SCHEMATIC DIAGRAM

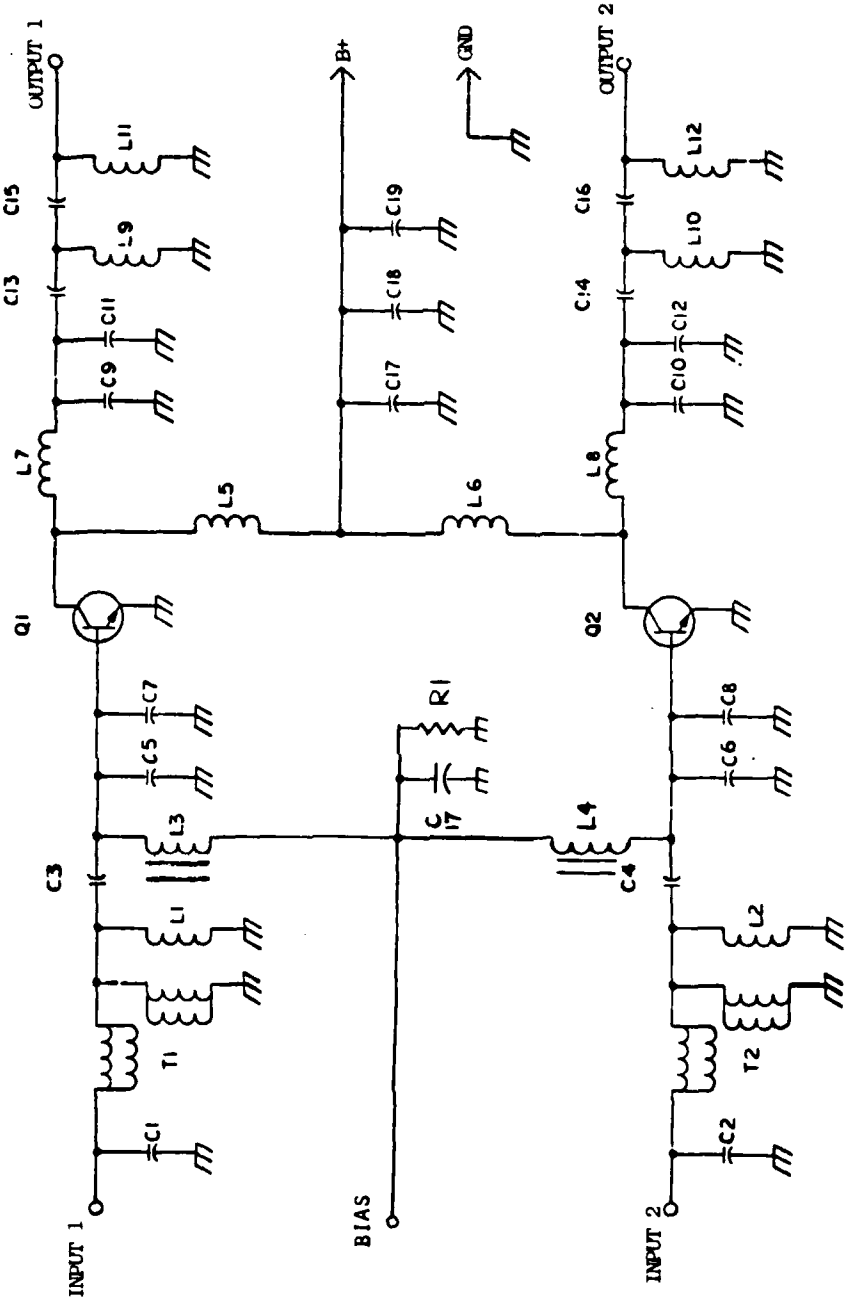

FIGURE 4.3.1a
HIGH POWER DUAL AMPLIFIER
SCHEMATIC DIAGRAM

dual is controlled by a temperature sensitive circuit that compensates for ambient temperature changes in the amplifier heat sink.

The Tunable Cavity schematic diagram is shown in Fig. 4.3.2. R.F. from the gain stages is connected to the cavity input transformer T1A. The cavity is tuned by selecting one or more capacitors (C1, C4, C5, C8, C9 . . . C36) to produce the desired amplitude and phase response. This is accomplished by controlling the bias applied to PIN diodes CR1 through CR18. L1 through L18 R.F. decouple the bias applied to the PIN diodes to prevent spurious filter operation. Transformer T1B couples the filtered R.F. energy out of the cavity.

The schematic diagram for the Phase Shifter is shown in Fig. 4.3.3. H1, H2 and H3 are 90° quadrature hybrids. Hybrid H1 in conjunction with coaxial lines L1 - L12 and CR1 - CR10 provides the selectable phase shift depicted in Fig. 4.3.3a. CR1 through CR10 are PIN diodes. Phase shift is controlled by "turning on" the appropriate pairs of diodes to produce the desired delay. Hybrid H2 and diodes CR11 and CR12 operate in a similar manner to produce an additional phase shift as shown in Fig. 4.3.3.b. The circuit of Hybrid H3 and varactor diodes CR13 through CR16 provide the analog phase shift as shown in Fig. 4.3.3.c.

Not only does the two pole filter provide amplitude selection and filtering of wideband noise, but it also provides a large phase vs. frequency slope. It is this slope which provides excellent noise performance, and data discussed later in this report indicates that improving the slope improved noise.

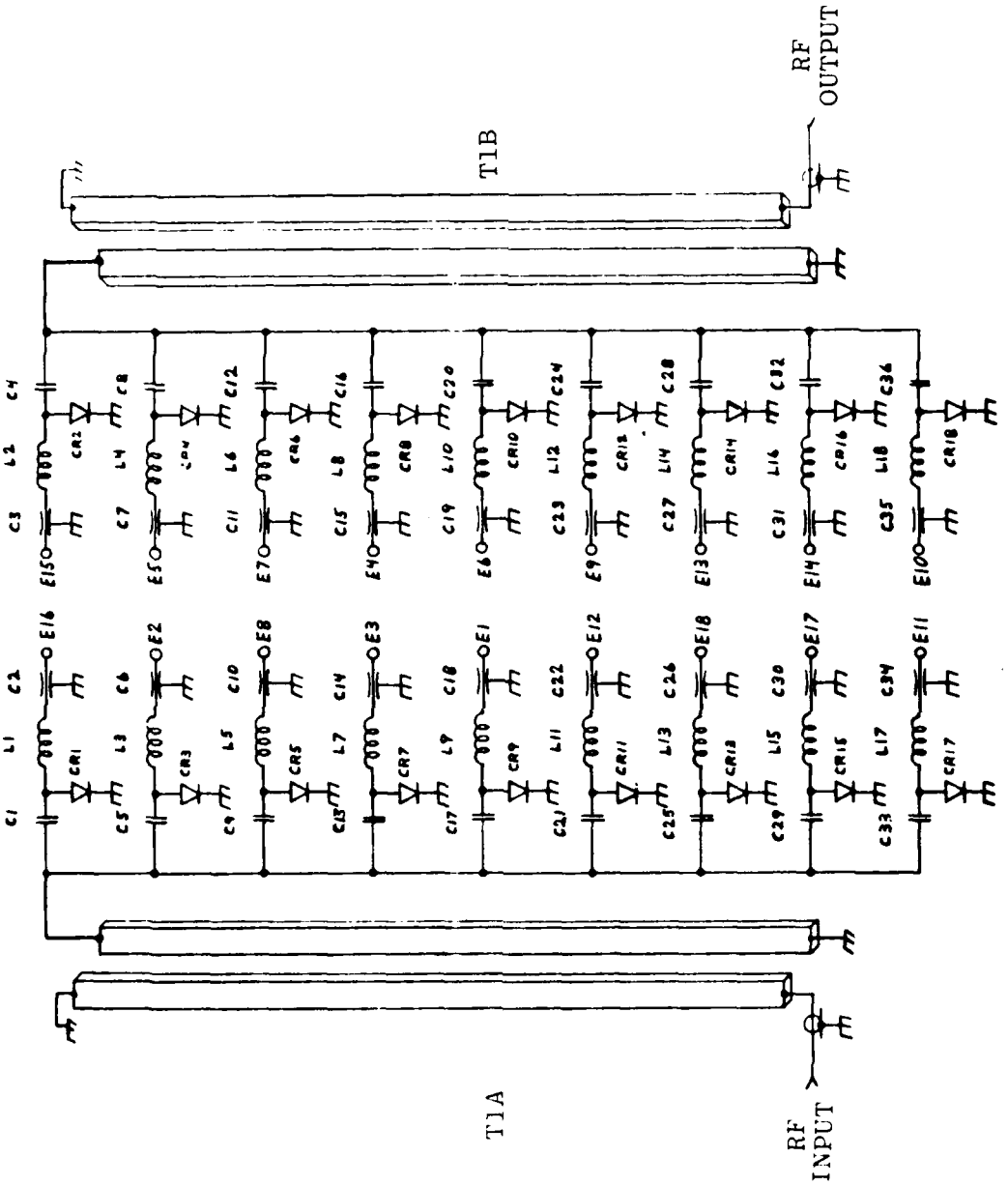

FIGURE 4.3.2
TUNABLE CAVITY
SCHEMATIC DIAGRAM

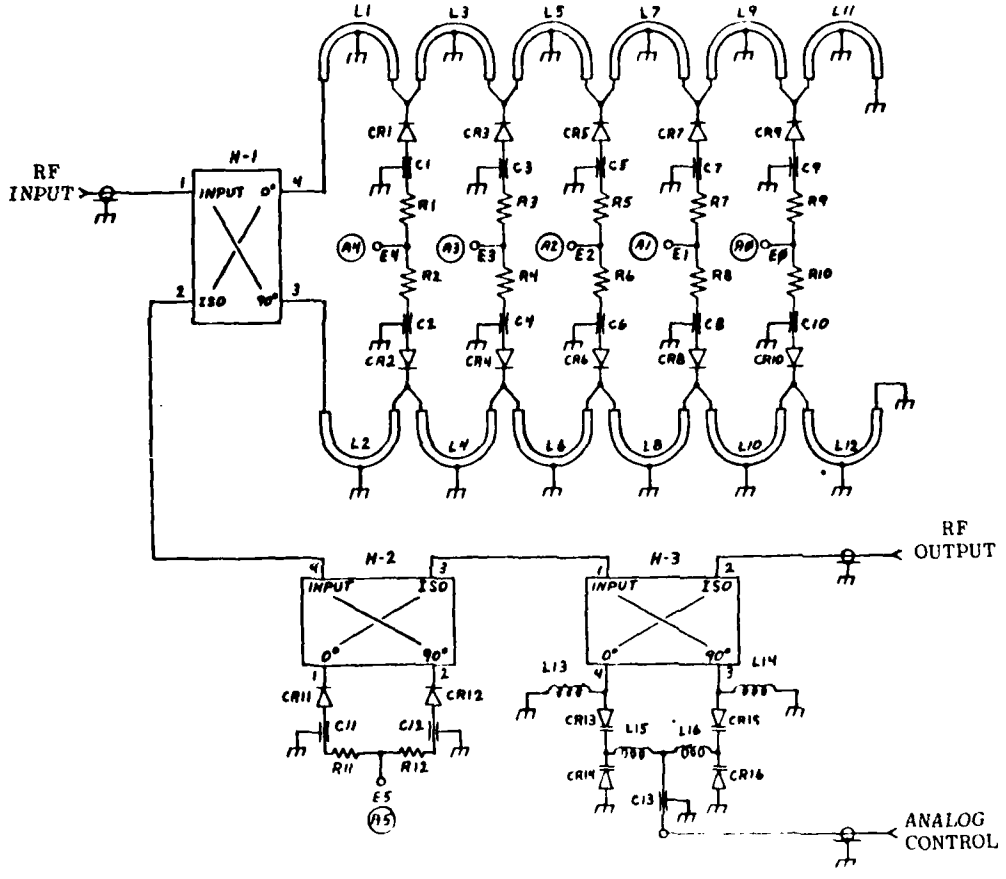

FIGURE 4.3.3
PHASE SHIFTER
SCHEMATIC DIAGRAM

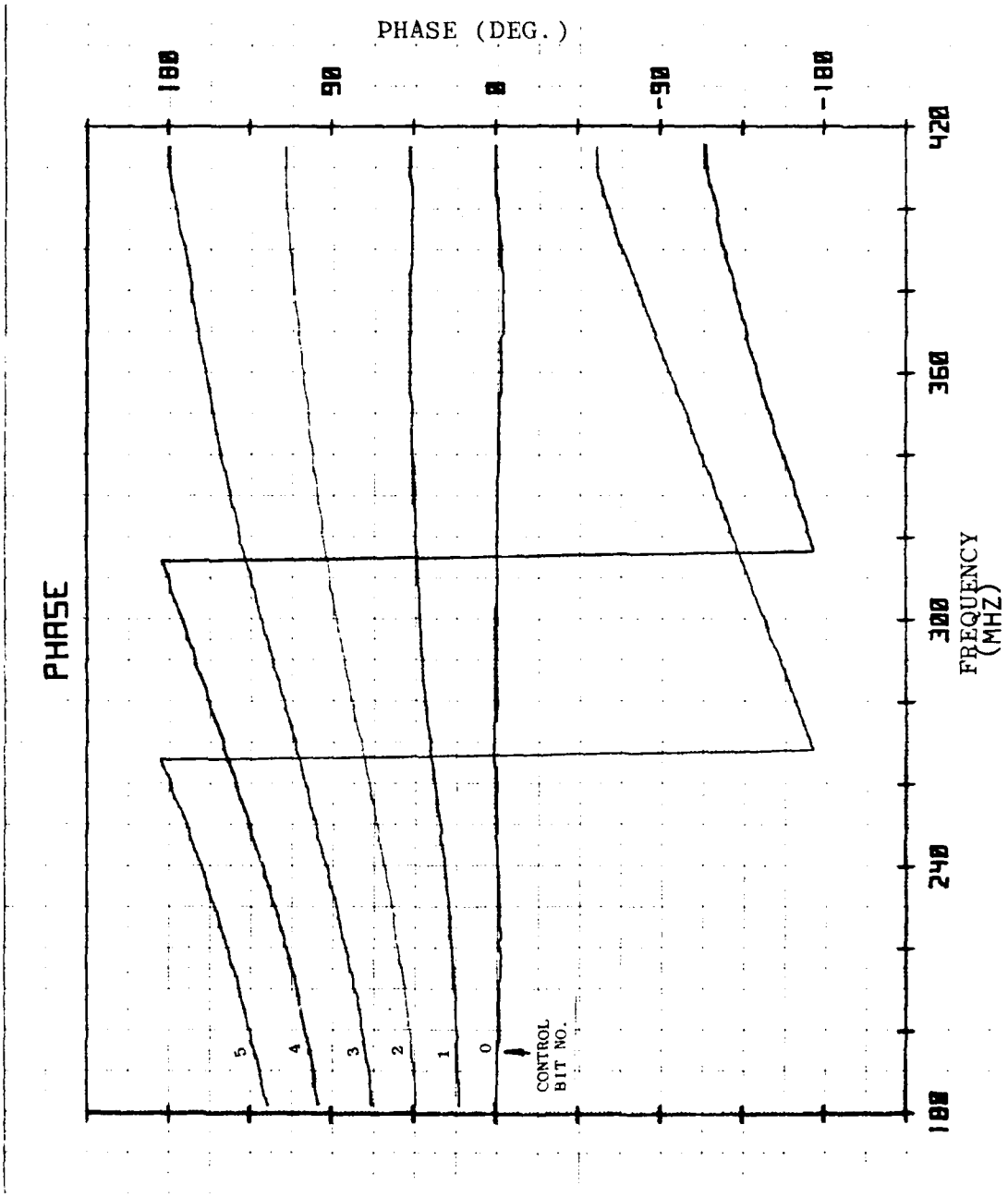

FIGURE 4.3.3a
PHASE SHIFT vs FREQUENCY,
6 BIT PHASE SHIFTER

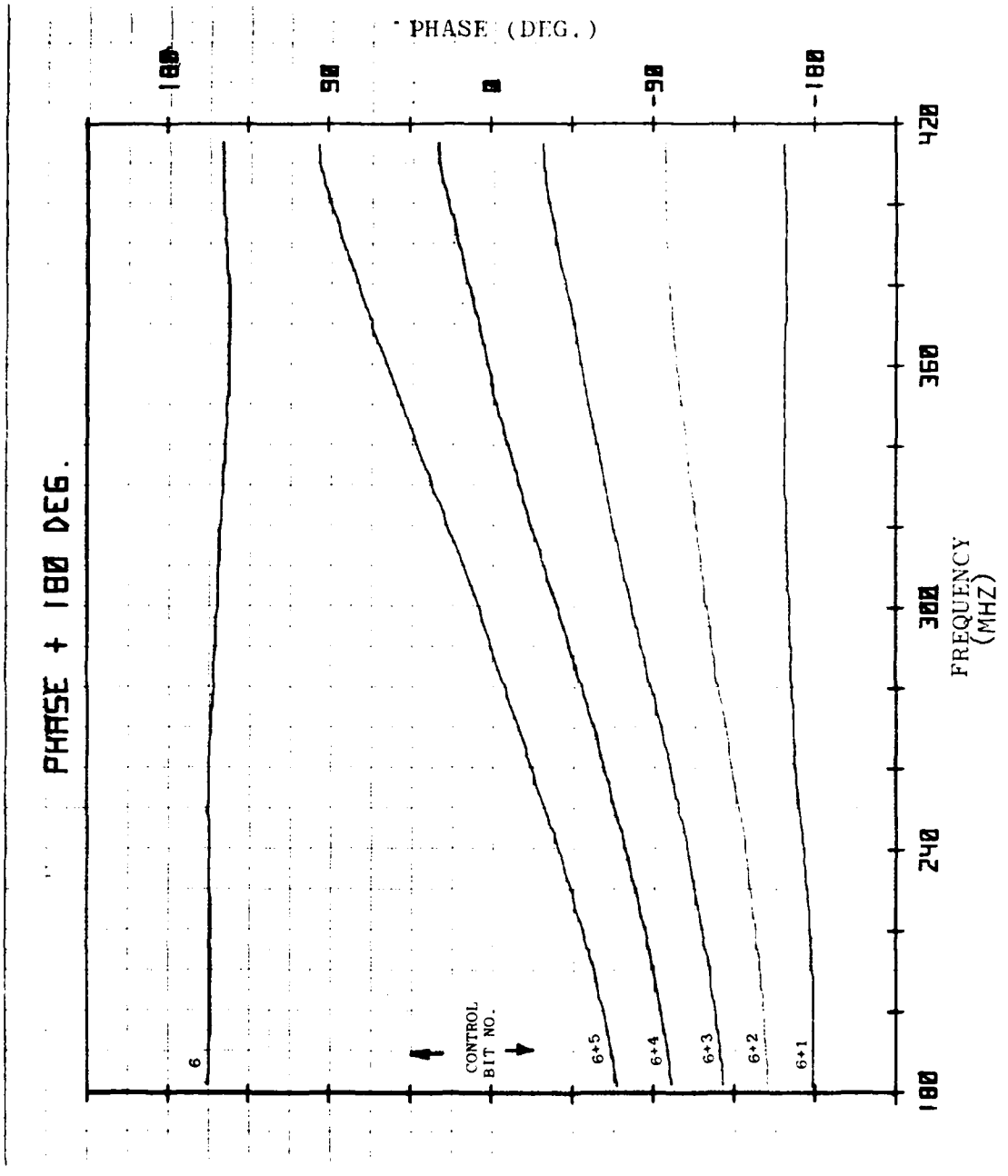

FIGURE 4.3.3b
PHASE SHIFT vs FREQUENCY,
6 BIT PHASE SHIFTER

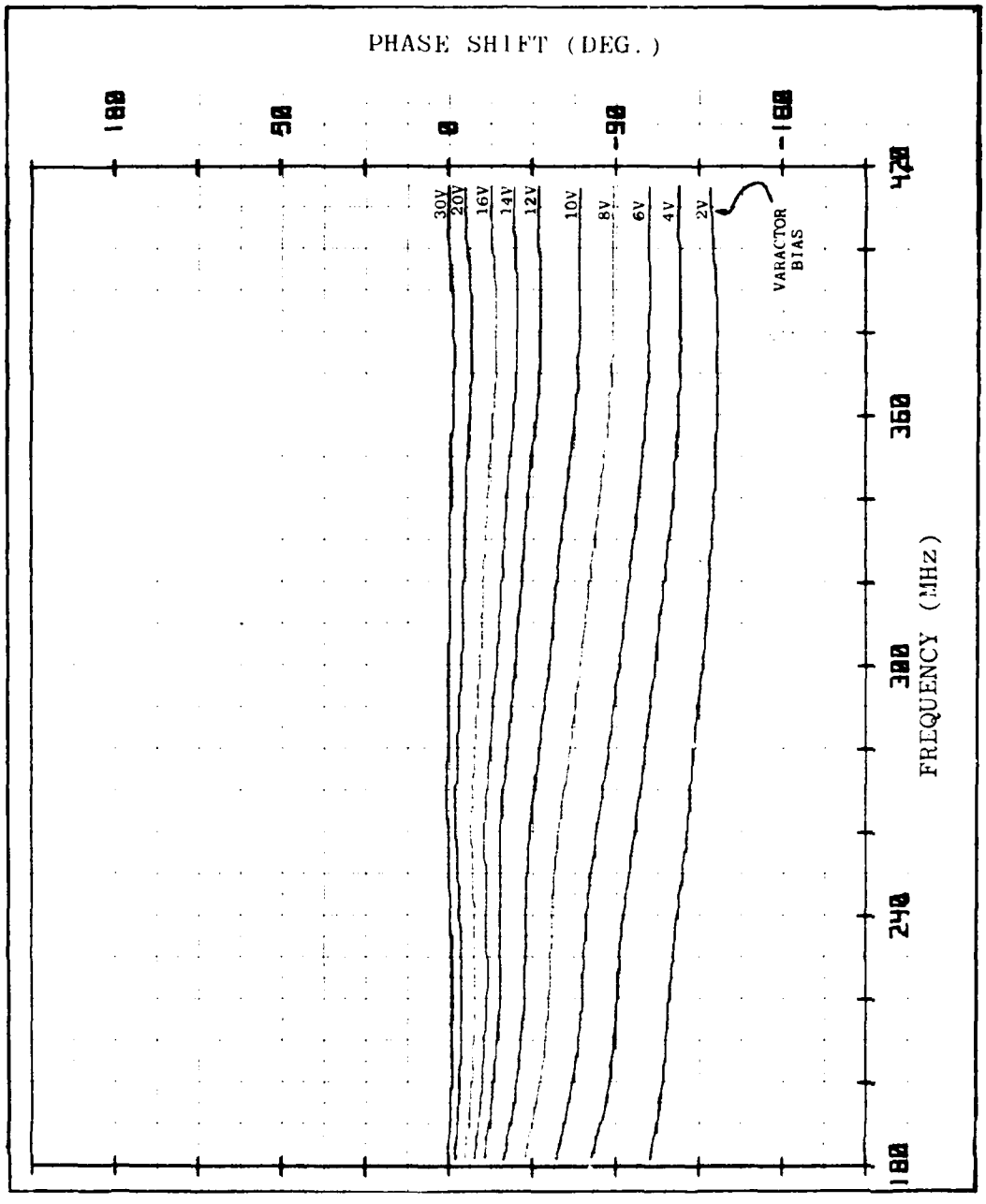

FIGURE 4.3.3c
PHASE SHIFT vs FREQUENCY, ANALOG PHASE SHIFTER

It is possible to provide increased phase slope without amplitude selection through the use of a length of cable in the feedback. However, if the loop amplitude response is still large at frequencies offset from the carrier where the phase passes through 360^{o}, noise sidebands will actually degrade near those offset frequencies. (See Fig. 6.3.5). In addition, if open loop gain is greater than unity at those frequencies, then false lock is a possibility. Thus, the better approach is to increase both amplitude and phase selection with improved Q filters.

5.0 CONSTRUCTION AND OPERATION

5.1 Oscillator Description

The complete oscillator consists of an oscillator assembly and a control assembly. The oscillator assembly houses the RF sections while the control assembly contains the switching elements for programming the oscillator frequency.

5.1.1 Control Unit

The lower subchassis of the control unit houses the D.C. power control for the oscillator. See Fig. 5.1.1. Two independent switches provide selective control of the oscillator's active power stage (S2) and the cavity/phase shift controlling section (S1). Also in the subchassis is the analog frequency control bias supply. This provides at J34 a variable D.C. voltage, +6 volts to +27.5 volts for manual frequency control.

The rear apron is divided into 3 sections, two finned heat sinks and a cable entrance panel. One heat sink is used to mount the resistors that provide the constant current required by the PIN diodes for cavity tuning. The other heat sink is used to mount the level shifter and transistor power switches that are used to remotely control the rate of channeling between any two oscillator frequencies. Convection provides adequate cooling when the controller is operated in a $25^{o}C$ nominal environment.

The sloped front panel was built to provide easy access to the 19 frequency control programming switches and the 33 external frequency control programming jacks. A set of cables is provided to allow the patching of the frequency control bits (J1-J24) to the driver jacks (J26-J33).

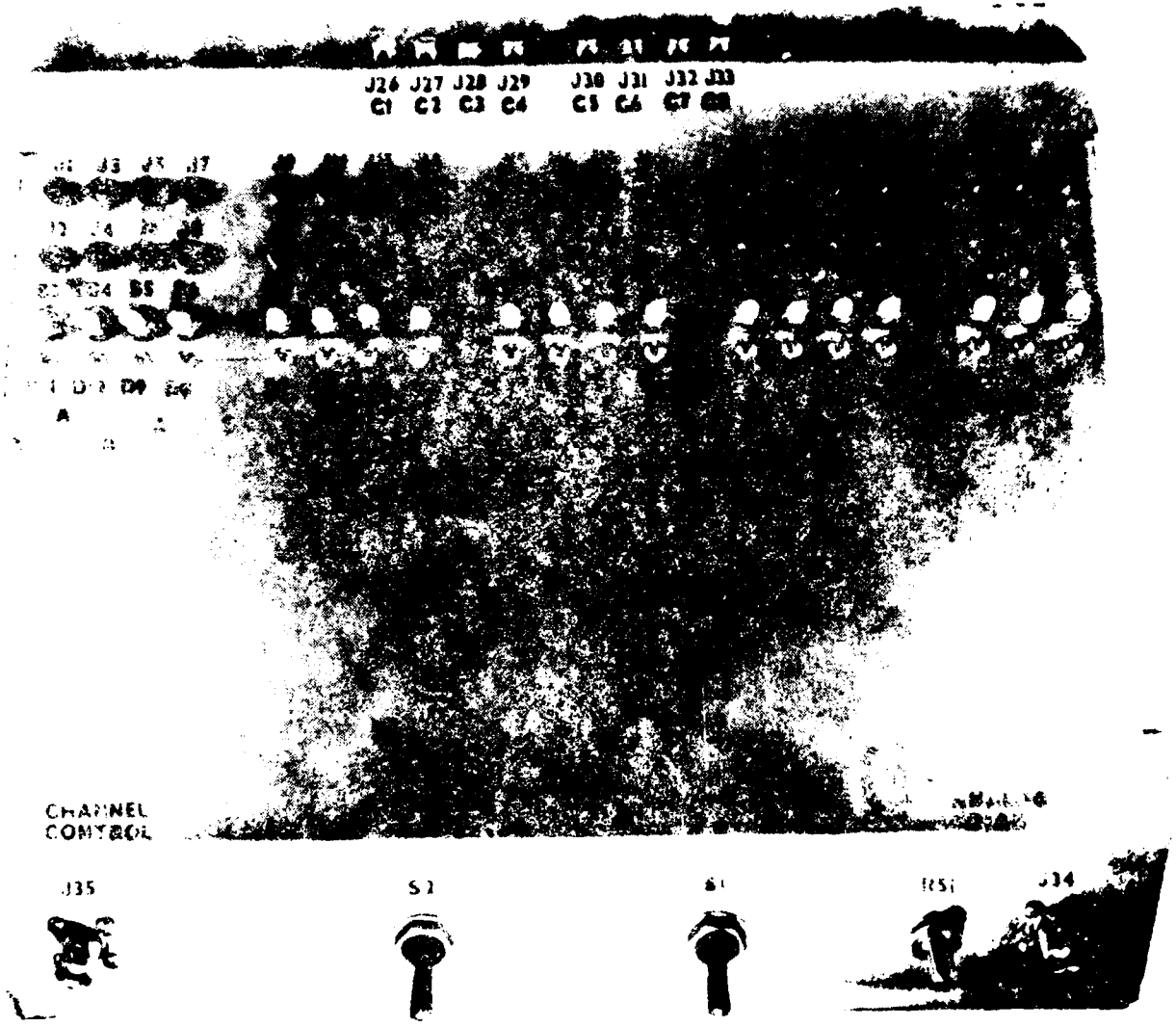
J26 J27 J28 J29 J30 J31 J32 J33
C1 C2 C3 C4 C5 C6 C7
CHANNEL
CONTROL
J35
S1
J34

5.1.2 Oscillator Assembly

The oscillator chassis houses a blower cooled heat sink that is used to mount all of the major oscillator components with the exception of the phase shifter. (See Fig. 5.1.2).

On the heat sink adjacent to the blower is the electronically tuned filter. The filter was positioned on the coolest section of the heat sink to decrease the magnitude of the thermal transients that are produced by the dual amplifier. The heat dissipated by the dual is not constant but varies with frequency.

Mounted on top of the filter is the coupler used to split RF energy between the output load connected to J2 and the phase shifter that is mounted against the front panel.

Adjacent to the filter is the dual amplifier with its bias stabilizer. Next to the bias stabilizer is the VMOS amplifier and the VMOS power control switch.

J3 and J4 are mounted on the front panel to enable open loop testing of the oscillator elements. J5, the analog control input, is mounted on the front panel below J3 & J4. J2 is the oscillator RF output and is mounted on the right of the front panel. The 60 Hz 115 VAC cord that provides blower power enters at the left rear of the chassis. The main power and control connector J1 is mounted on the rear of the chassis above the blower.

Cooling air enters the chassis through a series of holes drilled in the left side. The air flows over a baffle installed to permit cooling air to flow over the electronically tuned filter tuning elements. Air then flows underneath the baffle and enters the inlet of the blower B1. Air exits the blower and flows through the heat sink and then exits out the right side of the main chassis.

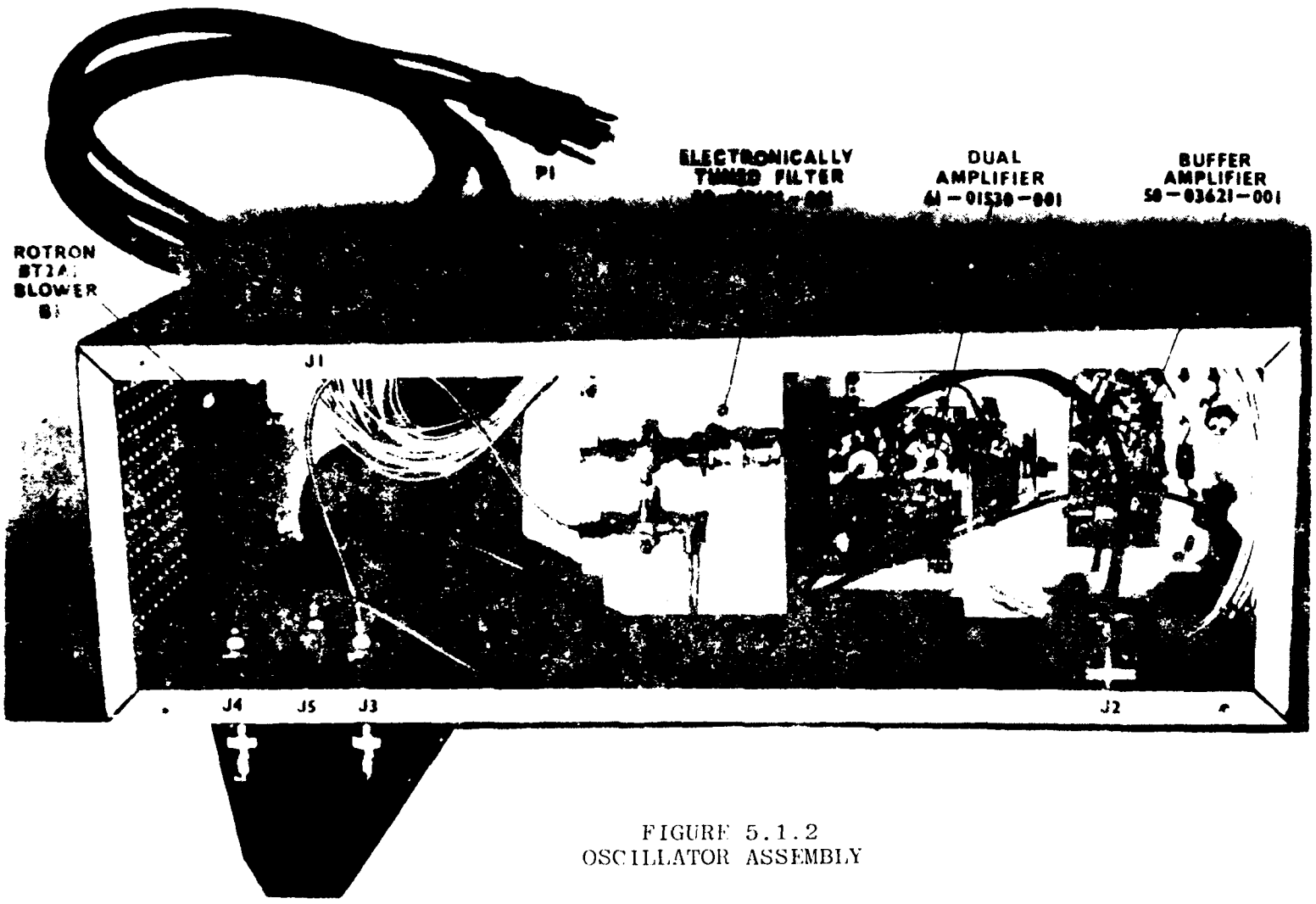

FIGURE 5.1.2
OSCILLATOR ASSEMBLY

5.2 Oscillator Operation and Testing

The two assemblies are interconnected at J1 at the rear of the RF unit with a 36 wire cable originating in the control unit and terminated with P1. Internal analog frequency control is supplied through a shielded coaxial cable connected between RF unit J5 and control unit J34. See Figure 5.2.1.

When installed, W1, the jumper cable supplied for interconnecting J3 and J4 on the RF unit, closes the oscillator loop. Only when the supplied cable is used will the tuning codes shown in Table 6.1a be valid.

The cable may be temporarily removed to open the oscillator loop to enable testing or alignment of individual oscillator elements.

Power is supplied to the oscillator through 4 pair of banana jacks and one AC line cord. The oscillator power requirements are shown in Table 5.2

TABLE 5.2

OSCILLATOR POWER REQUIREMENTS

JACK NO.	VOLTAGE	CURRENT
AC PLUG	115 VAC-60 Cycle	0.18A
P4	+28V	5.6A
P5	+22V	0.48A
P3	+4V	12 A
P2	-150V	12 mA

5.2.1 Determination of Tuning Codes

CAUTION - WARNING

Any attempt to operate the oscillator without the blower in the RF unit activated may damage components and result in failure of the oscillator. Activate blower prior to supplying power to the oscillator.

Figure 5.2.1A indicates the test circuit that determines the tuning code for oscillator operation at any frequency between 225 MHz and 400 MHz.

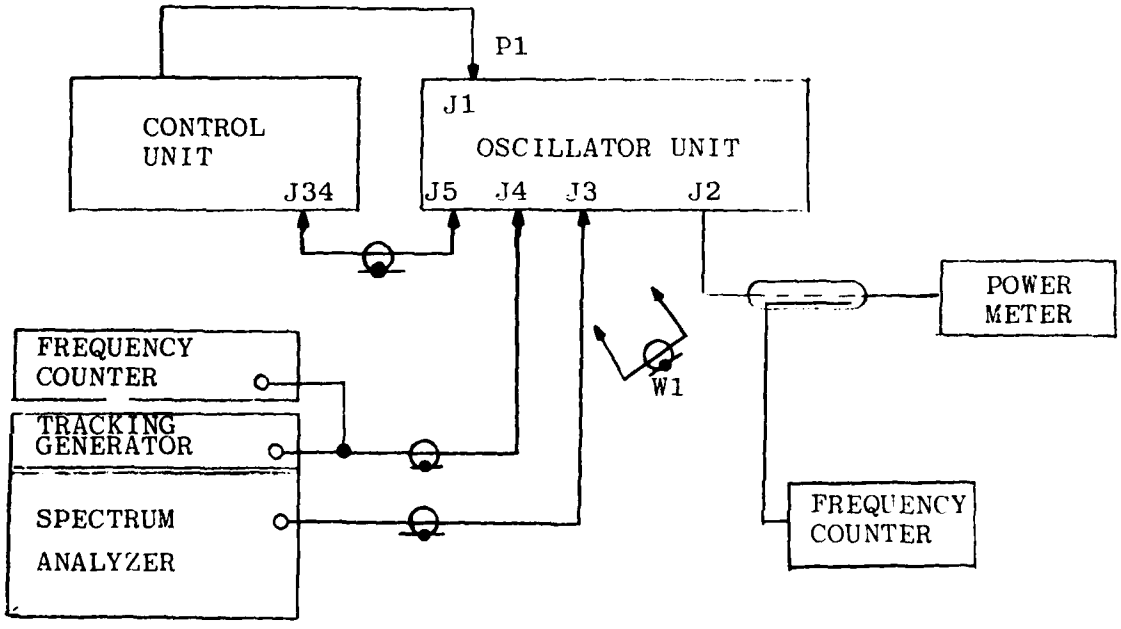

FIGURE 5.2.1a
OSCILLATOR TEST CIRCUIT

By tuning the spectrum analyzer and tracking generator to the desired operating frequency, the spectrum analyzer display produced the characteristic response of a bandpass filter.

The Frequency Control Bits D0 through D11 were exercised to produce a well balanced display centered around the desired operating frequency consistent with maximum gain. The gain is dependent upon frequency and varies from 3.2 dB to 7.5 dB.

After the code for the D bits was determined the loop was closed by installing Cable W1. See Fig. 5.2.1b.

A bias of 11 volts was supplied to the analog frequency control connector (J5). The phase shifter Bits A0 through A5 were then exercized to adjust the oscillator as close as possible to the desired operating frequency. Once the optimum "A" bits were selected, the analog voltage was varied to fine tune the oscillator.

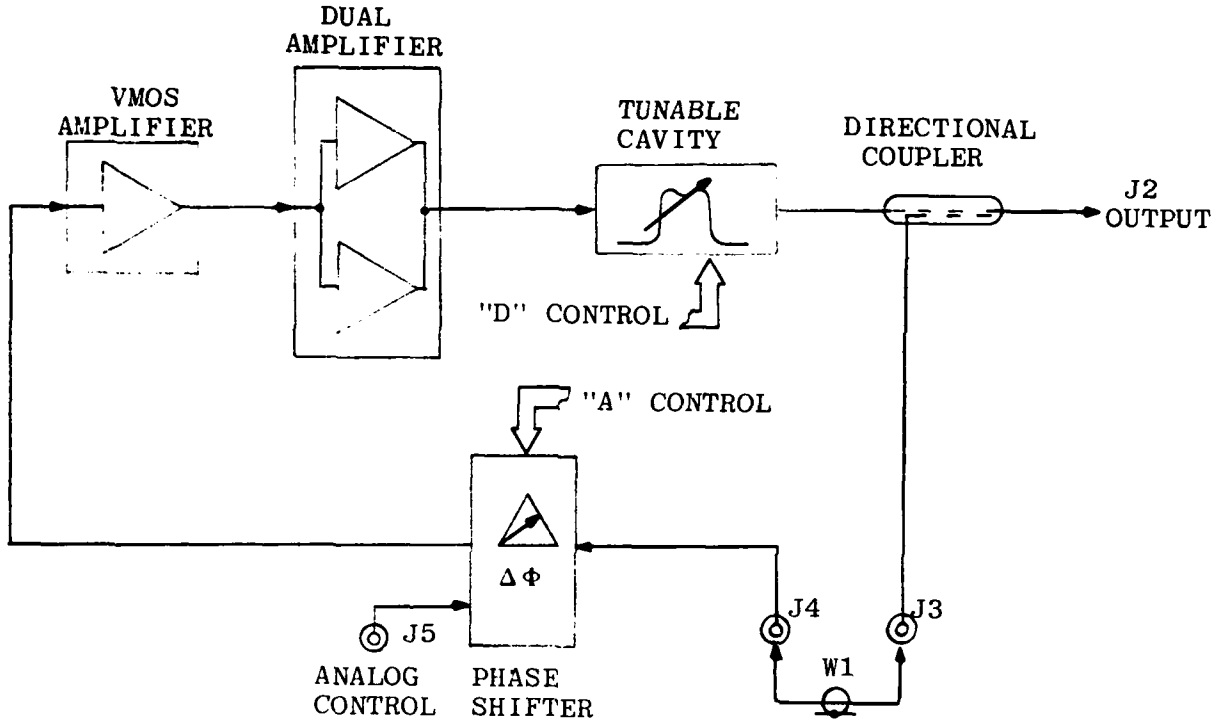

FIGURE 5.2.1b
OSCILLATOR BLOCK DIAGRAM

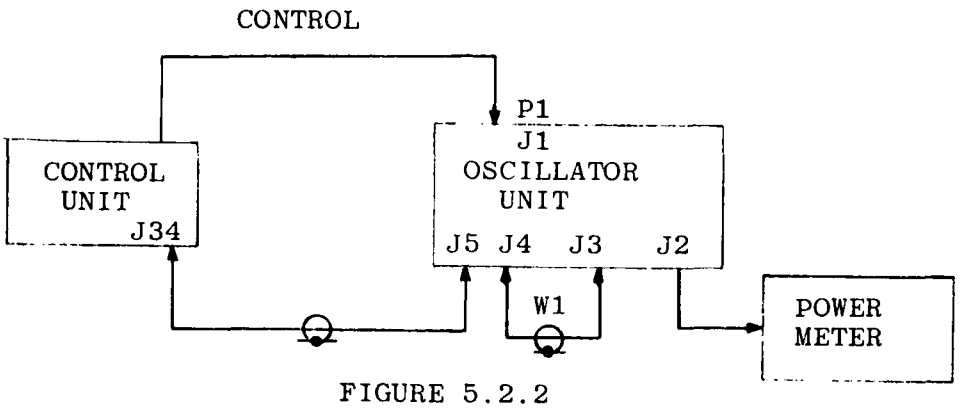

FIGURE 5.2.2
POWER OUTPUT MEASUREMENT

5.2.2 Measurement of Oscillator Output Power

The test circuit shown in Fig. 5.2.2 was used to measure the power output of the oscillator.

By adjusting switches D0 to D11 and A0 to A5 to codes determined as described in 5.2.1, power output at any frequency may be determined.

5.2.3 Load Stability

Fig. 5.2.3 shows the test circuit used to measure the load sensitivity of the oscillator under approximately 3:1 & 1.5:1 VSWR. The VSWR that results from the shorted 3 dB and 6 dB pad may be calculated using the equations:

$$VSWR = \frac{1 + \Gamma}{1 - \Gamma}$$

where

$$\Gamma = \frac{1}{\text{Log}^{-1}\left(\frac{L_R}{20}\right)}$$

L_R = Return Loss
= 6 dB for 3 dB pad
=12 dB for 6 dB pad

The oscillator was terminated with a 50 ohm load and the output frequency was noted. The appropriate VSWR termination was attached to the end of the variable length air line. The frequency of the oscillator was monitored while varying the length of the line. The frequency deviation was compared to the 50 ohm loaded case. The maximum frequency deviation was recorded.

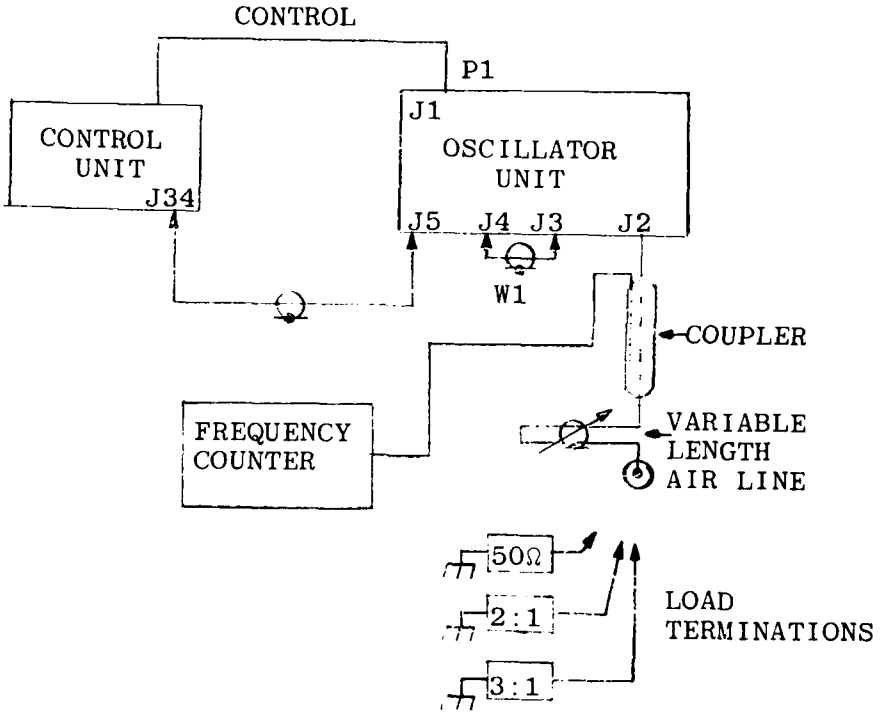

FIGURE 5.2.3
LOAD STABILITY TEST CIRCUIT

5.2.4 Settling Time

Settling time is the period required for the oscillator output frequency to enter and stay within a specified error band centered around a reference frequency after a programmed step change in frequency.

Two sets of frequencies were selected to demonstrate the oscillators channeling ability. Figure 5.2.4 lists the frequency codes and indicates which bits were selected to be toggled.

Figure 5.2.4a is a simplified schematic of the current switching, channeling circuits. Level shifter, Q1 and Q2, converts the $\pm$10V channel control signal to the drive required to operate the high current switch Q3. With Jumpers J15 to J26 and J13 to J27 installed and switches S9 and S11 off, resistors R12 and R13 limit the forward current supplied to the PIN diodes to approximately 1 amp when Q3 is biased on. When Q3 turns off, the PIN diodes are turned off by bias supplied from -150V through R11 and R31-R7 and R33-R9 combinations. By the proper selection of the frequency codes and corresponding patching of the jumpers the oscillator may be remotely channeled between most any two frequencies.

LONG HOP (400-288) 112 MHz

BIT NOS FREQUENCY	D11	D10	D9	D8	D7	D6	D5	D4	D3	D2	D1	D0	A5	A4	A3	A2	A1	A0	B0
400	1	1	1	1	1	1	1	1	1	1	0	1	1	1	1	1	0	1	0
288	0	1	1	0	1	1	0	1	0	1	0	1	1	1	1	0	1	1	0
BITS TO BE TOGGLED	X			X		X			X							X	(X)		

(X) = DOESN'T CARE

SHORT HOP (400-383) 14 MHz

400	1	1	1	1	1	1	1	1	1	1	0	1	1	1	1	1	0	1	0
386	1	1	1	1	1	0	1	1	0	1	0	1	0	1	1	0	1	1	0
BITS TO BE TOGGLES						X			X				X			X	(X)		

(X) = DOESN'T CARE

FIGURE 5.2.4
FREQUENCY HOP PROGRAMMING CODES

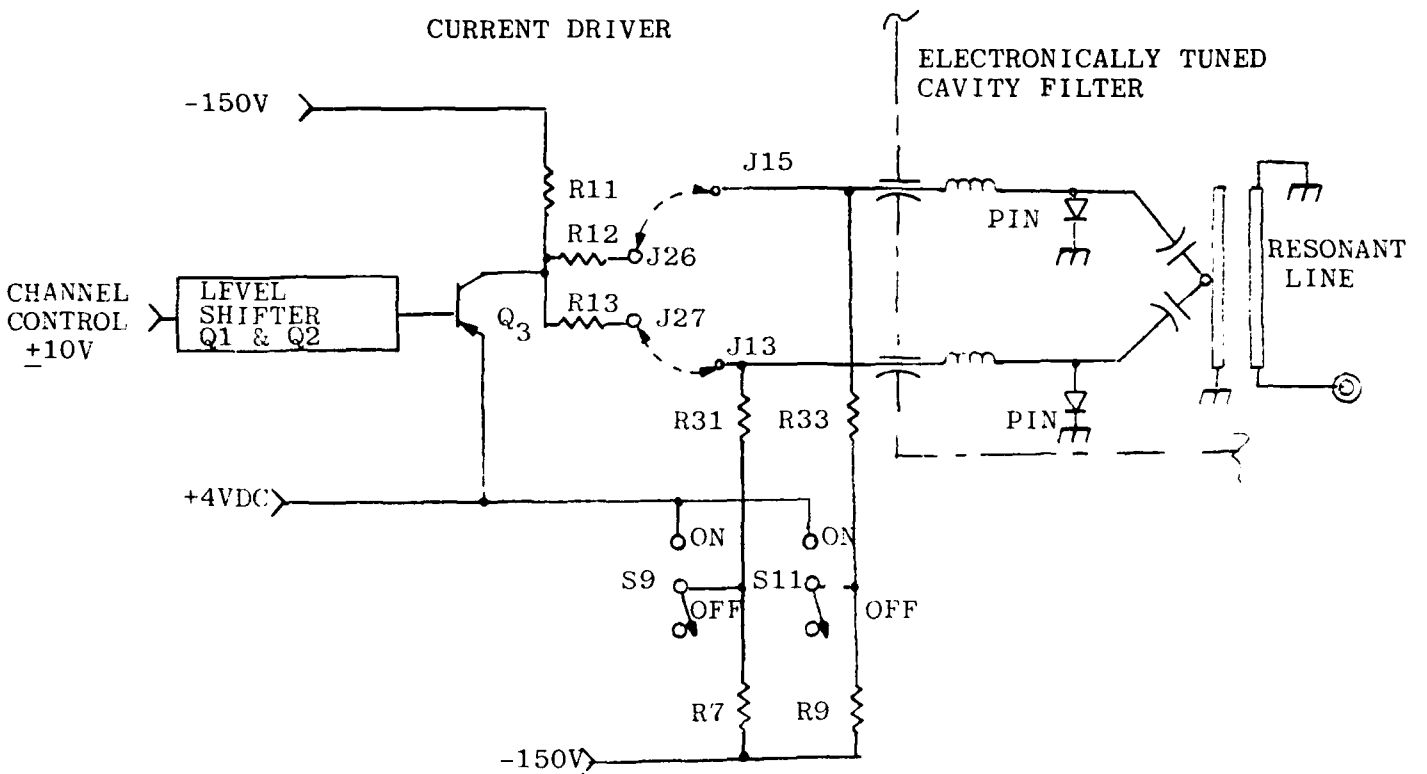

FIGURE 5.2.4a
SIMPLIFIED DIODE DRIVE CIRCUIT

Figure 5.2.4b shows the test setup used to measure the frequency agility of the oscillator. The signal generator was adjusted to provide a carrier centered within the frequency discriminator when the oscillator was tuned to the frequency of interest. The function generator was disconnected temporarily. The resulting oscilloscope display was calibrated. By varying the frequency of the signal generator, the carrier was offset in 100 kHz increments and the discriminator output voltage for each offset was noted on the oscilloscope. The display was adjusted to view both positive and negative deviations as a full screen display. The frequency of the signal generator was retuned to provide a carrier centered within the discriminator. The function generator was connected and it's frequency was adjusted to present a CRT display consistent with the time interval to be measured.

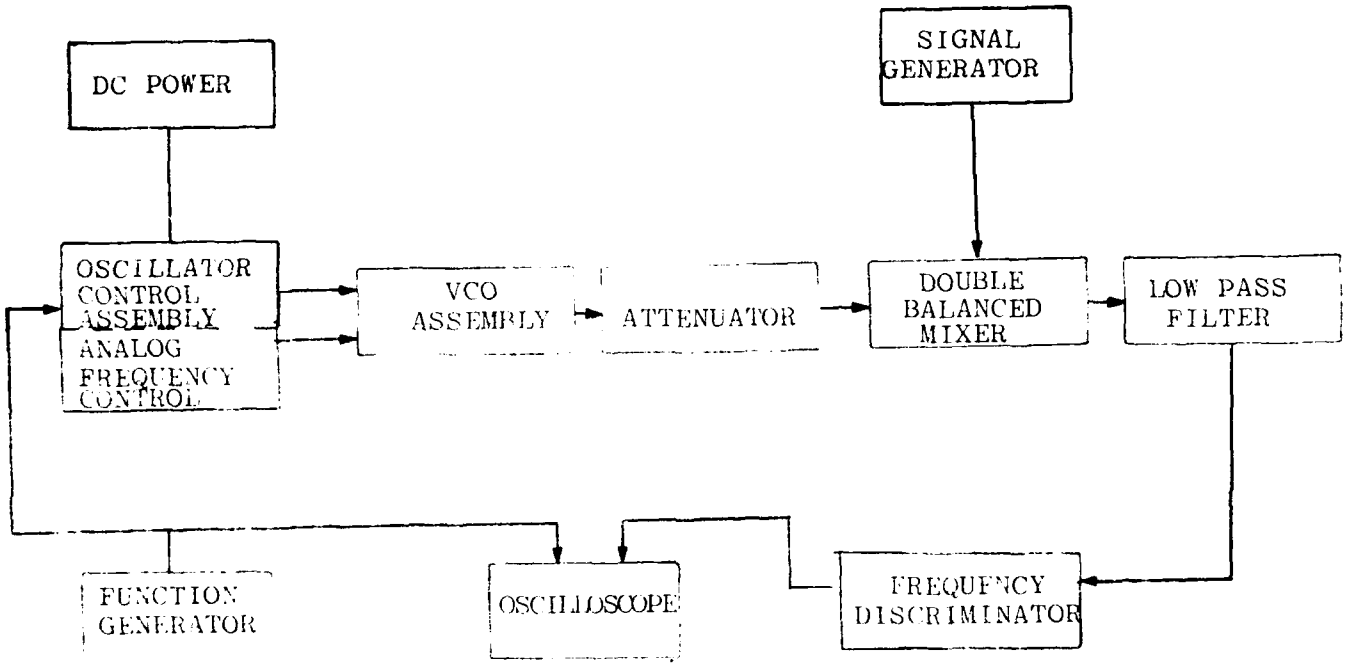

FIGURE 5.2.4b
FREQUENCY HOPPING TEST SETUP

AD-A113 253 E-SYSTEMS INC ST PETERSBURG FL ECI DIV F/G 9/5
ELECTRONICALLY TUNABLE PHASE LOCKED LOOP OSCILLATOR.(U)
FEB 82 M BALASIS, M R DAVIS, C R JACKSON F30602-80-C-0133
UNCLASSIFIED 60-62244 RADC-TR-81-400 NL

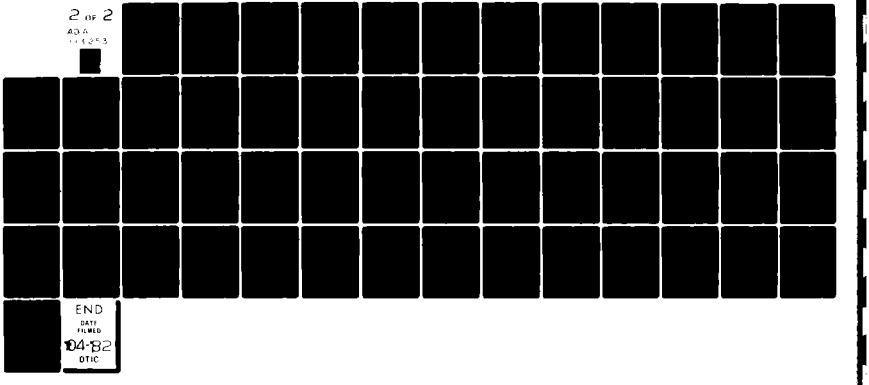

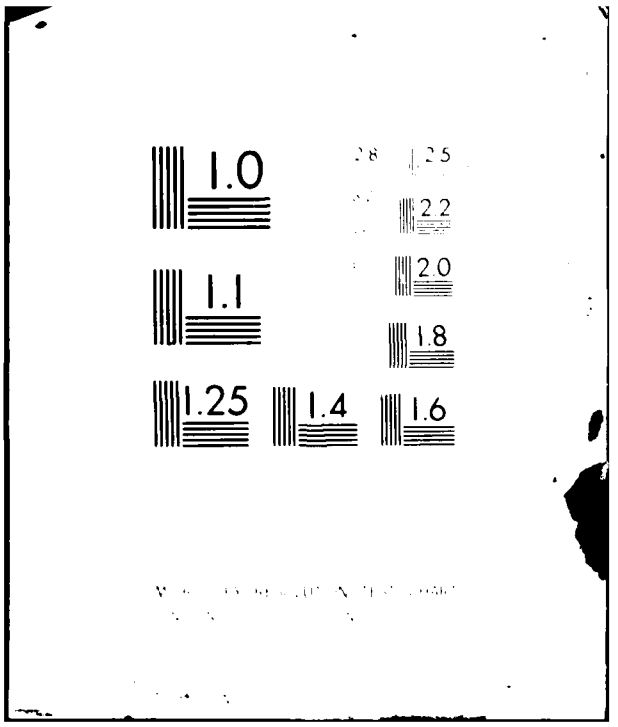
1.0
1.1
1.25
1.4
1.6
1.8
2.0
2.2
2.5

The frequency error after the prescribed time was then read from the CRT display and then recorded. The oscilloscope trigger was inverted, the signal generator readjusted to the second frequency plus discriminator offset, the function generator disconnected, and the calibration was repeated. The function generator was connected and the frequency error noted on the oscilloscope was recorded.

5.2.5 Current Drain

Figure 5.2.5 shows the test set up used to measure the oscillator power consumption.

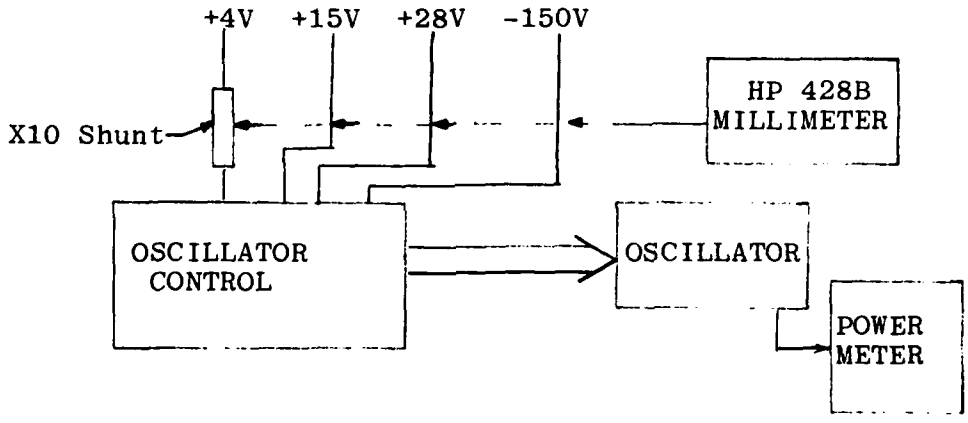

Figure 5.2.5

POWER CONSUMPTION TEST SETUP

The current was measured at 3 frequencies (225, 290 and 400 MHz). The HP428B was used to measure the current by direct clip-on attachment with one exception. The current measurement of the +4V supply was metered by using a times ten shunt. The currents measured (measurement X10 in the +4V case) were recorded.

5.2.6 Measurement of Output Noise Power

Standard laboratory techniques of measuring carrier signal-to-noise ratios are dynamic range limited at 80 to 100 dBc/Hz. A carrier notching method that increases measurement to >200 dBc/Hz was devised.

5.2.6.1 Noise Measurement Test Set

Figure 5.2.6.1.1 shows the basic configuration of the noise test set. The following describes the elements of the test set:

Directional Coupler	Samples VCO to provide input to frequency stabilizer.
3 dB Pad	Provides isolation to VCO from tunable notch filter which has tendency to change input impedance while tuning and pull VCO.
Tunable Notch	Low loss notch filter tuned by FR-171 UHF bandpass filter and 2 circulators in series.
Tunable Bandpass	Provides extra attenuation to notched carrier and eliminates VCO harmonics from saturating LNA and spectrum analyzer.
Low Noise Amp	Provides additional gain required and lowers overall analyzer noise figure to 5 dB.

5.2.6.1.1 Signal Handling Limitations

The signal handling capability of the combined LNA and analyzer can be predicted. The LNA can handle an input signal

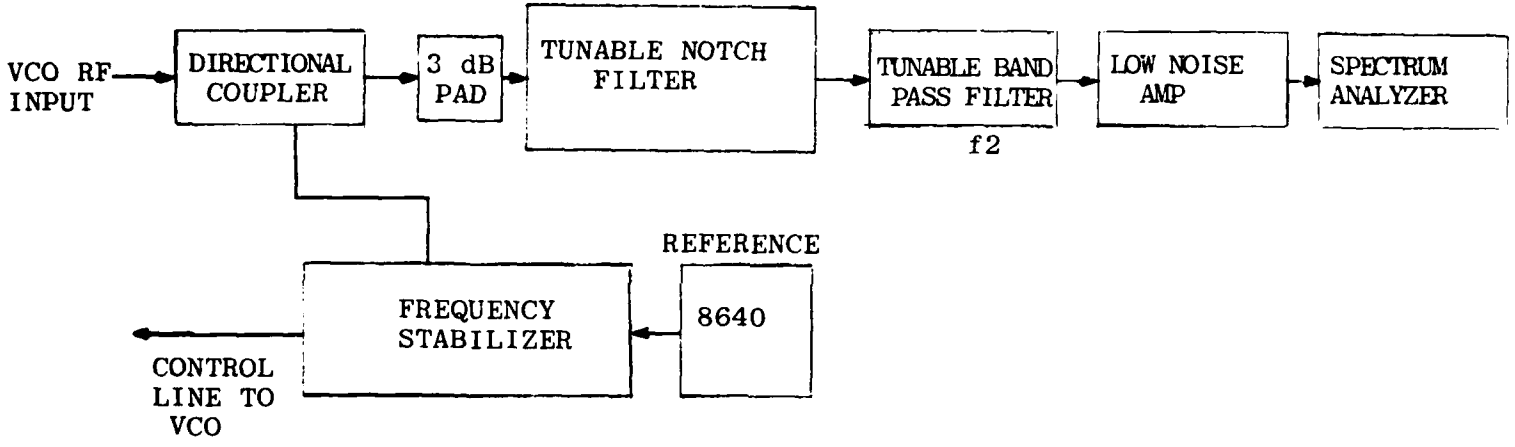

FIGURE 5.2.6.1.1
NOISE MEASUREMENT TEST SET

of -25 dBm without exceeding the output 1 dB compression point of +8 dBm. Given a combined total noise figure of 5 dB for the LNA and Analyzer the noise floor at the input of the LNA is:

5 dB	Noise Figure
-174 dBm/Hz	Thermal Noise @25^{o}C
-169 dBm/Hz	Equivalent Noise

The maximum signal-to-noise of a -25 dBm carrier that can be resolved is:

-25 dBm	Carrier
-(-169 dBm/Hz)	Noise Floor
144 dBc/Hz	Signal-to-Noise

Figure 5.2.6.1.2 shows the single sideband phase noise contribution that may be expected from the HP 8568A spectrum analyzer.[35] The noise floor for measurements at Fourier offsets greater than 500 kHz is determined by the phase noise contribution of the spectrum analyzer alone (-140 dBc/Hz). Therefore, the LNA signal-to-noise is not the limiting factor.

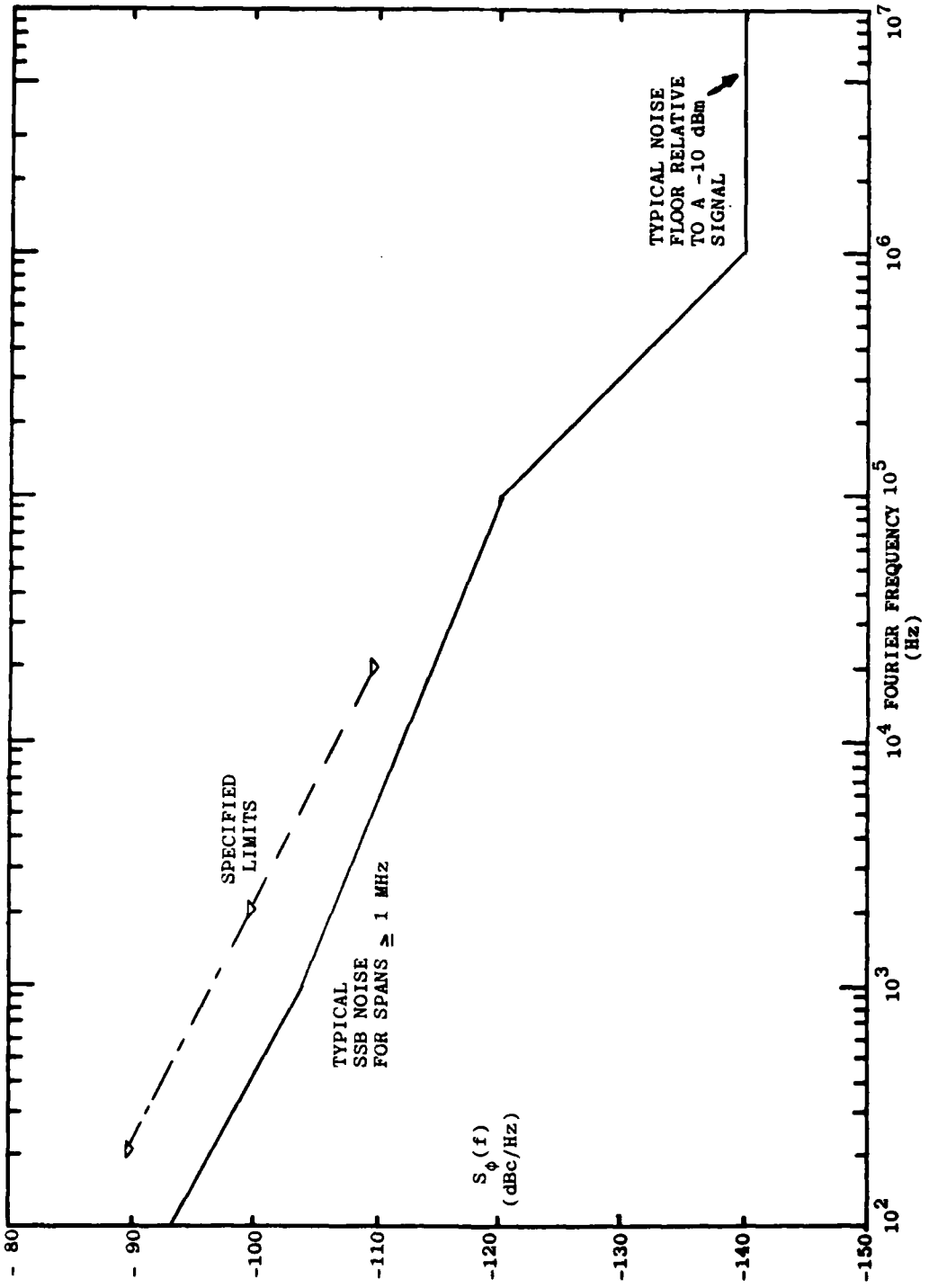

FIGURE 5.2.6.1.2
SPECTRUM ANALYZER NOISE OPERATION

Then it is obvious that to measure a carrier whose phase noise power at an offset of 500 kHz is -200 dBc/Hz, we need an additional increase of 70 to 80 dB in dynamic range. This is achieved by the notching and preselection process.

-140 dBc/Hz	ANALYZER
-70 dB	NOTCH
-210 dBc/Hz	TOTAL

5.2.6.1.2 Noise Floor Limitations

The noise figure of the complete setup is:

ITEM	CONTRIBUTION
3 dB Pad	3 dB Attenuation
Notch	1 dB Loss
Preselector	1 dB Loss
LNA/Analyzer	5 dB Noise Figure
	10 dB System Noise Figure

Examining the phase noise of a 10 watt (+40 dBm) carrier, the measurement floor is:

System Floor = -174 dBm/Hz + 10 dB	=	-164 dBm/Hz
Signal = + 40 dBm (10 watts)	=	40
Setup Signal-to-Noise Measurement Floor	=	-204 dBc/Hz

Accurate measurements may be made on 10 watt carriers whose noise is as low as -204 dBc/Hz. As noise performance approaches -204 dBc appropriate corrections must be made to eliminate the error caused by the addition of system noise to oscillator noise.

For example:

System Noise = -204 dBc/Hz

Measurement = -199 dBc/Hz

$$10 \text{ LOG } \left| \text{Log}^{-1}\left(\frac{-199}{10}\right) - \text{Log}^{-1}\left(\frac{-204}{10}\right) \right| = -200.7$$

Corrected Value = -200.7 dBc/Hz

5.2.6.1.3 Frequency Stability Limits

The short term frequency stability of most unlocked, variable frequency oscillators is insufficient to maintain the carrier precisely within the very narrow bandwidth of the notch. Slight ambient temperature fluctuations alone can create frequency changes of several kilohertz. This frequency drift reduces the depth of the notch from 70 to 40 or 30 dB. The resulting desensitization causes a subsequent reduction in measurement capability. Note that for gross frequency drifts power sufficient to damage elements in the testing system could exist.

To eliminate the short term frequency drifts, the frequency stabilizer shown in Figure 5.2.6.1.3 was constructed and incorporated into the test system.

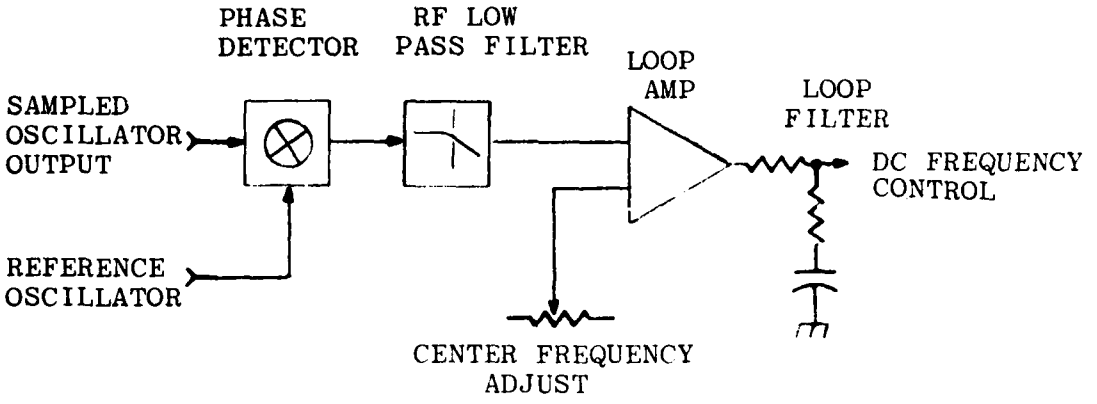

FIGURE 5.2.6.1.3
FREQUENCY STABILIZER

The stabilizer has a maximum closed loop bandwidth of 100 Hz. This very narrow bandwidth eliminates any broadband noise contribution from the reference oscillator at measurement offsets greater than a few kilohertz.

The coupler at the VCO output (Figure 5.2.6.1.1) samples the oscillator R.F. power. This signal is compared to a reference frequency in the frequency stabilizer (Figure 5.2.6.1.3) by a double balanced mixer used as a phase detector. The output of the mixer is filtered and amplified. The closed loop gain characteristics of the stabilizer/oscillator are modified by a lag filter. The elements of the filter were chosen and the gain of the amplifier set to provide a closed loop response as indicated above. The stabilizer drives the analog frequency control port of the high power voltage controlled oscillator.

The potentiometer adjusts the oscillator center frequency (stabilizer resting voltage) to within capture range of the loop.

5.2.6.2 Measurement of Single Sideband Noise Power

The measurement of the single sidcband noise power was performed at 5 frequencies within the range of the oscillator. In addition to measuring the SSB noise power, a calibration factor was also measured and later used to compensate for instrumentation.

5.2.6.2.1 Noise Power Measurement

The single sideband noise power was measured using the test system shown in Figure 5.2.6.1.1. A frequency of operation was selected and the HP VCO programmed. The reference oscillator was adjusted for an output at the same frequency as the HP VCO. The stabilizer potentiometer was adjusted until the oscillator was locked at the required operating frequency. Once stabilized the selective notch was adjusted. With the carrier properly notched, the analyzer noise level measurement and video averaging functions were enabled. The spectrum analyzer noise level measurement function reads out the RMS noise level normalized to a 1 Hz bandwidth. The filter, f2, was adjusted to the frequency offset from the carrier where the measurement was to take place. The analyzer dispersion was reduced to zero (cw), resolution bandwidth of 1 kHz (normalized to 1 Hz) selected and center frequency chosen for the same offset as filter f2. 50 video averages were performed and the resultant data recorded. Measurements were performed at offsets of 500 kHz, 1, 2, 5 and 10 MHz from the carrier for each of the 5 frequencies in the test plan.

5.2.6.2.2 After the noise measurement was performed, the system gain from HP VCO output to analyzer input was measured at each of the prescribed offsets. The oscillator power output was measured and a calibration factor for each offset was determined.

$$C_f = P_o + G$$

where:

C_f = Calibration Factor

P_o = Power Out (dBm)

G = System Gain (dB)

5.2.6.3 Computation of SSB Noise Power

The 1 Hz normalization performed within the analyzer corrects for the analyzer's logarithmic amplifier response, detector response and the noise power bandwidth of the selected analyzer resolution bandwidth. The only remaining computation is the summing of the calibration factor and the noise power in dBm/Hz to arrive at noise power in dBc/Hz for each point measured.

$$N_{(dBm/Hz)} + C_f = N_{(dBc/Hz)}$$

6.0 TECHNICAL RESULTS

A performance verification test was executed to compare the characteristics of the oscillator to the goals and requirements as outlined in paragragh 2.4. The tests were performed as described in the test plan (submitted in accordance with data item 0002-A003) and as described in section 5.2.

6.1 Tuning Range (Ref. SOW 4.1.1.4 and 4.1.1.1).

The requirement is complete coverage of the 225 to 400 MHz band by a combination of digital tuning bits and an analog voltage. This engineering unit provides analog coverage of greater than $\pm$1 MHz. Therefore, a digital code was derived for 2 MHz increments. See the following:

Table 6.1a Digital code versus frequency
Table 6.1b Analog tuning range
Figure 6.1 Graphic display of analog tuning range

Conclusion: The oscillator exhibits complete coverage of the 225 MHz to 400 MHz frequency range.

TABLE 6.1 a
HIGH POWER VCO TUNING CODES

DESIRED FREQUENCY (MHz)	GROUP "D" 11 10 9 8	7 6 5 4	3 2 1 0	GROUP "A" 5 4 3 2	1 0
225	0 0 0 0	0 1 0 1	0 1 0 1	0 1 1 0	1 1
226	0 0 0 0	0 1 0 1	0 1 0 1	0 1 0 1	1 1
228	0 0 0 0	1 0 1 1	0 1 0 1	0 1 0 1	1 1
230	0 0 0 0	1 0 1 1	0 1 0 1	0 0 1 1	1 1
232	0 0 0 0	1 1 1 1	0 1 0 1	0 0 1 1	1 1
234	0 0 0 1	0 0 0 1	0 1 0 1	1 1 1 1	1 1
236	0 0 0 1	0 1 0 1	0 1 0 1	1 1 1 1	1 1
238	0 0 0 1	0 1 0 1	0 1 0 1	1 1 1 1	1 0
240	0 0 1 0	0 0 0 1	0 1 0 1	1 1 1 1	0 1
242	0 0 1 0	0 1 0 1	0 1 0 1	1 1 1 1	0 1
244	0 0 1 0	0 1 0 1	1 1 0 1	1 1 1 0	1 1
246	0 0 1 0	1 0 0 1	0 1 0 1	1 1 1 0	1 1
248	0 0 1 0	1 0 0 1	1 1 1 1	1 1 0 1	1 1
250	0 0 1 0	1 1 0 1	0 1 1 1	1 1 0 1	1 1
252	0 0 1 1	0 0 0 1	0 1 0 1	1 0 1 1	1 1
254	0 0 1 1	0 0 1 1	1 1 1 1	0 1 1 1	1 0
256	0 0 1 1	0 1 0 1	0 1 0 1	0 1 1 1	1 0
258	0 0 1 1	0 1 1 1	1 1 1 1	0 1 1 1	0 1
260	0 0 1 1	1 0 0 1	0 1 0 1	0 1 1 1	0 1
262	0 0 1 1	1 0 1 1	1 1 1 1	0 1 1 0	1 1
264	0 1 0 1	0 0 0 1	0 0 0 0	0 1 1 0	1 1
266	0 1 0 1	0 0 0 1	1 1 1 1	0 1 1 0	1 1
268	0 1 0 1	0 1 0 0	0 1 0 1	0 1 0 1	1 1
270	0 1 0 1	0 1 0 1	0 1 0 1	0 1 0 1	1 1
272	0 1 0 1	0 1 1 1	1 1 1 1	0 0 1 1	1 1
274	0 1 0 1	1 0 0 1	1 0 0 1	0 0 1 1	1 1
276	0 1 1 0	0 1 0 1	0 1 1 1	0 0 1 1	1 1
278	0 1 1 0	0 1 0 1	0 1 1 1	1 1 1 1	1 0
280	0 1 1 0	0 1 0 1	0 1 1 1	1 1 1 1	0 1
282	0 1 1 0	1 0 0 1	0 1 0 1	1 1 1 1	0 1
284	0 1 1 0	1 0 0 1	1 1 0 1	1 1 1 0	1 1
286	0 1 1 0	1 1 0 1	0 1 0 0	1 1 1 1	0 1
288	0 1 1 0	1 1 0 1	0 1 0 1	1 1 1 0	1 1
290	0 1 1 1	0 0 0 1	0 1 0 1	1 1 0 1	1 1
292	0 1 1 1	0 0 0 1	1 1 1 1	1 0 1 1	1 1
294	0 1 1 1	0 1 0 1	0 0 0 0	1 0 1 1	1 1
296	0 1 1 1	0 1 0 1	0 1 0 1	1 0 1 1	1 1
298	0 1 1 1	1 0 0 0	0 1 0 0	0 1 1 1	0 1

TABLE 6-1a(Cont'd)
HIGH POWER VCO TUNING CODES

DESIRED FREQUENCY (MHz)	GROUP "D" 11 10 9 8	7 6 5 4	3 2 1 0	GROUP "A" 5 4 3 2	1 0
300	0 1 1 1	1 0 0 1	1 1 0 1	0 1 1 1	0 1
302	0 1 1 1	1 0 1 1	1 1 1 1	0 1 1 1	0 1
304	0 1 1 1	1 1 0 0	0 1 0 1	0 1 1 0	1 1
306	0 1 1 1	1 1 1 1	0 0 0 1	0 1 1 0	1 1
308	0 1 1 1	1 1 1 1	1 1 1 1	0 1 0 1	1 1
310	1 0 1 1	1 1 0 1	0 1 0 0	0 1 0 1	1 1
312	1 0 1 1	1 1 1 1	1 1 0 1	0 1 0 1	1 1
314	1 1 0 0	1 1 0 1	0 1 1 1	0 0 1 1	1 1
316	1 1 0 1	0 0 0 1	0 1 0 1	1 1 1 1	1 0
318	1 1 0 1	0 0 0 1	0 1 1 1	1 1 1 1	0 1
320	1 1 0 1	0 1 0 1	0 0 0 1	1 1 1 1	1 0
322	1 1 0 1	0 1 0 1	0 1 0 1	1 1 1 1	0 1
324	1 1 0 1	0 1 0 1	1 1 1 1	1 1 1 1	0 1
326	1 1 0 1	1 0 0 0	0 1 0 0	1 1 1 1	0 1
328	1 1 0 1	1 0 0 1	0 1 0 1	1 1 1 1	0 1
330	1 1 0 1	1 0 0 1	0 1 0 1	0 1 1 1	1 1
332	1 1 0 1	1 0 0 1	0 1 0 1	0 1 1 1	1 0
334	1 1 0 1	1 1 0 1	0 0 0 0	1 1 1 0	1 1
336	1 1 0 1	1 1 0 1	0 0 0 1	1 1 0 1	1 1
338	1 1 0 1	1 1 0 1	0 1 0 1	1 0 1 1	1 1
340	1 1 0 1	1 1 0 1	0 1 1 1	0 1 1 1	0 1
342	1 1 0 1	1 1 1 1	1 1 1 1	0 1 1 0	1 1
344	1 1 1 0	1 0 0 1	0 0 0 0	0 1 1 1	0 1
346	1 1 1 0	1 0 0 1	0 1 0 1	0 1 1 1	0 1
348	1 1 1 0	1 0 0 1	0 1 0 1	0 1 1 0	1 1
350	1 1 1 0	1 0 0 1	0 1 0 1	1 1 1 1	1 1
352	1 1 1 0	1 0 0 1	1 1 1 1	0 0 1 1	1 1
354	1 1 1 0	1 1 0 1	0 0 0 0	0 1 0 1	1 1
356	1 1 1 0	1 1 0 1	0 0 0 1	0 0 1 1	1 1
358	1 1 1 0	1 1 0 1	0 1 0 1	1 1 1 1	1 0
360	1 1 1 1	0 0 0 1	0 1 0 1	1 1 1 1	1 0
362	1 1 1 1	0 0 0 1	0 1 1 1	1 1 1 1	0 1
364	1 1 1 1	0 0 0 1	1 1 1 1	1 1 1 1	0 1
366	1 1 1 1	0 0 0 1	1 1 1 1	1 1 1 0	1 1
368	1 1 1 1	0 1 0 1	0 0 0 0	0 1 1 1	1 1

TABLE 6-1a(Cont'd)
HIGH POWER VCO TUNING CODES

DESIRED FREQUENCY (MHz)	GROUP "D" 11 10 9 8	7 6 5 4	3 2 1 0	GROUP "A" 5 4 3 2	1 0
370	1 1 1 1	0 1 0 1	0 1 0 0	1 1 1 0	1 1
372	1 1 1 1	0 1 0 1	0 1 0 1	0 1 1 1	1 0
374	1 1 1 1	0 1 1 1	0 1 1 1	0 1 1 1	1 0
376	1 1 1 1	0 1 0 1	1 1 1 1	0 1 1 1	0 1
378	1 1 1 1	1 0 0 0	0 0 0 1	0 1 1 1	0 1
380	1 1 1 1	1 0 1 1	0 1 0 0	1 1 0 1	1 1
382	1 1 1 1	1 0 1 1	0 1 0 0	0 1 1 1	0 1
384	1 1 1 1	1 0 1 1	0 1 0 0	0 1 1 0	1 1
386	1 1 1 1	1 0 1 1	0 1 0 1	0 1 1 0	1 1
388	1 1 1 1	1 0 1 1	1 1 1 1	1 1 1 1	1 1
390	1 1 1 1	1 1 0 0	0 1 0 1	1 1 1 1	1 1
392	1 1 1 1	1 1 0 0	0 1 0 1	0 1 0 1	1 1
394	1 1 1 1	1 1 0 1	0 0 0 1	1 1 1 1	1 0
396	1 1 1 1	1 1 0 1	0 0 0 1	0 0 1 1	1 1
398	1 1 1 1	1 1 0 1	0 1 1 1	1 1 1 1	0 1
400	1 1 1 1	1 1 1 1	1 1 0 1	1 1 1 1	0 1
402	1 1 1 1	1 1 1 1	1 1 0 1	1 1 1 0	1 1

Table 6.1b Analog Tuning Range

FREQUENCY SELECTED	ANALOG VOLTAGE (VDC	OUTPUT FREQUENCY (MHz)	TUNING RANGE (Δf) (MHz)	TOTAL RANGE (Δf) (Mhz)
225	6.00	223.664	-1.34	2.57
	11.26	225.00	-0-	
	28.00	226.230	+1.23	
280	6.00	278.130	-1.87	3.00
	12.31	280.00	-0-	
	28.00	281.120	+1.12	
340	6.00	337.500	-2.50	4.17
	12.82	340.000	-0-	
	28.00	341.670	+1.67	
350	6.00	347.810	-2.19	4.27
	11.39	350.000	-0-	
	28.00	352.080	+2.08	
400	6.00	397.710	-2.29	4.89
	11.85	400.000	-0-	
	28.00	402.600	+2.60	

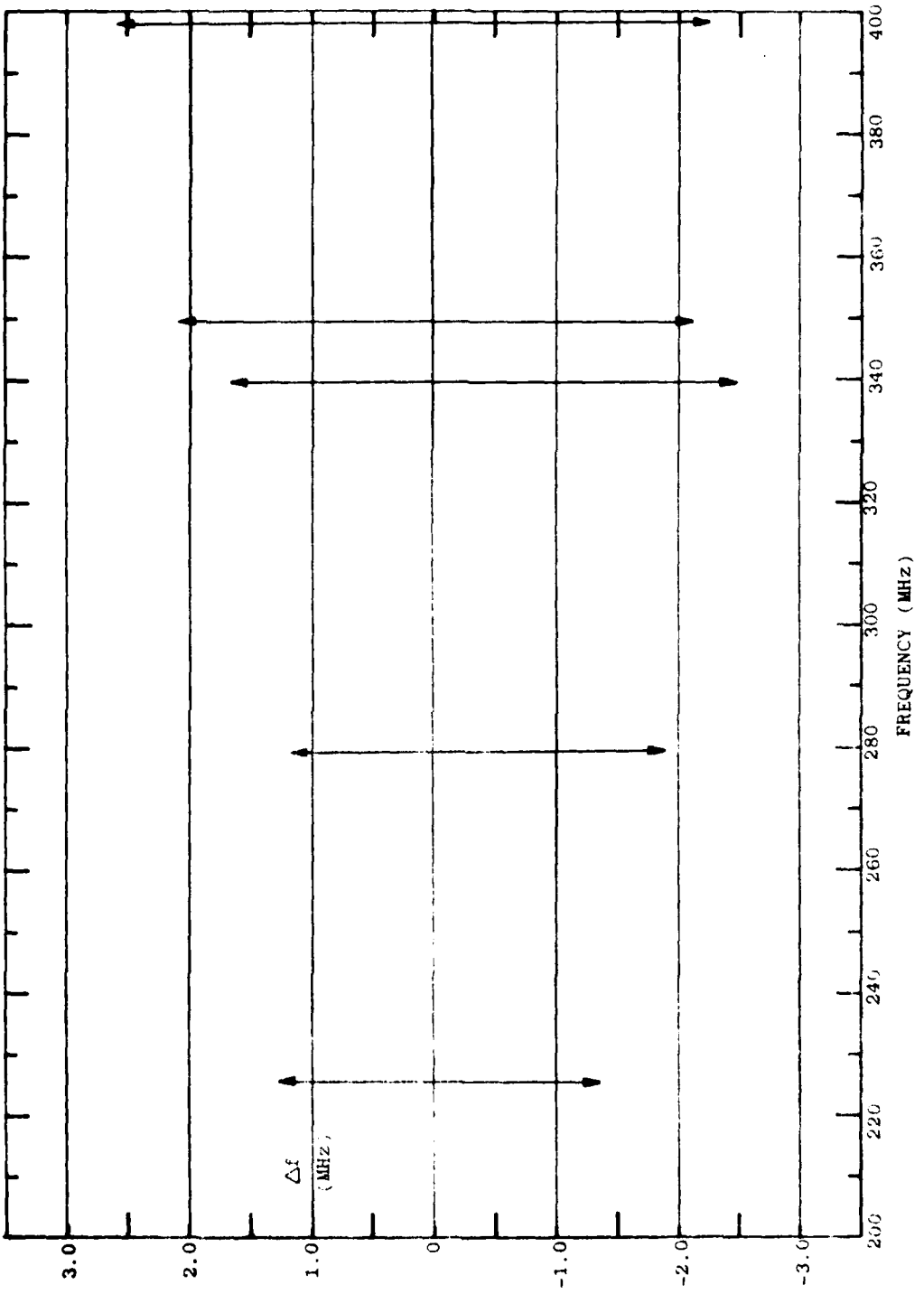

FIGURE 6.1

ANALOG TUNING RANGE

6.2 Power Output (Ref. SOW 4.1.1.2)

The oscillator power output is presented in Table 6.2 and graphed in Figure 6.2. The power output varies less than ±1 dB from a nominal +40.5 dBm (11.22 watts). The oscillator power output exceeds the +33 dBm (2 watt) requirement.

Table 6.2 RF Power Output

FREQUENCY (MHz)	POWER OUT (dBm)	
400	39.55	
390	39.97	
380	40.21	
370	39.97	NOTE: Requirement
360	40.34	is +33 dBm
350	40.59	minimum power
340	41.05	output
330	41.40	
310	41.10	
300	40.95	
290	41.52	
280	41.20	
276	41.45	
240	41.10	
225	40.59	

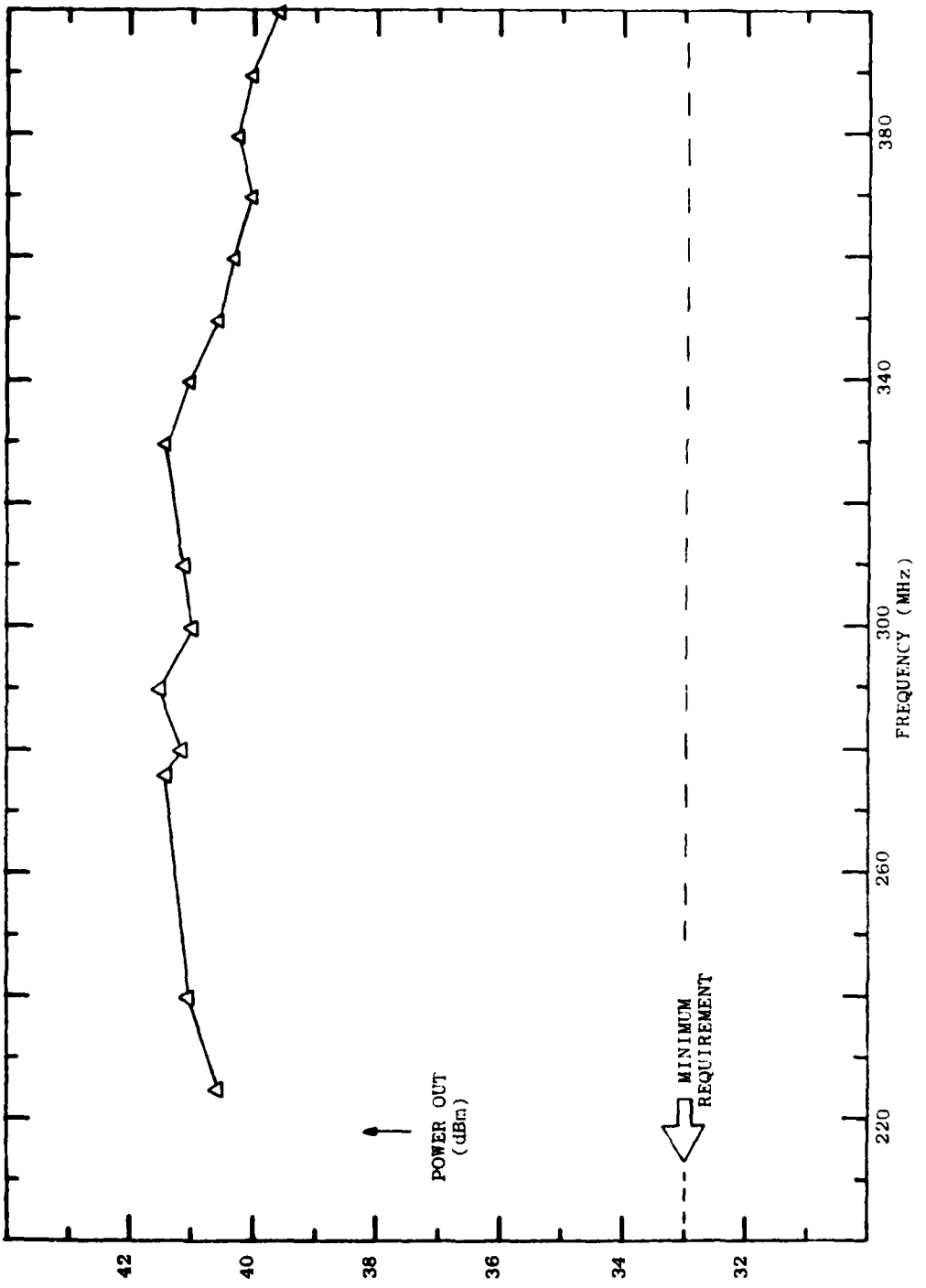

FIGURE 6.2
OSCILLATOR POWER OUTPUT vs FREQUENCY

6.3 Output Noise (Ref SOW 4.1.1.3)

6.3.1 Acceptance Test Data

The phase noise performance was measured at 5 output frequencies across the band and is illustrated by Graphs 6.3.1a through 6.3.1e.

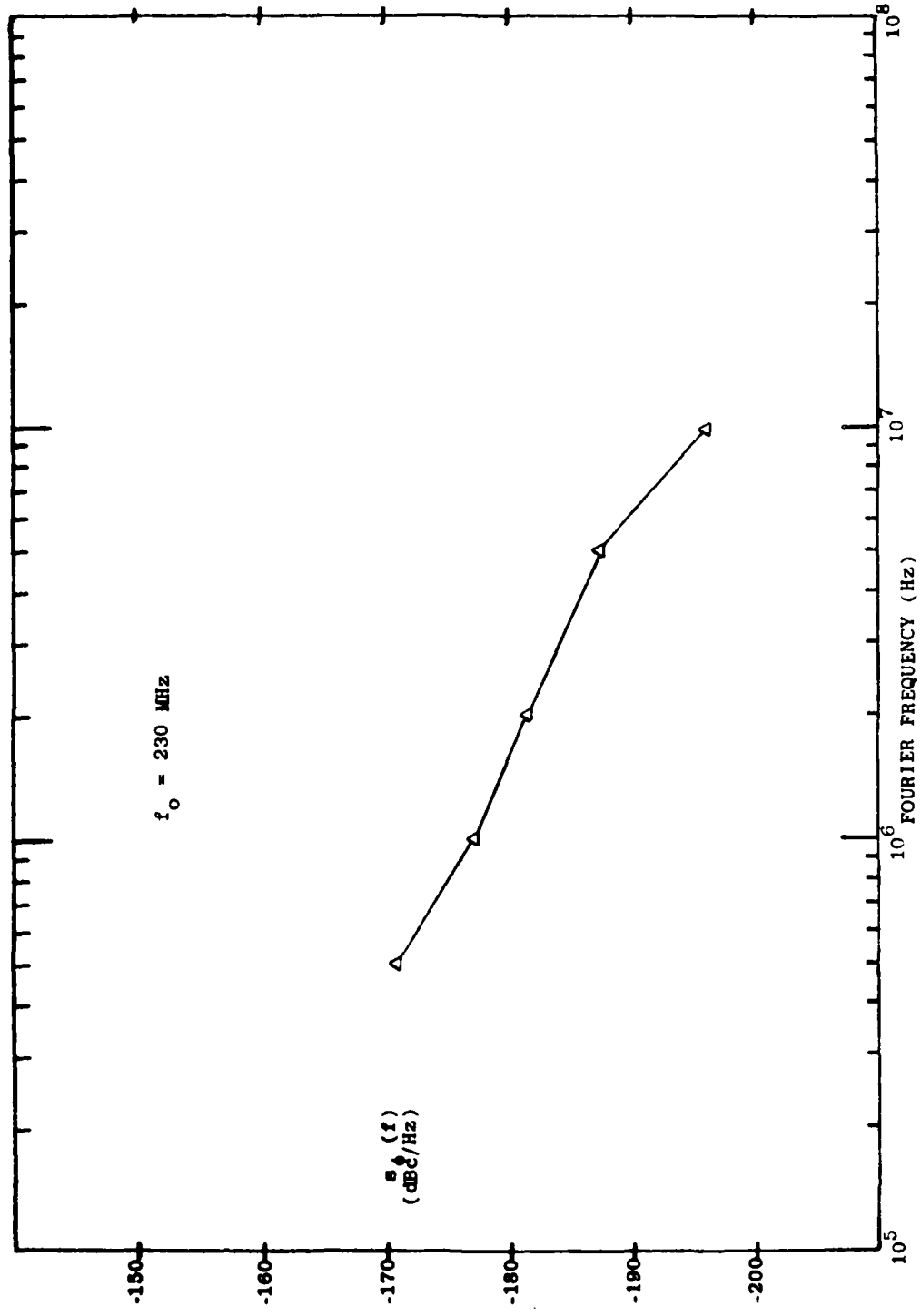

FIGURE 6.3.1a

OSCILLATOR NOISE PERFORMANCE

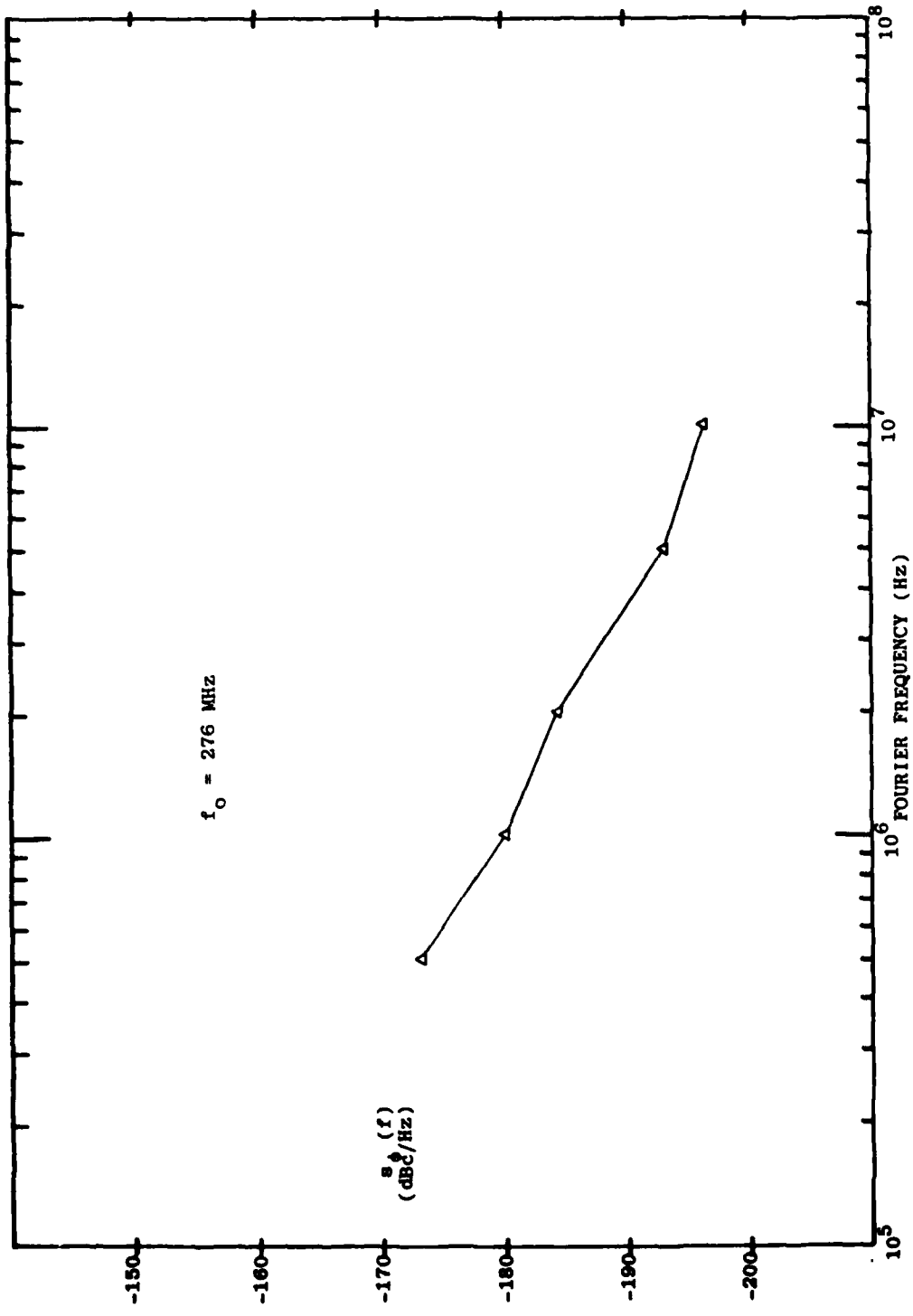

FIGURE 6.3.1b
OSCILLATOR NOISE PERFORMANCE

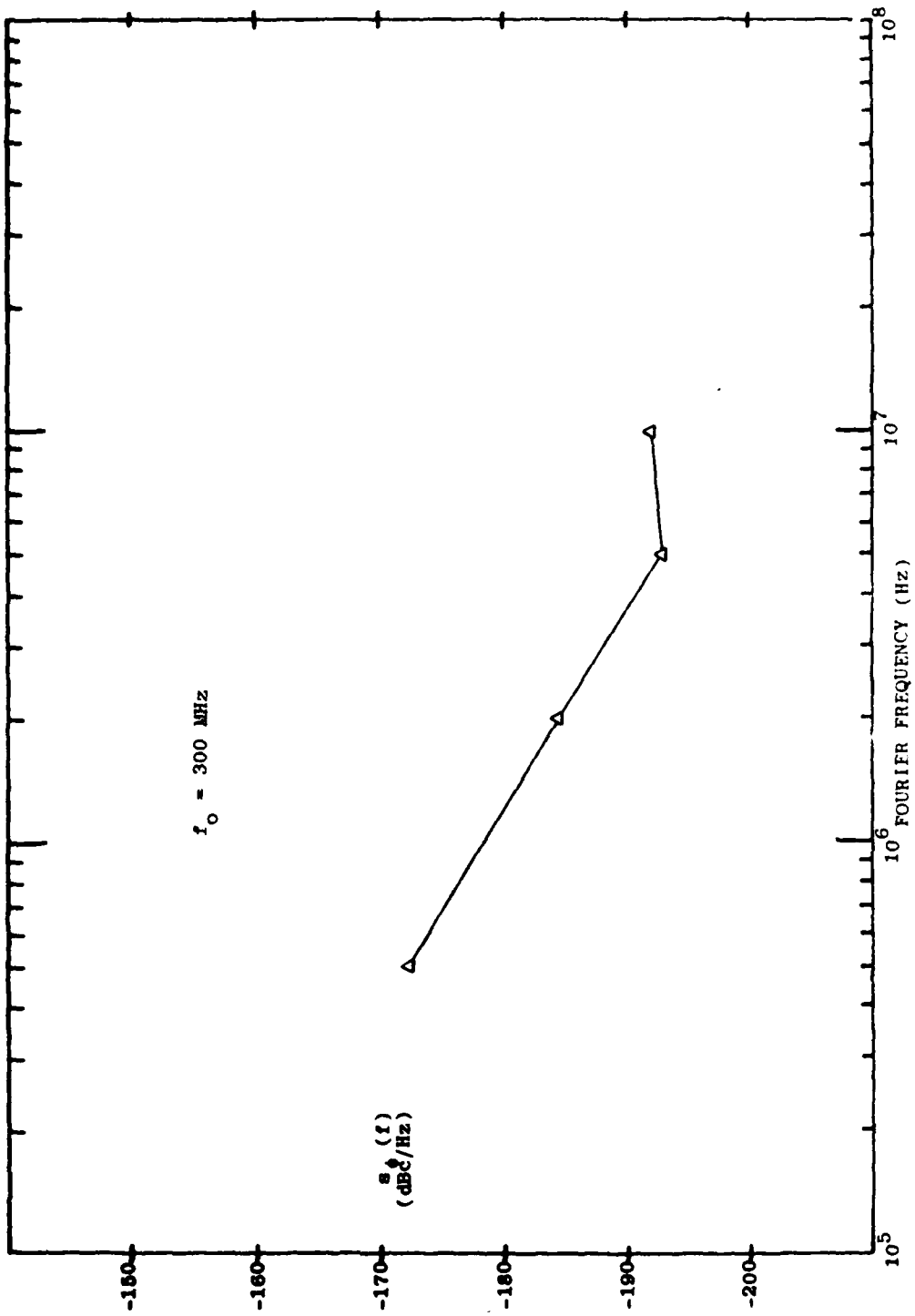

FIGURE 6.3.1c
OSCILLATOR NOISE PERFORMANCE

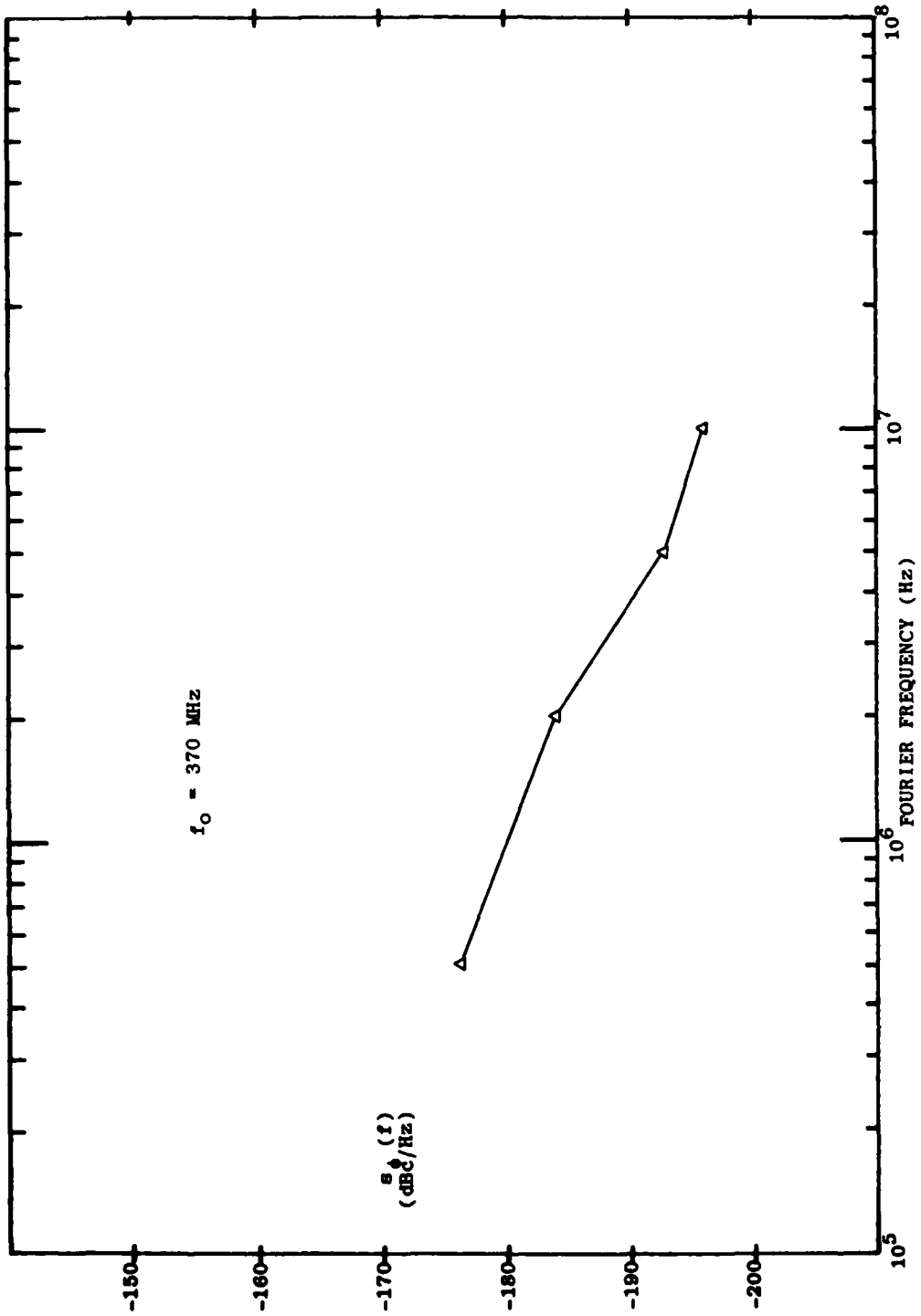

FIGURE 6.3.1d
OSCILLATOR NOISE PERFORMANCE

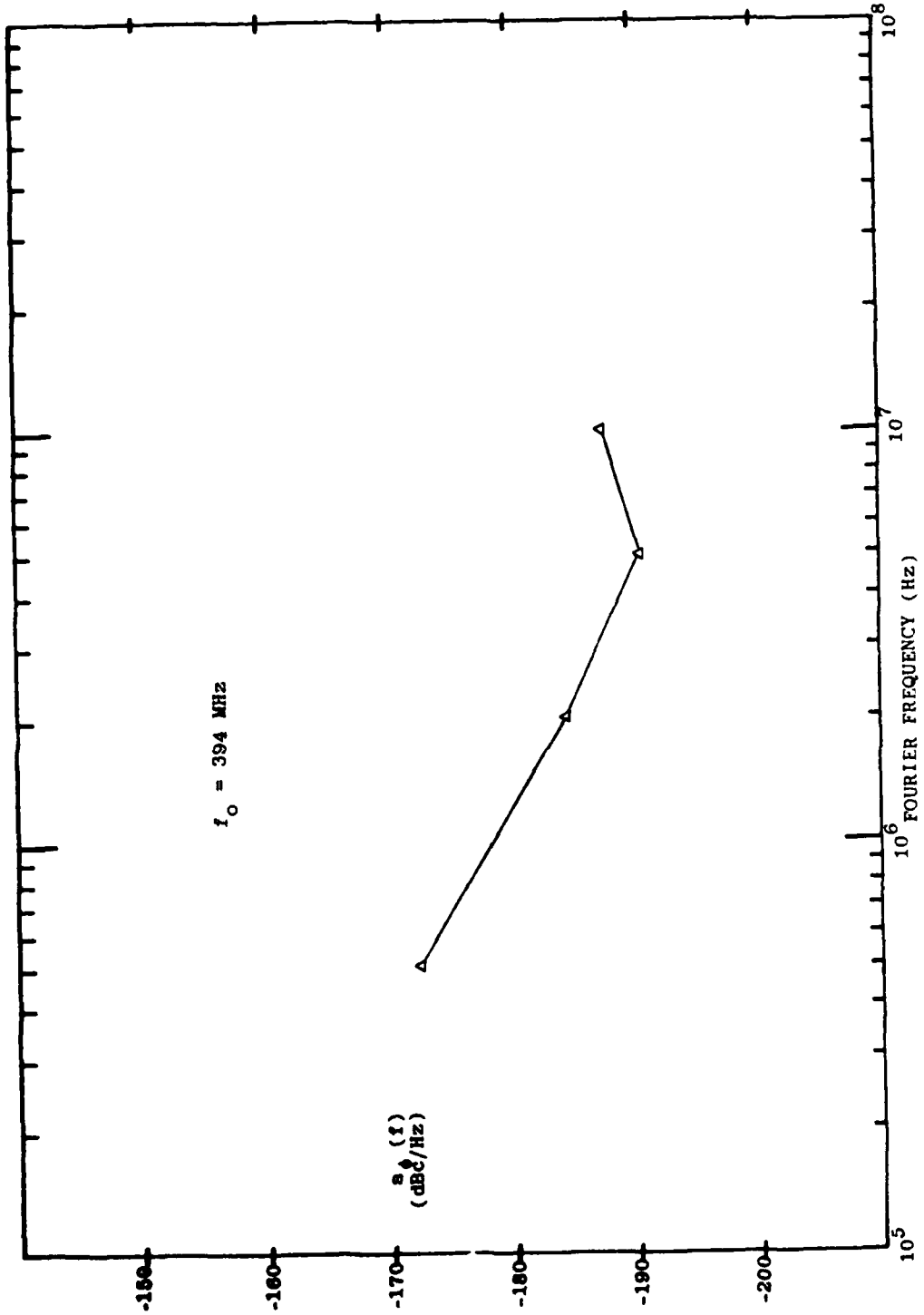

FIGURE 6.3.1e
OSCILLATOR NOISE PERFORMANCE

6.3.2 Evaluation of Higher Q Resonators

The oscillator phase noise performance achieved during this contract is significantly improved compared to present day UHF systems. However, the experimental model does not meet the design goals established for this effort. To gain further understanding of the problem, we ran phase noise tests by replacing the two-pole resonator with an experimental model resonator presently in development at ECI under separate funding. Figures 6.3.2a and 6.3.2b illustrate the comparative data at two output frequencies. The resonator Q's are approximately 25 and 100 respectively.

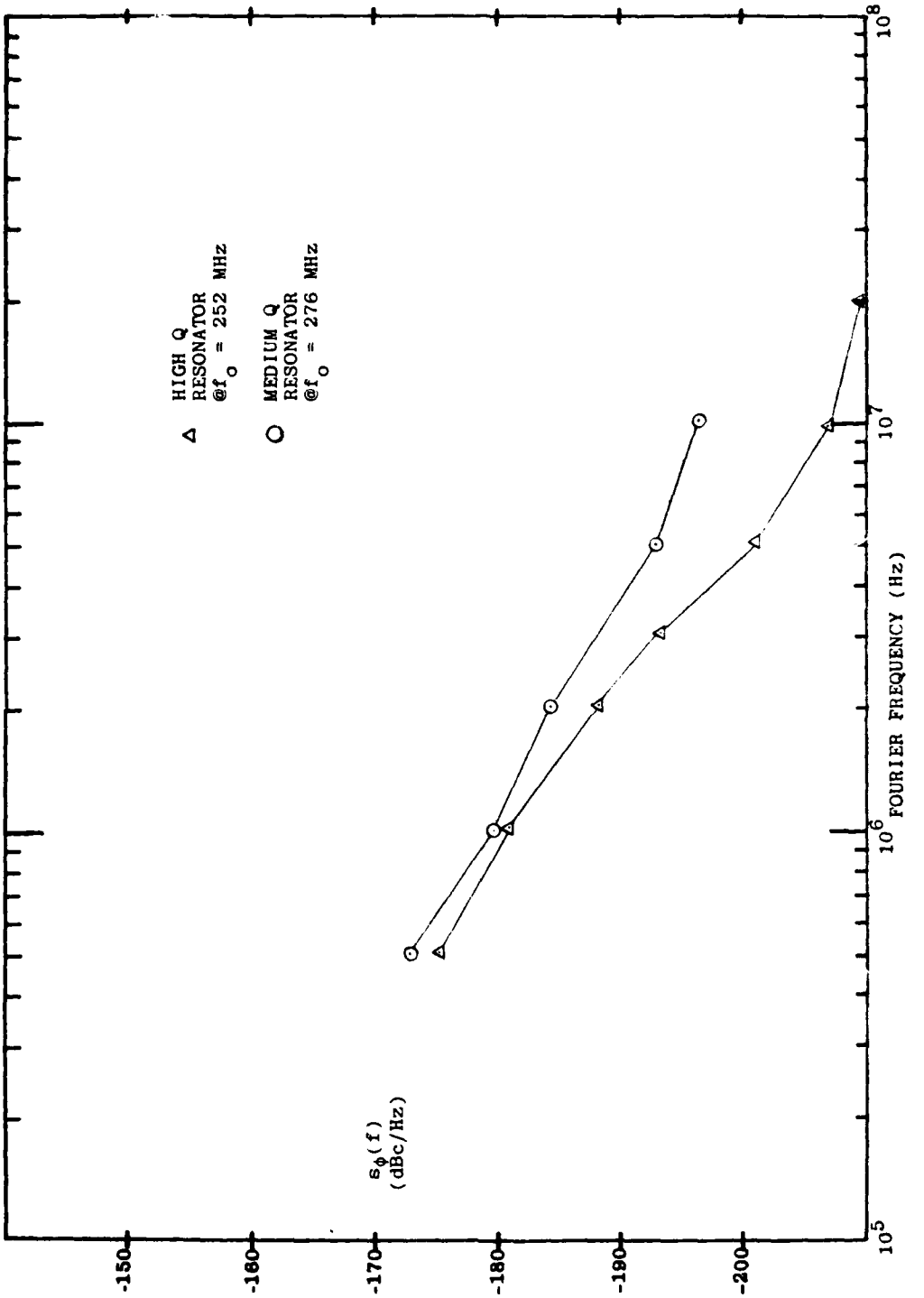

FIGURE 6.3.2a OSCILLATOR PERFORMANCE
WITH DIFFERENT Q RESONATORS

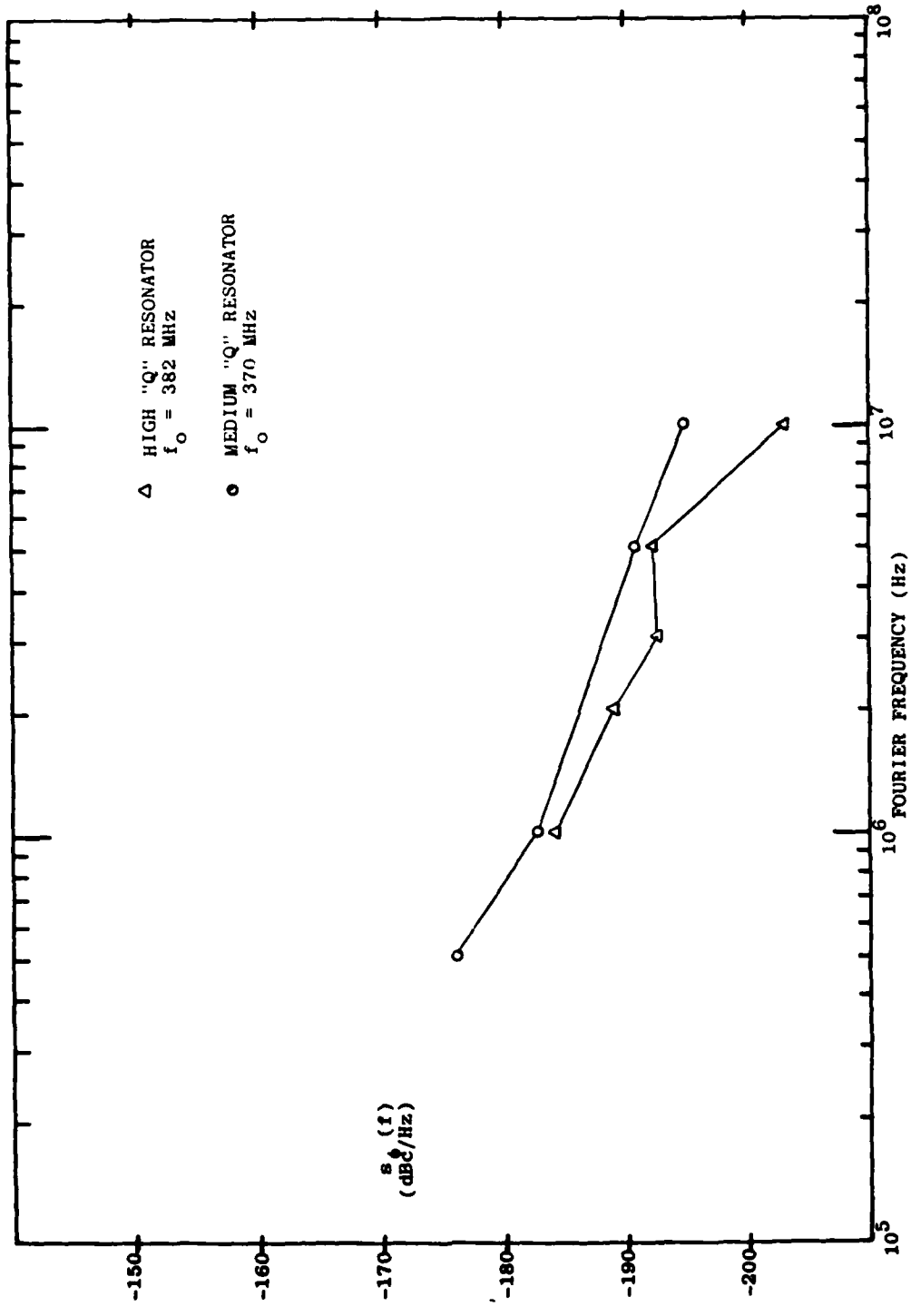

FIGURE 6.3.2.b
OSCILLATOR PERFORMANCE WITH DIFFERENT "Q" RESONATORS

Conclusion: Significant improvement is gained in phase noise performance by utilization of higher Q resonators especially at offset frequencies above 5 MHz.

6.3.3 Upper and Lower Sideband Phase Noise

An observation made during the test phase of the contract was that the phase noise is not perfectly balanced about the carrier. That is, one sideband noise spectra may be lower than the opposite side. A test was set up where the oscillator was positioned at the center of the 2-pole resonator (f=300 MHz). Figure 6.3.3 illustrates the phase noise performance. No definite cause was identified. This should be considered carefully in future work.

6.3.4 Non-symmetrical Tuning Effects on Phase Noise.

To further understand what circuit parameters effect phase noise performance, we intentionally tuned the oscillator to the edge of the 2 pole filter pass band measured the upper and lower sideband phase noise spectra. The VCO was tuned to the upper side of the band-pass resulting in the performance of Figure 6.3.4.

6.3.5 Operation with Delay Line

Several articles [19] in literature address the use of a delay element to enhance phase noise in an oscillator. The basic principle is the utilization of a steep slope (phase vs frequency) presented by the long delay element to drastically reduce phase noise. We experimented with an 80 nsec delay line (coaxial cable) in the feedback path of the high power oscillator. The resonator and power splitter added an additional 50 nsec for a total delay of 135 nsec. Figure 6.3.5 illustrates the resultant at 386 MHz. Note the noise responses that occur

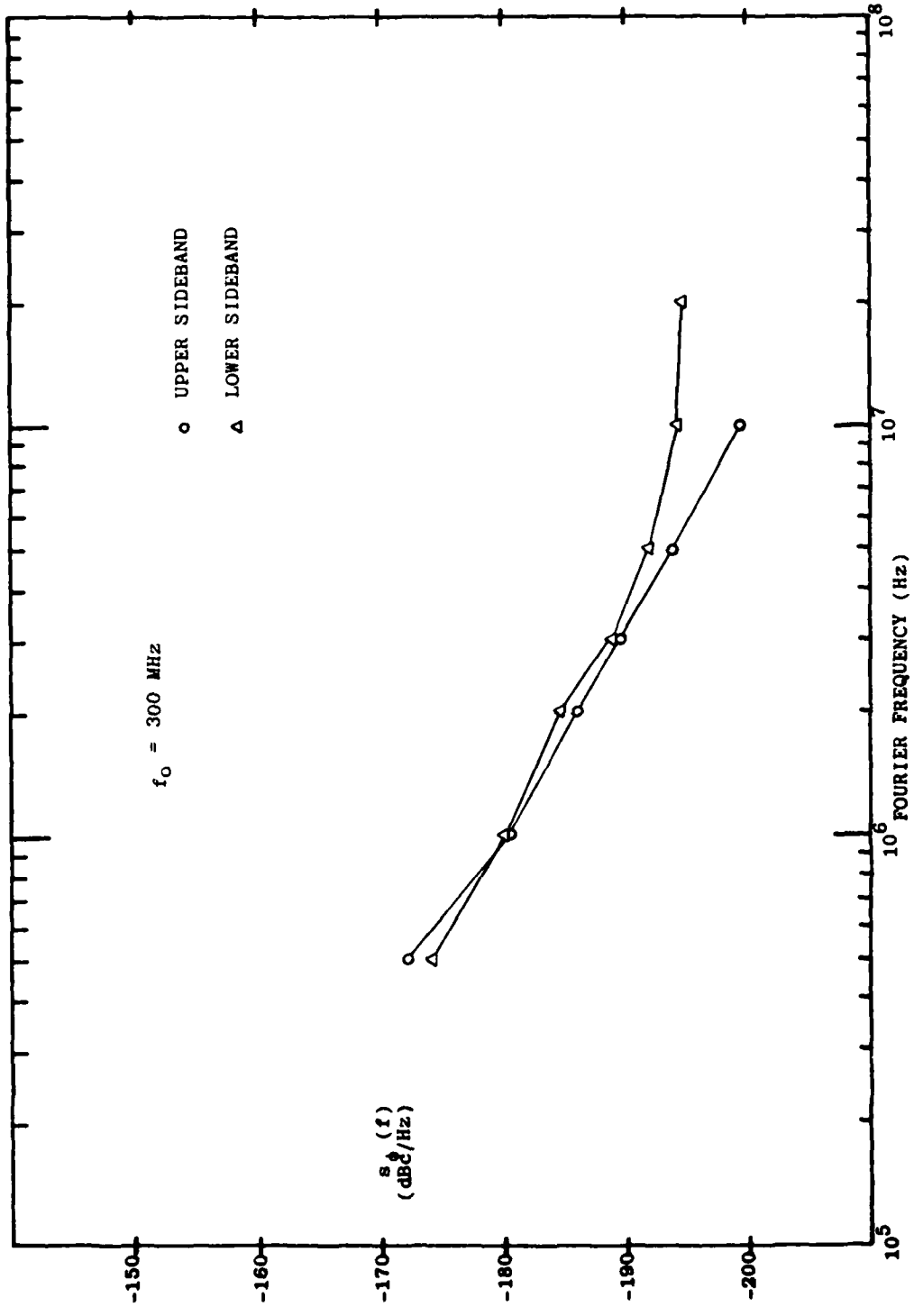

FIGURE 6.3.3
SYMMETRICALLY TUNED OSCILLATOR NOISE PERFORMANCE

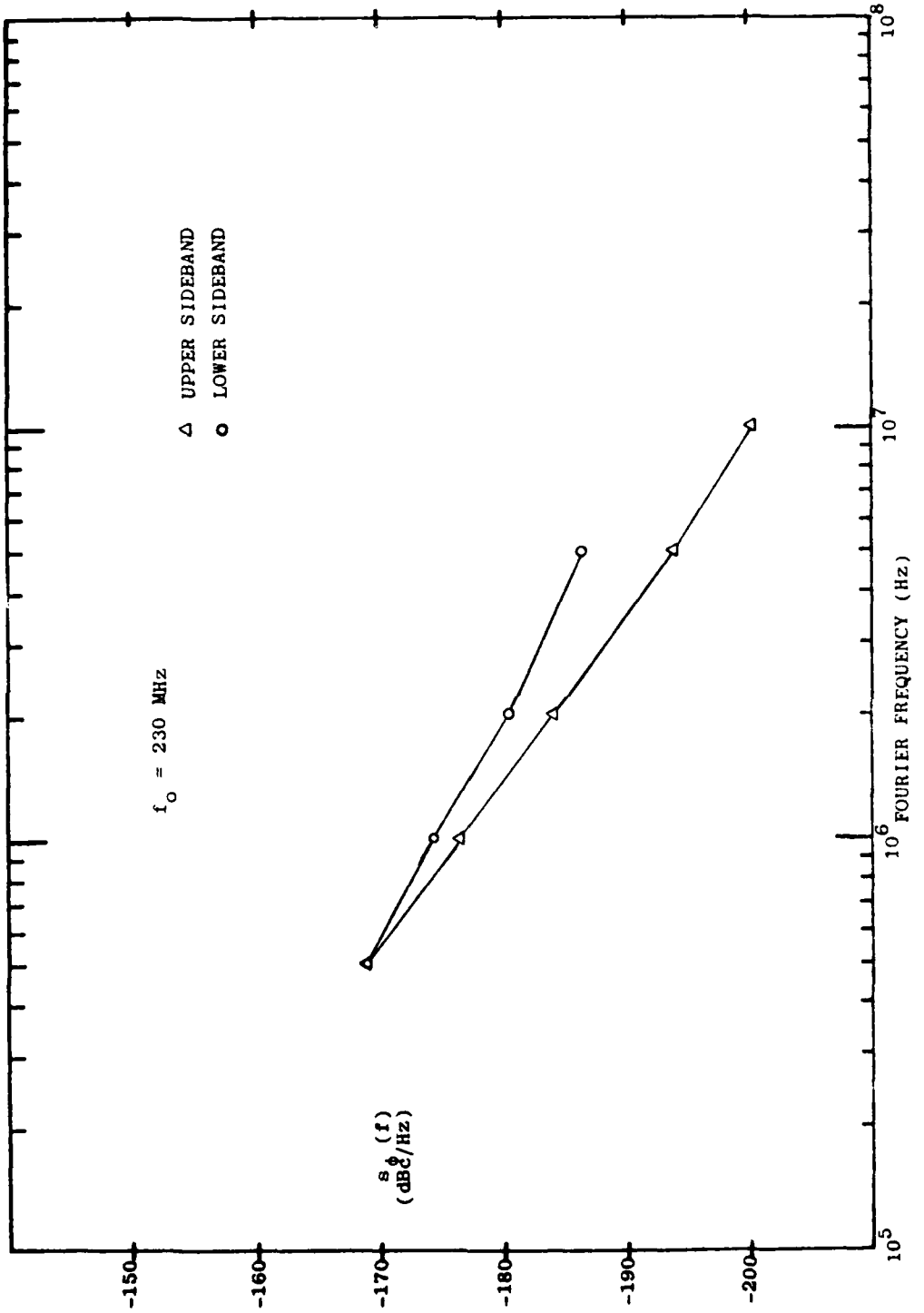

FIGURE 6.3.4
EFFECTS OF NON-SYMMETRICAL TUNING

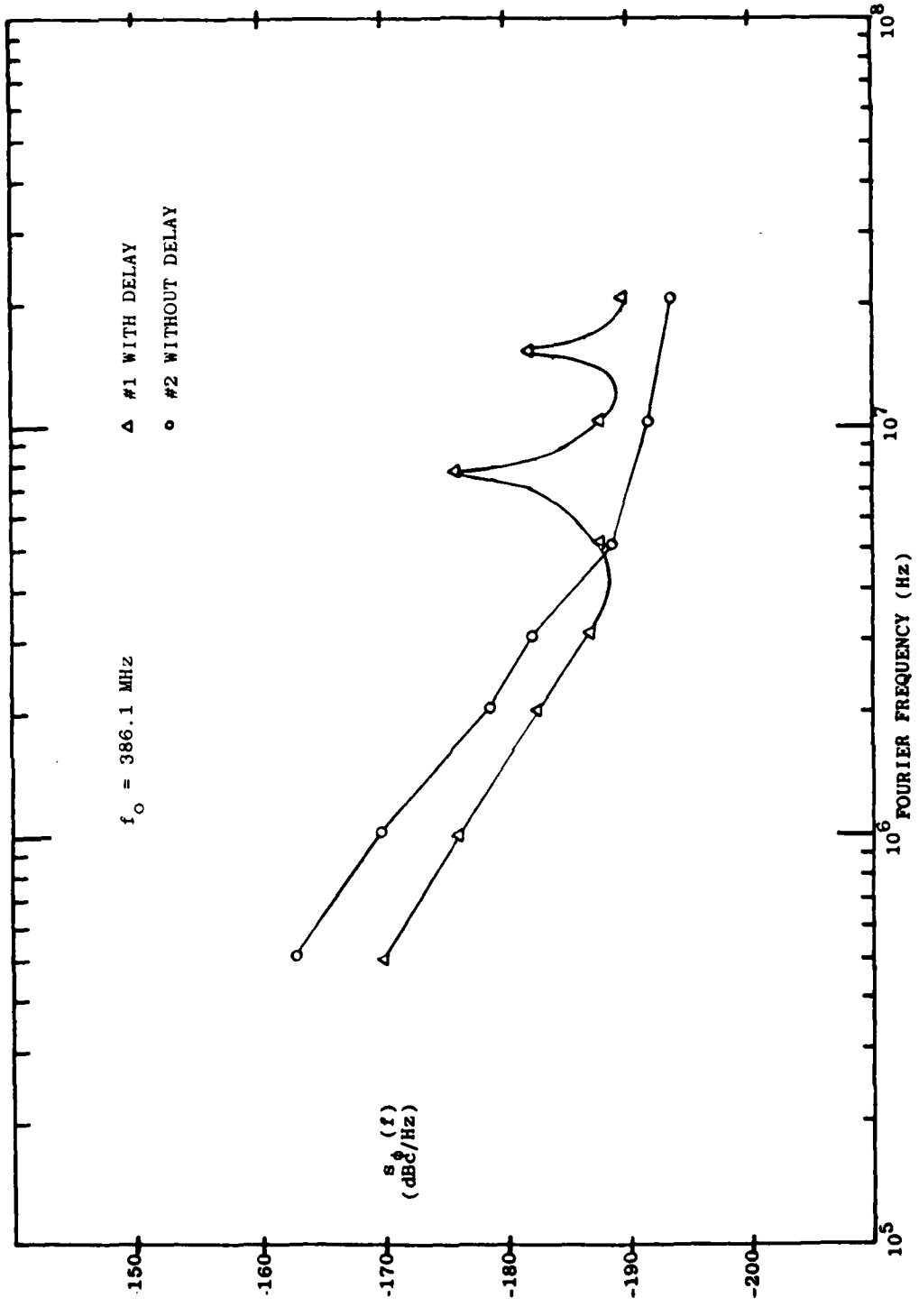

FIGURE 6.3.5

PHASE NOISE UNDER TWO FEEDBACK DELAY CONDITIONS

at 7.5 MHz and again at 15 MHz. These responses occur at Fourier Frequency, f and multiples where:

$$f = \frac{1}{t}$$

and t = total delay implemented in the feedback of the oscillator. The obvious close-in improvements are somewhat balanced by the noise peaks.

6.4 Oscillator Settling Times (Ref SOW 4.1.1.4)

Table 6.4 presents the results of the oscillator settling tests.

Table 6.4 Oscillator Settling

HOP FROM	HOP TO	ERROR	TIME
400 MHz	288 MHz	100 kHz	6.8 usec
288 MHz	400 MHz	100 kHz	(1) 68 usec
400 MHz	386 MHz	650 kHz	10 usec
		100 kHz	230 msec
386 MHz	400 MHz	620 kHz	(1) 60 usec
		100 kHz	240 msec
Specification		to within Loop Capture Range	100 usec

(1) Total includes 60 usec caused by switching delay in control box.

It reveals that the VCO exhibits post-tuning-drift of 100 to 600 kHz on long frequency hops. The VCO course tunes to within this range almost immediately, but has a very long settling time to its final frequency due to thermal time constants. When locked to a stable reference in a wide band phase locked loop, however, the initial offset is tracked out by the loop. A negligible phase change remains due to the slow change in VCO tuning caused by the post-tuning-drift.

To better understand the effects of post-tuning-drift on frequency settling, the following section is included.

6.4.1 Loop Lock-up Time and Capture Range for Wideband Phase-locked Loops.

ECI is presently working on an IR&D project to develop fast hopping frequency synthesizers. A multiple loop design is planned, with each loop having a bandwidth of 100 kHz. Loop reference frequencies will be approximately 1 MHz, with divider ratios of 100-400 to yield the UHF output frequencies. See Fig. 6.4.1a for a typical loop in the multiple loop design.

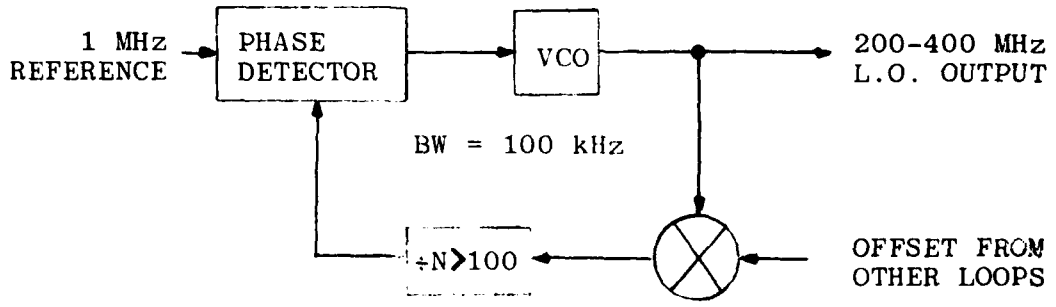

FIGURE 6.4.1a
TYPICAL SYNTHESIZER
LOOP

Lock-in range is defined as the frequency offset over which the unlocked loop will acquire lock without cycle skip (with only a phase transient). The UHF lock-in range is approximately equal to loop BW times the division ratio, greater than 10 MHz in the loops planned. A frequency offset of 10 MHz will never fall out of lock, but will see only a phase transient.

For the case where the frequency offset is well within the lock-in range a simplification of the loop model allows an estimate of the frequency settling time. The loop acts as a one-pole low pass filter with a time constant

$$\tau = \frac{1}{Wn} = \frac{1}{2\pi BW}$$

The frequency offset appears as a unit step input to the filter and the response is a simple exponential decay. (See Fig.6.4.1b)

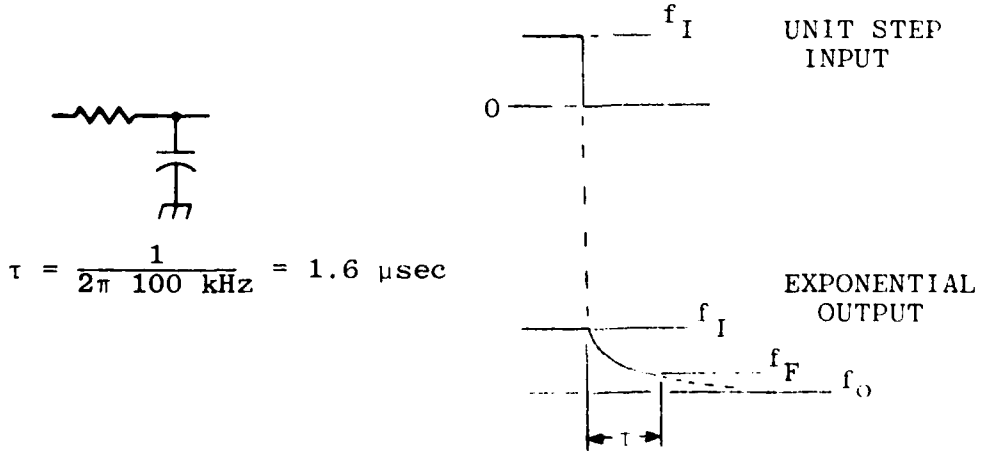

Figure 6.4.1b
LOOP RESPONSE TO EXPONENTIAL DECAY

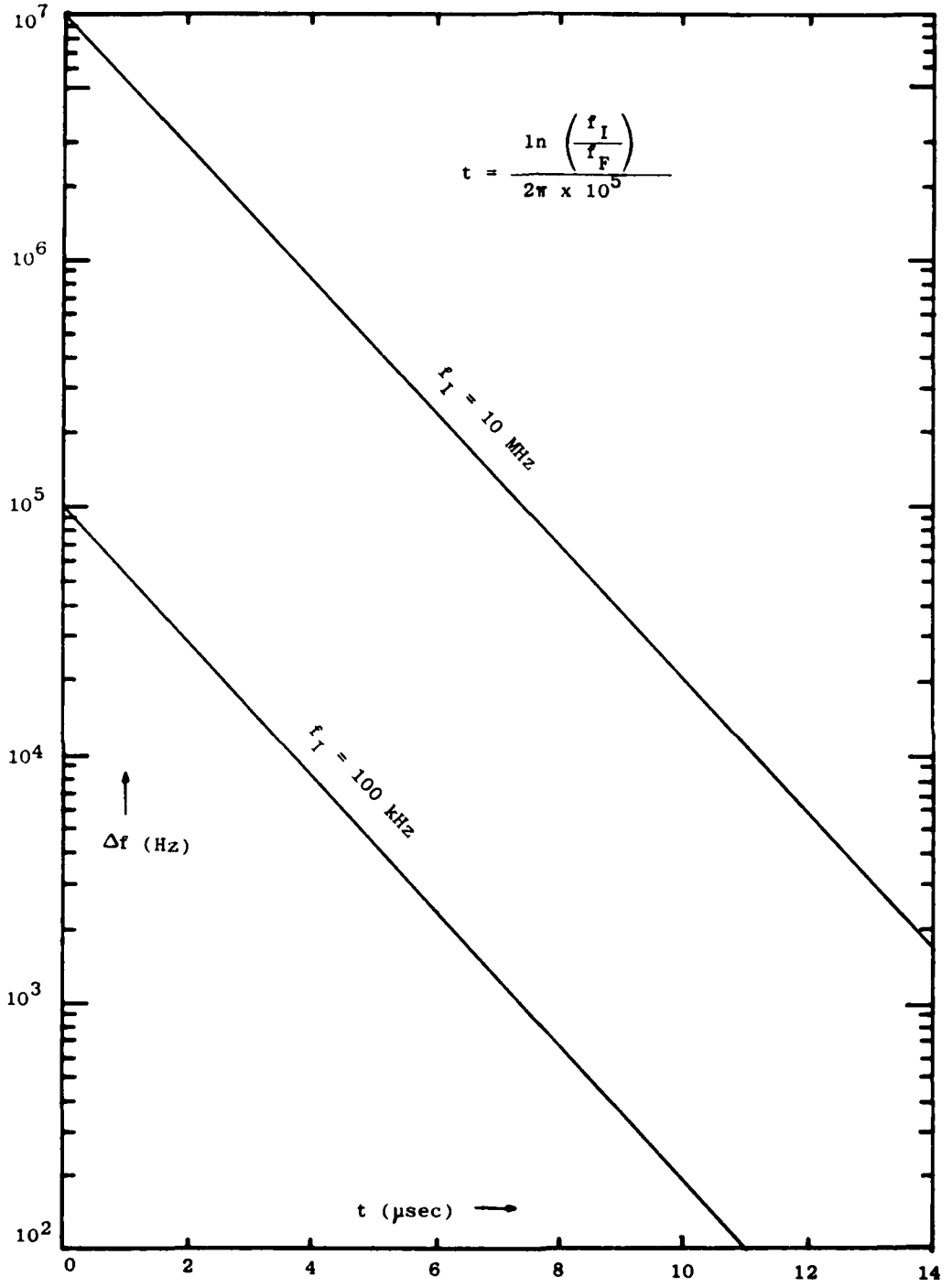

FIGURE 6.4.1c
TIME TO SETTLE AFTER STEP
CHANGE IN FREQUENCY

The output frequency offset f_F is related to initial off-set f_I and time by the equations:[34]

$$f_F = f_I e^{(-t/\tau)} \quad , \quad t = \tau \ell n (f_I / f_F)$$

Table 6.4.1 and Figure 6.4.1c show that loops of this type have settling times well within the 100 us limit.

TABLE 6.4.1
TIME TO SETTLE AFTER STEP CHANGE IN FREQUENCY

f_I	f_F	TIME TO SETTLE
100 kHz	1 kHz	7.4 uSec
500 kHz	500 Hz	11 uSec

6.5 Oscillator Load Stability (Ref SOW 4.1.1.5)

The amount of frequency deviation from desired frequency caused by terminating the oscillator in loads other than 50Ω is shown in Figure 6.5.

The oscillator exhibits less than 0.2% pulling at 300 MHz with a 3 to 1 VSWR. The exceptional improvement at 400 MHz was not investigated, (see Figure 6.5). This oscillator load isolation is sufficient for transceiver applications.

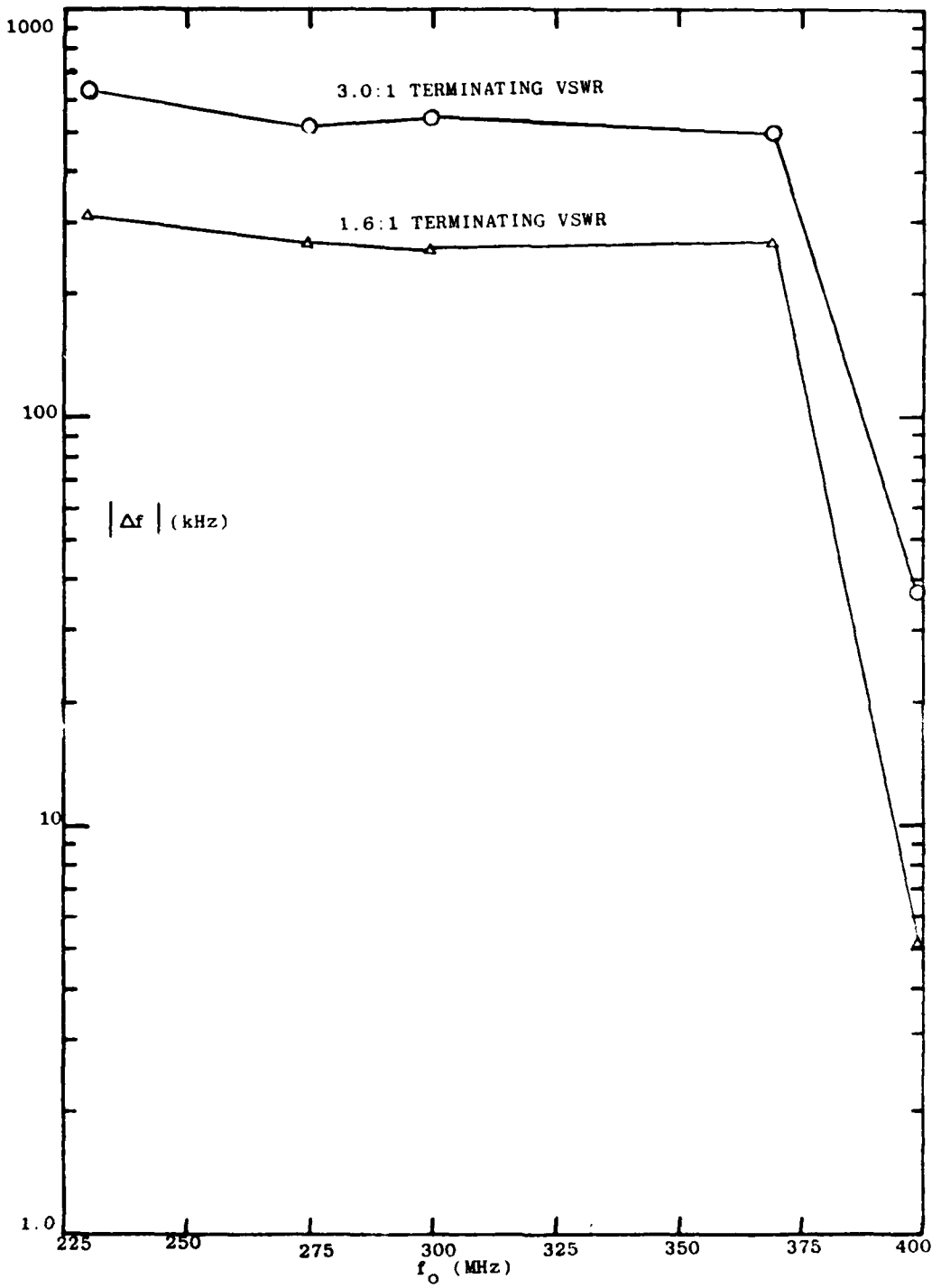

FIGURE 6.5
LOAD STABILITY

6.6 D.C. Current Drain (Ref. SOW 4.1.1.6)

Table 6.6 presents the D.C. power consumption of the oscillator at three frequencies.

Table 6.6 D.C.Power

Frequency	225 MHz	290 MHz	400 MHz
D.C.POWER			
-150V	9 mA	9 mA	2.5 mA
+4 V	8.8 A	6.25 A	0.9 A
+28 V	4.2 A	3.6 A	2.6 A
+22V	360 mA	390 mA	370 mA

7.0 RECOMMENDATIONS FOR FURTHER RESEARCH AND DEVELOPMENT

The high power VCO developed under this contract has substantially furthered the understanding of wideband low noise oscillator designs intended for high signal purity communications applications. The following paragraphs address areas to concentrate further research and development.

7.1 Higher Q Resonator

This project has illustrated that one main factor affecting inband phase noise is the phase slope of the tunable filter. The greater the slope of phase vs frequency, the lower the noise. Measurements using an experimental filter with a higher Q did indeed show improved phase noise. As both components and design techniques improve, a tunable filter with Q in excess of 150 should easily be realized.

7.2 Receive LO Applications

The high power VCO provides about 10 watts output. For both transmitter and receiver-transmitter equipments this is compatible. For receive only applications, a lower power version should be implemented. The obvious advantages are lower power consumption, less heat, smaller size. There is one question to consider though in such a task - as power out is lowered, say from 10 watts to 1/2 watt, what happens to the noise figure (and stage gains) of stages? The signal-to-noise qualities of a different design must be carefully considered. A configuration similar to the final design without the bipolar duals is a recommended starting point.

7.3 Packaging

This unit is a brassboard model intended to demonstrate design principles only. Since we are dealing with high power

PRECEDING PAGE BLANK-NOT FILMED

levels, the packaging concepts must be more in line with transmitter techniques rather than typical synthesizer packaging. Significant reductions in size and weight are natural next steps. The re-packaging must be compatible with overall heat-sinking of the entire equipment. An important factor also is vibration effects. The synthesizer phase locked loop will attenuate minor vibration effects but careful attention must be given to this packaging requirement.

7.4 Frequency Programming

The VCO is course tuned with digital steps and fine tuned with an analog voltage adjusting the varactor bias in a variable phase shifter. The present brassboard uses mechanical toggle switches for the digital inputs. We propose the development of a ROM that receives TTL codes from thumbwheel switches or a remote electrical programmer and generates a frequency code to the VCO. This development would also include a TTL-to-bipolar driver to interface the PIN diode circuits.

7.5 Integration with Frequency Synthesizer

The ultimate application for the HP VCO is as the radio frequency signal source in a frequency synthesizer where the final output frequency is stabilized to a highly stable reference source. Indirect phase locked loop techniques will be applied where a correction voltage generated within a phase detector causes the VCO to attain the frequency stability of the house-standard. Several problems must be solved in order to meet the overall objectives.

7.5.1 Low Spurious

To fully obtain the advantages of this low noise oscillator care must be taken to attenuate all spurious paths to the VCO.

As we approach signal-to-noise requirements of 200 dB, a whole new set of problems unfold concerning spurious. Typical present-day equipment with 50 to 80 dBc spurious requirements are orders-of-magnitude away in performance. Five major areas requiring careful attention are:

- Electro-static pick-up
- Magnetic pick up
- DC power line susceptibility
- Analog control line (out-of-band filtering)
- RF effects backward through buffers, etc.

As we consider -200 dBc/Hz noise levels, we begin to push packaging technology, for basic shielding capabilities. It would not be uncommon to find that double and triple shielding techniques are necessary to utilize this oscillator's full capabilities.

7.5.2 Phase Locked Loop Considerations

This design provides an analog control line for locking the VCO to a stable reference. Both digital and analog tuning are required because of the high power present in the resonator (approaches 30 watts). The loop problem that must be solved is the control line sensitivity variation experienced over the 225 to 400 MHz band. Since one PLL design criteria is to maintain nearly constant loop-bandwidth, a method must be devised to compensate for VCO sensitivity changes. This is not a trivial problem since the compensation technique must be very fast, low noise, and spurious free.

7.6 Active Devices

We are in the midst of significant improvements in the semi-conductor industry. One key characteristic that we look for is

device noise figure while operating at high power levels. The V-MOS FET was the first device to surpass UHF bipolar devices at power levels above 1 watt. Bipolars have made a significant recovery and should be considered for future evaluation. GaS FET's are extremely low noise devices at medium power levels and should also be given attention.

7.7 Tuning Elements

Presently the switch-tuned capacitor technique provides the best RF performance for an electronically tuned device operating at high power levels. Varactors are very limited in signal handling. Electronically variable magnetic devices are somewhat slow in tuning response and also very low Q for UHF applications. The PIN diodes require significant forward dc current to turn them on hard enough to reduce RF losses within the resonator. We will continue to work with diode vendors to encourage the development of very low on-resistance devices for this application.

7.8 Post Tuning Drift

Post tuning drift is best summarized as secondary tuning effects within the oscillator that pulls it off frequency after the frequency code change is made. Such effects are often related to thermal changes within the RF elements. Minute changes in device phase shift characteristics, for example, will pull the oscillator off frequency.

This characteristic is extremely important for frequency agile systems since frequency will be constantly changing. Adequate demodulation of the hopped carrier can only begin after the carrier has settled within the receiver IF bandwidth.

For phase locked transmitters and receive LO's, post tuning drift frequency errors are tracked out if the PLL bandwidth is significantly faster than the drifts. Careful attention must be given to this characteristic in the VCO and related circuits. General guide-lines are:

1. Eliminate as many effects as possible by component selection.
2. Provide good heat-sinking to critical components such as the oscillator transistor and tuning elements.
3. Provide a wide bandwidth loop to track off effects.

7.9 Oscillator Buffering

The VCO will be followed by active stages to increase power and provide isolation between the oscillator and various standing wave ratio loads. A significant design consideration for very low noise equipment will be the gain and noise figure of following stages. For example, a 100 watt output power amplifier stage may have about 10 dB gain and a 20 dB noise figure. The noise power from the PA is -174 dBm/Hz + 10 dB gain +20 dB noise figure = -144 dBm/Hz. The signal is +50 dBm. Therefore, S/N = 50 (-144) or 194 dBc.

The 200 dBc S/N desired can never be accomplished with this PA unless a narrowband filter is added at the output. Research must continue to lower the G·N (gain-noise figure product) of high power amplifier stages.

REFERENCES

PRECEDING PAGE BLANK-NOT FILMED

REFERENCES

1
J.K.Clapp, Frequency Stable LC Oscillators, IRE August 1954

2
Jiri Vackar, "LC Oscillators and Their Frequency Stability", pp 1-9, Tesla Tech. Reports, Czechoslovakia, December 1949.

3
G.B. Jordon, "The Vackar VFO, a Design to Try", The Electronic Engineer, February, 1968.

4
L.R.Malling, "Phase-Stable Oscillators for Space Communications Including the Relationship Between the Phase Noise, the Spectrum, the Short-Term Stability, and the Q of the Oscillator", Proc. of IRE, July 1962.

5
W.A.Edson, "Noise in Oscillators", Proc. of IRE, August 1960.

6
Kaneyuki Jurokawa, "Noise in Synchronized Oscillators", IEEE Trans. on Microwave Theory, April 1968.

7
D.B.Leeson, "Simple Model of Feedback Oscillator Noise Spectrum", Proc. IEEE, p. 329, February 1966.

8
G.Sauvage, "Phase Noise in Oscillators: A Mathematical Analysis of Leeson's Model", IEEE Trans. on Inst. & Meas., Vol. IM-26 No. 4, December 1977.

9
J.A.Mullen, "Background Noise in Nonlinear Oscillators," Proc. of IRE, August 1960.

10
D.Scherer, "Today's Lesson - Le. n About Low-Noise Design", Microwaves, April 1979.

11
R.B.Shields, "Review of the Specification and Measurement of Short-Term Stability", Microwave Journal, June 1969.

12
L.S.Cutter and C.L.Searle, "Some Aspects of the Theory and Measurement of Frequency Fluctuations in Frequency Standards", Proc. of IEEE, February 1966.

13
D.B.Leeson, "Short Term Stable Microwave Sources", The Microwave Journal, June 1970.

14
D.W.Allan, "Statistics of Atomic Frequency Standards", IEEE Proc., Vol. 54, No. 2, 1966.

15
L.Peregrino, D.W. Ricci, "Phase Noise Measurement Using a High Resolution Counter with On-Line Data Processing", 30th Annual Frequency Control Symposium, June 1976.

16
R.Vessot, L.Mueller, J.Vanier, "The Specification of Oscillator Characteristics from Measurements Made in the Frequency Domain", Proc. of IEEE, February 1966.

17
R.A.Baugh, L.S.Cutter, "Precision Frequency Sources", The Microwave Journal, June 1970

18
M.Dydyk, "A Step-by-Step Approach to High-Power VCO Design", Microwaves, February 1979.

19
F.Telewski, et.al., "Delay Lines Give RF Generator Spectral Purity, Programmability", Electronic Magazine, August 28, 1980.

20
J.Millman, "Vacuum-Tube and Semiconductor Electronics", McGraw Hill Book Co., New York, pg. 488, 1958.

21
H.Vollers and L.Clairborne, "RF Oscillator Control Utilizing Surface Wave Delay Lines", Proc. of 28th Annual Symposium on Frequency Control, p 256, 1974.

22
R. Rippy, "A New Look at Source Stability", Microwaves, August 1976.

23
C.L.Farell, "Designing FET Oscillators", IEEE Magazine, January 1967.

24
D.B.Leeson, "Simple Model of Feedback Oscillator Noise Spectrums", Proc. of IEEE, February 1966.

25
D.R.Lohrmann, "Determine Transmitter Noise Figure", Electronic Design 13, June 12, 1975.

26
C.V.Anderson, "Metal-Film Resistors", Electronic Design 17, August 16, 1978.

27
A.Troianello and D.E.Wheatley, "The Impact of Bulk Alloys on Resistor Technology", EDN Magazine, June 5, 1973.

28
J.Gonda, "Large Signal Transistor Oscillator Design", 1972, IEEE G-MTT International Symposium.

29
J.Beif and R.Chaffin, "Power Transistor Amplifier Design Using Large Signal S Parameters", 1973 IEEE G-MTT.

30
R.Chaffin and W. Leighton, "Large-Signal S Parameter Characteristization of UHF Power Transistors", 1973 IEEE G-MTT.

31
G. R. Basawapatna and R.B.Stanfliff, "A Unified Approach to the Design of Wide-Band Microwave Solid-State Oscillators", IEEE Trans. on MTT, Vol. MTT-27, No. 5, May 1979.

32
B.G.Malcolm, "Frequency Pulling: What Happens to Oscillator Stability with Load Variations?", MSN, June/July 1975.

33
A.W.Vemis, "Specifying Isolation to Limit Frequency Pulling", Microwaves, May 1976.

34
"Frequency Synthesis by Phase Lock", John Wiley, New York, Page 213.

35
Application Note 270-2, "Automated Noise Sideband Measurements using the HP8568P Spectrum Analyzer". Hewlett Packard.

APPENDIX A

General Oscillator Noise Model

Leeson's simple model assumes the output is taken from the amplifier as follows:

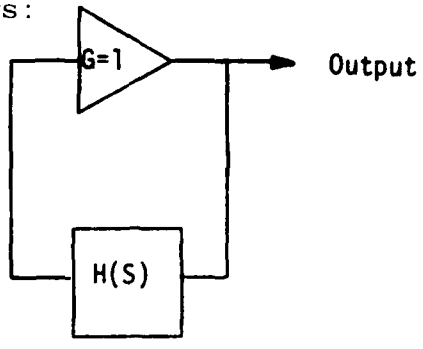

A more realistic model would be one with an amplifier with gain >1 and a feedback network adjusted to provide the desired loop gain. The oscillator output should also be taken after the resonator in the model as follows:

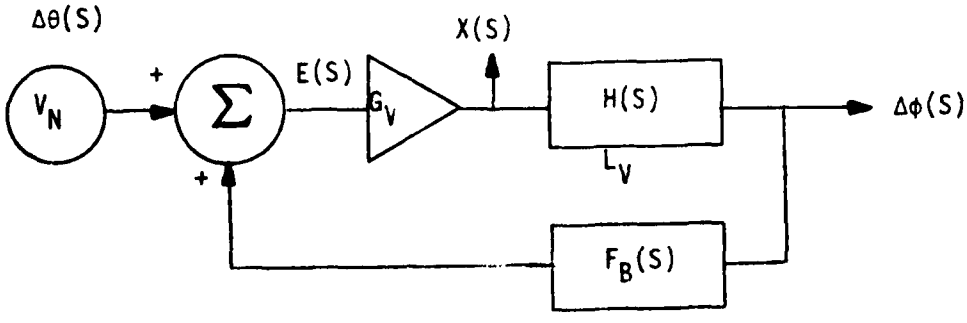

Where:

$H(S)$ = resonator transfer function

$F_B(S)$ = feedback transfer function

$E(S)$ = amplifier input

$\Delta\theta(S)$ = input phase noise

$\Delta\phi(S)$ = output phase noise

$X(S)$ = output phase noise for Leeson's model

G_V = voltage gain

L_V = voltage loss

First, let's show that this more general model is equivalent to Leeson's model when the output is taken at the amplifier output and the amplifier has unity gain. The transfer function is:

$$\frac{X(S)}{\Delta\theta(S)} = \frac{G_V}{1 - F_B(S)H(S)G_V}, \text{ and for } G_V = F_B(S) = 1$$

$$\frac{X(S)}{\Delta\theta(S)} = \frac{1}{1 - H(S)}$$ which is the same phase servo transfer equation

Next, let's show what happens when the gain and feedback ratios are included. Assuming a single tank circuit as the bandpass response, then the equivalent lowpass transfer function of the resonator is:

$$H(j\omega) = L_V\left(\frac{1}{1 + j\omega 2QL/\omega_o}\right)$$

$$\frac{X(j\omega)}{\Delta\theta(j\omega)} = \frac{G_V}{1 - \frac{F_B(j\omega)G_V L_V}{1 + j\omega 2Q_L/\omega_o}}$$

for $F_B(j\omega) = F_B$, i.e., the voltage feedback ratio is not frequency sensitive.

$$\frac{X(j\omega)}{\Delta\theta(j\omega)} = \frac{G_V L_V (1 + j\omega 2Q_L/\omega_o)}{(1 - F_B G_V L_V) + j\omega 2Q_L/\omega_o}$$

The power transfer function is:

$$\left|\frac{X(f)}{\Delta\theta(F)}\right|^2 = \frac{GL\left[1 + \left(\frac{2QL}{f_o}\right)^2\right]}{(1 - \sqrt{F_B GL})^2 + f^2\left(\frac{2QL}{f_o}\right)^2}$$

where G, L, and F_B are power ratios.

The power spectral density of the output phase noise is the product of the phase spectral density of the input noise sources with the phase transfer function of the oscillator.

$$S(f) = [\alpha f^{-1} + \beta f^0] \left|\frac{X(f)}{\Delta\theta(f)}\right|^2$$

$$= \left[\frac{FKTf_\alpha f^{-1}}{P_s} + \frac{FKT}{P_s}\right] \left\{\frac{GL\left[1 + f^2\left(\frac{2QL}{f_o}\right)^2\right]}{(1-\sqrt{F_B GL})^2 + f^2\left(\frac{2QL}{f_o}\right)^2}\right\}$$

$$= \frac{FKT\ GL}{P_s} \left(\frac{f_\alpha f^{-1} + f_\alpha f\left(\frac{2QL}{f_o}\right)^2 + f^2\left(\frac{2QL}{f_o}\right)^2 + 1}{(1-\sqrt{F_B GL})^2 + f^2\left(\frac{2QL}{f_o}\right)^2}\right)$$

Normally, the power out of the device, P_D, is measured rather than P_s and $P_s = \frac{P_D}{G}$, & $\sqrt{F_B GL} = 1$ for a linear oscillator so that for a single sideband spectral density:

$$S_{x(f)/2} = \frac{FKTG^2L}{2P_D}\left[f_a\left(\frac{f_o}{2Q_L}\right)^2 f^{-3} + \left(\frac{f_o}{2Q_L}\right)^2 f^{-2} + \frac{f_a}{f} + 1\right]$$

Except for the multiplication by GL, this equation is identical to the one derived from the simple model by Leeson. But, this equaiton is more general in that the amplifier gain and resonator loss are included.

Finally, let's consider what happens when the output is taken at the resonator output. The transfer function is:

$$\frac{\Delta\phi(S)}{\Delta\theta(S)} = \frac{GH(S)}{1 - GH(S)F_B}$$

Again, using the resonator equivalent transfer function of:

$$H(j\omega) = L_V\left(\frac{1}{1 + j\omega 2QL/\omega_o}\right)$$

$$\frac{\Delta\phi(j\omega)}{\Delta\theta(j\omega)} = \frac{G_V L_V\left(\frac{1}{1 + j\,2Q_L/\omega_o}\right)}{1 - G_V L_V F_B\left(\frac{1}{1 + j\omega 2Q_L/\omega_o}\right)}$$

$$\frac{\Delta\phi(j\omega)}{\Delta\theta(j\omega)} = \frac{G_V L_V}{(1 - G_V L_V F_B) + j\omega 2QL/\omega_o}$$

The power transfer function:

$$\left|\frac{\Delta\phi(f)}{\Delta\theta(f)}\right|^2 = \frac{GL}{(1-\sqrt{GLF_B})^2 + f^2\left(\frac{2Q_L}{f_o}\right)^2}$$

The power spectral density of the output phase noise is the product of the spectral density of the noise sources and the phase power transfer function of the oscillator.

$$S_{\Delta\phi(f)} = [\alpha f^{-1} + \beta f^0]\left|\frac{\Delta\phi(f)}{\Delta\theta(f)}\right|^2$$

$$\alpha = \frac{FKTf_\alpha}{P_s} \quad , \beta = \frac{FKT}{P_s}$$

$$S_{\Delta\phi(f)} = \frac{FKT}{P_s}\left[\frac{f_\alpha}{f} + 1\right]\left[\frac{GL}{(1-\sqrt{GLF_B})^2 + f^2\left(\frac{2Q_L}{f_o}\right)^2}\right]$$

The single sideband spectral density is one-half the value of $S\Delta\phi(f)$ The output power of the oscillator is normally measured rather than the input power and $P_s = P_o/GL$. These facts are included to show:

$$S_{\Delta\phi(f)/2} = \frac{FKT\ GL}{2P_o}\left[\frac{f_\alpha}{f} + 1\right]\left[\frac{GL}{(1-\sqrt{GLF_B})^2 + f^2\left(\frac{2Q_L}{f_o}\right)^2}\right]$$

When the oscillator is operating linearily:

$\sqrt{GLF_B} \approx 1$, so that the term $(1 - \sqrt{GF_B}L) \approx 0$.

$$S_{\Delta\phi(f)/2} = \frac{FKTG^2L^2}{2P_o}\left(\frac{f_o}{2Q_L}\right)^2\left[\frac{f_\alpha}{f^3} + \frac{1}{f^2}\right]$$

since $GL \approx \frac{1}{F_B}$

$$S_{\Delta\phi(f)/2} = \frac{FKT\ GL}{2P_o F_B}\left(\frac{f_o}{2Q_L}\right)^2\left[\frac{f_\alpha}{f^3} + \frac{1}{f^2}\right] = \text{single sideband spectral density}$$

MISSION
of
Rome Air Development Center

RADC plans and executes research, development, test and selected acquisition programs in support of Command, Control Communications and Intelligence (C^3I) activities. Technical and engineering support within areas of technical competence is provided to ESD Program Offices (POs) and other ESD elements. The principal technical mission areas are communications, electromagnetic guidance and control, surveillance of ground and aerospace objects, intelligence data collection and handling, information system technology, ionospheric propagation, solid state sciences, microwave physics and electronic reliability, maintainability and compatibility.

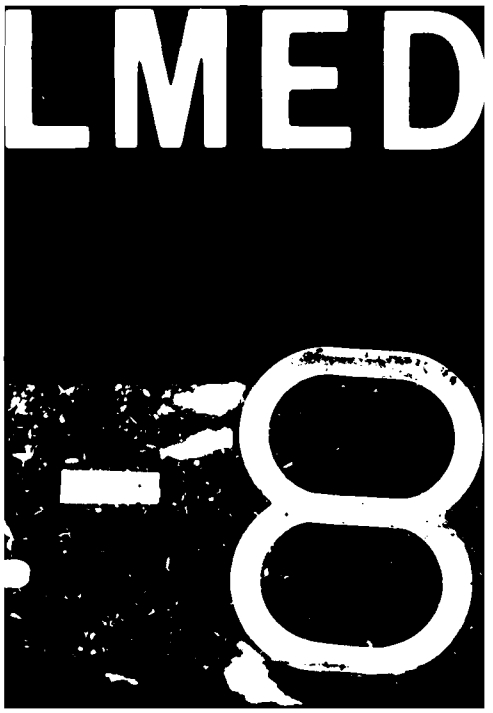
LMED
8